Functional characterization of Ubc6 and Ubc7 at the Doa10 ubiquitin ligase

Dissertation

zur Erlangung des akademischen Grades

doctor rerum naturalium

(Dr. rer. nat.)

im Fach Biologie

eingereicht an der

Lebenswissenschaftlichen Fakultät

der Humboldt-Universität zu Berlin

von

M.Sc. Annika Katharina Weber

Präsidentin der Humboldt-Universität zu Berlin

Prof. Dr.-Ing. Dr. Sabine Kunst

Dekan der Lebenswissenschaftlichen Fakultät

Prof. Dr. Bernhard Grimm

Gutachter/innen:

1. Prof. Dr. Thomas Sommer
2. Prof. Dr. Martin Scheffner
3. Prof. Dr. Claus Scheidereit

Tag der mündlichen Prüfung: 23.09.2016

Danksagung

An dieser Stelle möchte ich mich bei all jenen bedanken, welche mich bei der Erstellung dieser Arbeit in den letzten 4 Jahren unterstützt haben.

Ich danke meinem Doktorvater Prof. Thomas Sommer für die Möglichkeit diese Arbeit in seiner Gruppe anzufertigen, für seine vielseitigen Ideen und seinen Glauben in das Projekt.

Mein Dank gilt Dr. Ernst Jarosch für seine Unterstützung bei der Durchführung meines Projekts, seine große Hilfsbereitschaft und wissenschaftliche Beratung, sowie für das Korrekturlesen meiner Arbeit.

Ein großes Dankeschön geht an meine Kollegen aus der AG Sommer, die mich während meiner Zeit am MDC begleitet haben. Ihre Hilfsbereitschaft und die tolle und entspannte Arbeitsatmosphäre im Labor sorgen dafür, dass ich diese Zeit immer in sehr guter Erinnerung behalten werde. Corinna Volkwein und Mandy Mustroph möchte ich an dieser Stelle besonders danken für ihre exzellente technische Unterstützung. Ebenso möchte ich mich bei Jasmin Schlotthauer bedanken, welche mich im Zuge eines Praktikums sehr unterstützt hat.

Ich danke Dr. Oliver Popp und Dr. Gunnar Dittmar für die Durchführung der Massenspektrometrie Analysen dieser Arbeit.

Zuletzt möchte ich mich bei meinen Freunden, meiner Familie und meinem Lebensgefährten Torsten für ihre immerwährende Unterstützung, Motivation und Liebe und das Ertragen meiner Launen während der finalen Phase meiner Arbeit bedanken.

Zusammenfassung

Der Prozess der Proteinfaltung ist fehlerbehaftet und in dessen Verlauf entstehen zahlreiche Proteine mit einer unnatürlichen Konformation. Solche fehlgefalteten Polypeptide gefährden die zelluläre Proteinhomöostase, weshalb ihrer Anreicherung durch spezialisierte Proteinqualitätskontroll-Systeme (PQC's) entgegen gewirkt wird. Diese PQC's sorgen für die Beseitigung der unnatürlichen Proteine indem sie entweder deren Rückfaltung anregen oder ihren proteolytischen Abbau initiieren. Ein sehr bedeutender Qualitätskontrollmechanismus ist das Ubiquitin (Ub)-Proteasom-System (UPS), an dessen Ende der Abbau von Proteinen durch das 26S-Proteasom steht.

In *Saccharomyces cerevisiae* nimmt die membrangebundene RING-Ub-Ligase Doa10 eine bedeutende Rolle in der PQC des Endoplasmatischen Retikulums (ER) und des Nukleus ein. Doa10 katalysiert dabei die Verknüpfung K48-verbundener Ub-Ketten auf Proteine, die entweder in der ER-Membran oder löslich im Cytosol oder dem Nukleoplasma vorliegen. Diese Markierung leitet die Degradation dieser Proteine ein. Interessanterweise kooperiert Doa10, im Gegensatz zu anderen RING-Ub-Ligasen, mit zwei Ub-konjugierenden Enzymen (E2), um ihre Substrate zu prozessieren.

In dieser Arbeit wird veranschaulicht, wie die beiden hochspezialisierten E2 Enzyme Ubc6 und Ubc7 sequentiell agieren, um Doa10 Substrate zu modifizieren. Zuerst wird ein einzelnes Ub-Molekül Ubc6-abhängig an ein Substrat konjugiert (Initiation). Von diesem Rest ausgehen katalysiert Ubc7 die Ausbildung einer K48-verbundenen Ub-Kette (Elongation). Die Fähigkeit von Ubc6 nicht nur Lysine, sondern auch hydroxylierten Aminosäuren wie Serin und Threonin mit Ub-Molekülen zu verknüpfen, erweitert das Substratspektrum von Doa10 und ermöglicht die Prozessieren von Proteinen, die keine zugänglichen Lysinreste exponieren. Weiterhin wird gezeigt, dass ein Überangebot von Ubc6 den Doa10-abhängigen Substratabbau beeinträchtigt. Dies weist darauf hin, dass die Generierung eines effizienten Poly-Ub-Signals einer streng kontrollierten Koordination beider E2 Enzyme am Doa10-Ligase-Komplex unterliegt.

PQC, Proteinabbau, Doa10-Ub-Ligase, E2 Enzyme, Ubiquitylierung von Aminosäuren mit Hydroxylgruppe

Abstract

Protein folding is naturally error-prone and often gives rise to species that are trapped in an aberrant conformation. The accumulation of such terminally misfolded polypeptides, which threaten protein homeostasis, is prevented by elaborate protein quality control systems (PQCs). These PQCs remove misfolded proteins from the cell by either facilitating their refolding or by elimination through proteolysis. A major cellular PQC pathway is the ubiquitin (Ub) proteasome system (UPS), which facilitates protein degradation by the 26S proteasome.

In *Saccharomyces cerevisiae*, the membrane-bound RING-type Ub ligase Doa10 is a key player of PQC in the endoplasmic reticulum (ER) and the nucleus. Doa10 promotes lysine 48-linked poly-ubiquitylation of proteins that either reside in the ER membrane or are soluble in the cytosol or the nucleus and thereby labels them for degradation. Strikingly, in contrast to other RING Ub ligases, which typically employ a single Ub conjugating enzyme (E2) for substrate ubiquitylation, the Doa10 ligase requires two of such enzymes for client processing.

This study demonstrates that the highly specialized E2 enzymes Ubc6 and Ubc7 act in a sequential manner on Doa10 client proteins. In a first step Ubc6 attaches a single Ub molecule to a substrate (priming), which is followed by the elongation of this moiety with K48-linked Ub chains by Ubc7 (elongation). The ability of Ubc6 to conjugate Ub not only to lysine but also to hydroxylated amino acids like serine and threonine broadens the substrate range of Doa10 and allows processing of proteins, which do not expose accessible lysine residues. Overproduction of Ubc6 was shown to impair Doa10 dependent substrate degradation. Apparently, the generation of a productive K48-linked poly-Ub signal requires a tightly coordinated activity of the individual E2 enzymes at the Doa10 ligase complex.

PQC, protein degradation, Doa10 Ub ligase, E2 enzymes, non-canonical ubiquitylation of hydroxylated amino acids

Contents

1 Introduction

1.1 Ubiquitin and Ub-like proteins

Ubiquitin (Ub) is a highly conserved and essential polypeptide in eukaryotes that can be covalently attached to other proteins. Post-translational modification with Ub, known as ubiquitylation, regulates the function of proteins and thereby governs fundamental cellular processes like cell cycle progression, endocytosis, DNA damage repair and protein degradation [1]. The Ub molecule encompasses 76 amino acids that adopt a highly stable β-grasp fold through a number of hydrogen bonds and the formation of a hydrophobic core (figure 1.2 a) [2, 3]. This compact structure is important to preserve the functionality of Ub even during acute stress conditions [4–6]. The carboxyl-terminal six residues of Ub are highly flexible, which is a prerequisite for the attachment to target proteins [7]. Besides three conservative amino acid substitutions, Ub is identical from yeast to human, which demonstrates the functional importance of the Ub structure [8]. Indeed, specific regions on the surface serve as interaction platform for proteins with so-called Ub binding domains (UBDs) [9]. The association with such UBD containing proteins determines the fate of a client by routing it to specific cellular pathways. Most importantly, Ub can be conjugated to other Ub molecules in a controlled manner thereby forming Ub chains on the target. Individual Ub polymers expose different properties, which allows binding of only selected UBD proteins. This highly complex "Ub code" explains how such a small molecule can control highly divers cellular activities. Eukaryotic cells contain other Ub-like proteins (UBLs) that share a high degree of similarity in tertiary structure with Ub [10]. These UBLs are also covalently attached to target molecules through separate reaction mechanisms and regulate cellular processes like autophagy, splicing and development [11].

1.2 The ubiquitylation cascade

Post-translational modification of proteins with Ub is catalyzed by an enzymatic cascade involving three different kinds of proteins (figure 1.1). In a first step, the Ub activating enzyme (E1) forms a reactive thioester with the C-terminus of Ub under hydrolysis of ATP (E1~Ub) [12]. The E1 enzyme then transfers the activated Ub molecule to the active site cysteine of a Ub conjugating enzyme (E2) (E2~Ub) [13]. Finally, Ub ligases (E3) recruit E2~Ub complexes and bring them in close proximity to client proteins, which in turn promotes the conjugation of the Ub molecule to acceptor sites within the substrate [14]. As a typical product, the carboxy-group at the C-terminus of Ub is linked to the ε-amino group of a lysine residue by a stable isopeptide bond. This reaction is facilitated by the nitrogen atom in the amino-group, which acts as a nucleophile and attacks the thioester linkage at the electron-deficient carbonyl carbon of the C-terminus of Ub. Ub exposes seven lysine residues, which themself can serve as acceptor sites for further ubiquitylation. The addition of Ub molecules leads to the assembly of Ub chains on target proteins. E3 ligases are key players during substrate ubiquitylation because they assure the specificity of the reaction and in most cases they regulate the activity of the E2 enzymes. This is also reflected by their number in eukaryotic cells. Yeast cells contain one E1 enzyme, 13 E2 enzymes and around 100 E3 ligases [13]. In higher eukaryotes the number of E2 enzymes (40) and E3 ligases (600 to 1000) is considerably larger [15, 16]. Ub ligases can be classified into three subgroups. RING (Really Interesting New Gene)-type Ub ligases mediate direct transfer of Ub from the E2 enzyme to the target protein by providing a binding platform for E2~Ub complexes [14]. HECT (Homologous to E6AP Carboxy-Terminus) Ub ligases themself contain an active site cysteine to which the Ub molecule is transferred by an E2 enzyme before it is finally conjugated to a client protein [17]. The least well-studied Ub ligases are the RBR (RING between RING) ligases that combine features of both RING and HECT E3 ligases [18]. Ub ligases, which are specialized on transferring Ub moieties to already preassembled short Ub chains on client proteins, are so called E4 enzymes [19].

Similar to other post-translational modification ubiquitylation is reversible

[20]. Deubiquitinases (DUBs) remove Ub molecules from target proteins by hydrolyzing the isopeptide bond and thereby recycle Ub for other modification events. A balanced activity of Ub conjugation and deconjugation ensures the maintenance of a healthy cellular environment.

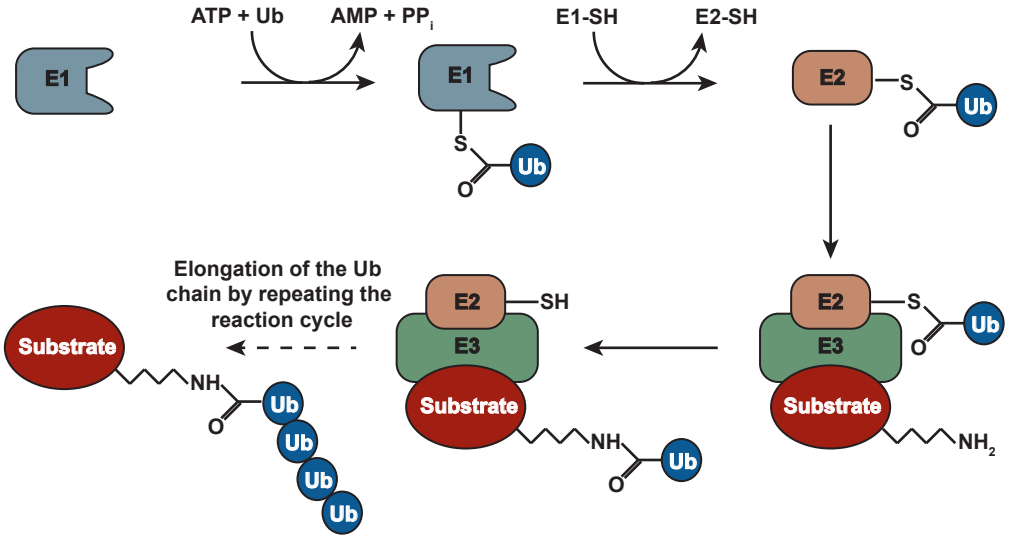

Figure 1.1 – Schematic representation of the ubiquitylation cascade. A Ub activating enzyme (E1) forms a reactive thioester with the C-terminus of a Ub molecule under consumption of ATP. In a second step, the activated Ub molecule is transferred to an active site cysteine of a Ub conjugating enzyme (E2). Subsequently a Ub ligase (E3) recruits charged E2 complexes and client proteins and mediates the conjugation of Ub to the target. Repetition of the ubiquitylation reaction results in the assembly of Ub chains on substrates.

1.3 The ubiquitin code

Ub modifications come in different shapes, which all affect client proteins in a distinct manner. In the recent years, progress in deciphering this Ub-code has been made to assign individual cellular functions to distinct types of Ub modifications [8]. Mono-ubiquitylation of clients controls their cellular localization and binding to other proteins, which modulates their activity [21, 22]. Some histones, for example, are regulated by post-translational modification with mono-Ub. Mono-ubiquitylation of histone H2A results in

silencing of gene expression and modification of histone H2B with mono-Ub is involved in the signaling cascade of homologous recombination upon DNA double strand breaks [23–25]. Multiple mono-ubiquitylation was also observed on proteins, which mostly causes degradation of the respective protein by the 26S proteasome or functional inactivation [26, 27]. Most importantly, Ub contains seven lysine residues and six of them are exposed on its surface (figure 1.2 a). These lysine residues themself can serve as target sites for Ub conjugation. Homogenous Ub chains differ in their abundance within cells with K48- and K63-linked chains making up the predominant forms and other species being only present in minor amounts [28–30]. The topology of Ub chains formed through linkages of different lysine residues are distinct in their conformation (figure 1.2 b,c).

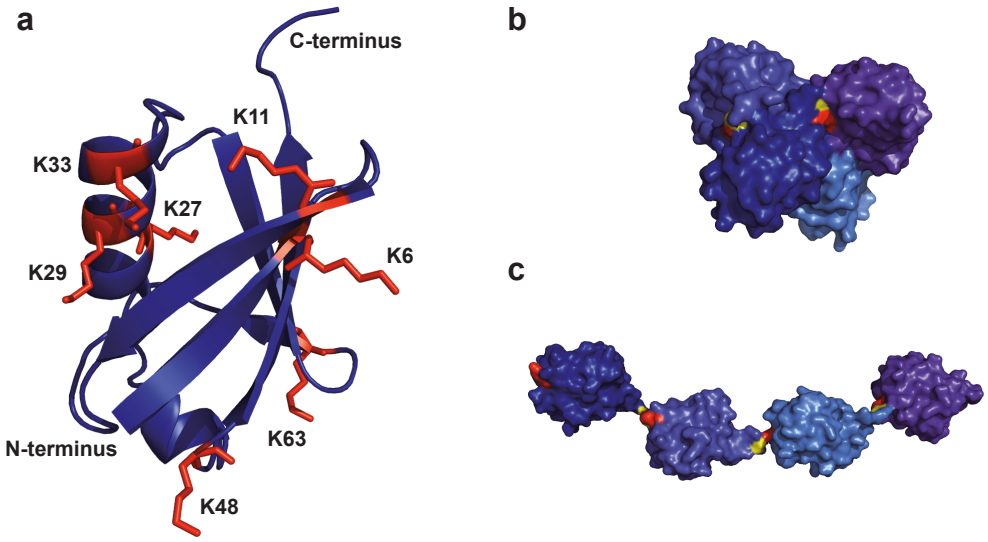

Figure 1.2 – Structure of single Ub and Ub chains. (a) Crystal structure of Ub with indicated C- and N-terminus. Lysine residues are highlighted in red (PDB ID: 1UBQ). **(b)** Crystal structure of a K48-linked tetra Ub polymer. The C-terminal glycine (yellow) and lysine 48 residue (red) are highlighted. (PDB ID: 2O6V) **(c)** Crystal structure of a K63-linked tetra Ub polymer. The C-terminal glycine (yellow) and lysine 63 residue (red) are highlighted (PDB ID: 3HM3). Structural figures were prepared using PyMOL [31].

K48-linked Ub chains, for example, adopt a compact structural arrangement where the single Ub molecules interact through a hydrophobic patch around

isoleucine 44 [32–34]. This closed conformation masks several putative interactions sites for UBD proteins. K48-linked Ub chains are mainly mediating protein degradation through the Ub proteasome system (UPS) [35, 36]. Similar conformations have been observed for K6-, K11- and K33-linked Ub species [37–40]. However, all structural arrangements of these di-Ub molecules vary in their conformation, which most likely accounts for their distinct functions within cells. K11-chains, for example, play an important role in cell cycle regulation in higher eukaryotes [41]. K6-linked Ub chains are less-well studied but recent findings indicate an involvement in mitochondrial homeostasis [42, 43] and K33-linked chains are suggested to take part in post-Golgi membrane trafficking [44]. On the contrary, Ub chains linked through lysine 29 and 63 display an open conformation, which results in a highly flexible and extended structure [39, 45–49]. Interaction sites on the surface of Ub are easily accessible in these polymers. K63-linked Ub chains are involved in several cellular processes as for example DNA repair, membrane protein transport and signal transduction [50]. In most cases K63-linked chains serve as scaffold for protein binding during these processes. The physiological role of K29-linked chains remains elusive but some experiments propose an involvement in epigenetic regulation and protein degradation [51, 52]. Ub chains, which are linked through lysine 27, are the least-well studied Ub polymers and no structure is available to date. K27 is buried within the Ub conformation (figure 1.2 a). Thus, linkage assembly would require some conformational rearrangements within the molecule [53]. Nevertheless, recent findings implicate that K27-linked Ub chains serve as scaffold during the DNA damage response similar to K63-linked Ub polymers [1]. It was shown that Ub chains are also assembled through linkages on the N-terminus of the Ub molecule (Met1-linked Ub chains) [53]. The resulting chains exhibit a linear conformation similar to K63-linked polymers that are involved in the regulation of inflammation and the immune response in higher eukaryotes [54, 55]. Corresponding to this variety of Ub chain geometries, there is a large number of UBDs, which specifically decode the conformational status of Ub polymers [56].

The biological relevance of homogenous assembled Ub chains is well established both *in vitro* and *in vivo*. In contrast, any significance of Ub chains

containing heterogeneous linkage types as well as branched K48- and K11-linked Ub chains remains to be shown. Initial experiments suggest a function of branched Ub chains at the Anaphase Promoting Complex (APC), which results in enhanced substrate recognition by the 26S proteasome [57, 58]. Recent findings demonstrate that Ub itself is post-translationally modified by phosphorylation and acetylation, which substantially expands the Ub code [1]. This new kind of modification might account for an additional layer of regulation in the Ub system.

1.4 Non-canonical ubiquitylation

In most cases Ub linkages are conjugated to ε-amino groups of lysine side chains within target proteins. However, in recent years several new "atypical" Ub acceptor sites were identified (figure 1.3) [59]. The N-termini of proteins harbor a reactive amino group similar to the one in a lysine side chain. N-terminal ubiquitylation was first identified at MyoD and subsequently shown for several other proteins [60, 61]. This non-canonical ubiquitylation event is not only important for the degradation of naturally occurring lysine-free proteins but also of some proteins, which harbor internal lysine residues [60, 62]. The reason why some proteins are ubiquitylated predominantly at their N-termini remains elusive. This modification might represent an adaptation to ensure the robust degradation of structural distinct proteins by one E2-E3 pair [63]. Interestingly, N-terminal ubiquitylation competes with N-terminal acetylation of proteins and thereby might create a new level for regulation of protein ubiquitylation and degradation [64, 65]. Besides the N-terminal amino group of proteins, other amino acids as serine, threonine and cysteine residues are implicated in being acceptor sites for Ub molecules. The side chains of these amino acids expose a nucleophile, which can attack the Ub thioester bond at the active site of the E2. Thioester bonds of cysteine residues and Ub molecules were shown to be relatively stable in cells thereby contradicting the claim that such linkage types would be rapidly dissociated in the reducing environment of the cytoplasm [66]. Ubiquitylation of cysteine residues has been reported for a couple of proteins. The peroxisomal membrane signal receptor Pex5, for example, is ubiquitylated at a conserved cysteine residue during translocation of proteins through the

peroxisomal membrane [67]. In most other cases cysteine ubiquitylation mediates degradation of the modified protein [68–72]. Targeting of cysteine residues for ubiquitylation might contribute for enhanced protein turnover during cell cycle events as it was proposed for the degradation of the transcription factor Ngn2 in mitosis [65]. Ubiquitylation of hydroxylated amino acids like serine and threonine residues was recently shown to initiate proteolysis of several proteins [68–70, 73]. TRCα, for example, is assumed to be ubiquitylated at its cytoplasmic tail involving serine residues, which in turn initiates degradation of the receptor [74]. Moreover, ubiquitylation of the non-secreted immunoglobulin light chain NS-1 was significantly diminished upon treatment with NaOH under wt conditions and only mutation of all lysine, serine and threonine residues significantly stabilized the protein [75]. Thus, ubiquitylation of hydroxylated amino acids seems to have a role in initiating proteolysis.

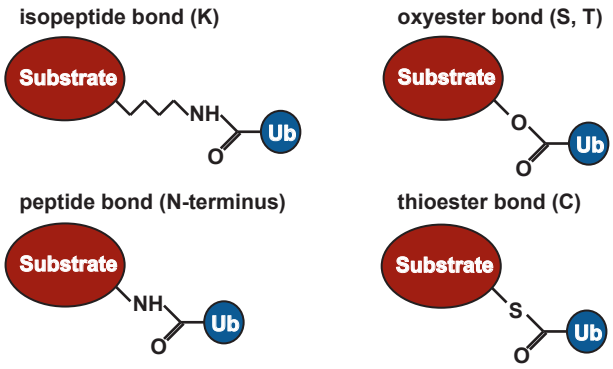

Figure 1.3 – Possible linkage types between Ub and proteins. The C-terminus of Ub can be covalently linked to several amino acids as lysine residues but also cysteine, serine and threonine residues and the N-terminus of proteins.

It is not known, whether certain proteins are specifically marked with Ub on hydroxylated amino acids to initiate their degradation or if such conjugations can only be observed when suitable lysine residues are not present on the client. Furthermore, most studies only indirectly indicate an involvement of other amino acids besides lysine during ubiquitylation or solely investigate modifications of lysine residues. Especially, cysteine, serine and threonine ubiquitylation still lack direct evidence and also the E2 enzymes catalyzing

such Ub conjugation are not identified to date. Summing up, it can be stated that non-canonical ubiquitylation occurs within cells. However, frequency and physiological relevance of such ubiquitylation events still need to be determined.

1.5 Ubiquitin conjugating enzymes

Ub conjugating enzymes (E2s) are often called "Ub carriers". Despite this name, they do not constitute passive components in the ubiquitylation reaction but play an active role in defining the length and conformation of the Ub chain. All E2 enzymes contain a Ub conjugating (UBC) domain, which harbors the catalytically active cysteine residue (figure 1.4) [76]. This domain folds into a compact structure of four α-helices, which surround a four-stranded anti-parallel β-sheet structure [77–79]. The majority of E2 enzymes exhibit a highly conserved HPN motif, which has an important structural role in organizing residues in close proximity of the active site cysteine (figure 1.4) [80, 81]. Furthermore, acidic "gateway" amino acids (UbcH5: asparagine 117, figure 1.4) are supposedly involved in activation of the attacking lysine residue during ubiquitylation [82–84]. E2 enzymes interact with the Ub activating enzyme (E1) to get charged with Ub [12]. A functional E1-E2 complex can be only established when the E1 enzyme itself is loaded with Ub. This event induces conformational changes within E1 that in turn make the E2 binding site accessible [85–87]. Charged E2 enzymes bind to E3 ligases to transfer Ub onto substrates. Some E2 enzymes specifically interact with only one appointed E3 enzyme whereas others display high promiscuity towards the selection of E3 ligases [13]. Association of E2 enzymes to ligases involves the α-helix 1 at the N-terminus as well as loops 4 and 7 of the E2 enzyme and only slight differences within these areas account for the specificity of the interaction [88–91]. Because E1 and E3 enzymes occupy overlapping docking sites, the E2 enzymes commit several rounds of binding and dissociation during Ub chain synthesis (figure 1.4) [92, 93].

Formation of Ub polymers starts with the attachment of the first Ub molecule to a target site within a client. This process is called Ub chain initiation or priming. Subsequently, additional Ub moieties are conjugated to this substrate-

linked Ub, which is termed chain elongation. Some E2 enzymes, like yeast Cdc34, catalyze both steps during client ubiquitylation [94]. However, both ubiquitylation reactions display differences in their mechanistic details. Thus, it has been postulated that some E3 ligase employ two E2 enzymes to catalyze both steps independently during chain assembly. *In vitro* studies on the Anaphase Promoting Complex (APC) for example, showed that the complex employs Ubc4 for the initial attachment of Ub to substrate proteins, while Ubc1 catalyzes subsequent extensions with homogeneous K48-linked Ub chains [95]. Chain elongating E2 enzymes evolved structural features to specifically recognize one lysine residue within the Ub molecule, which ensures the rapid synthesis of homogenous Ub chains [96]. This specificity is often a self-contained characteristic of the Ub conjugating enzyme that is not influenced through binding to its cognate E3 ligase [97, 98]. In contrast, chain initiating E2 enzymes are much more promiscuous in the selection of conjugation sites, which enables them to initiate ubiquitylation on many different substrates [96].

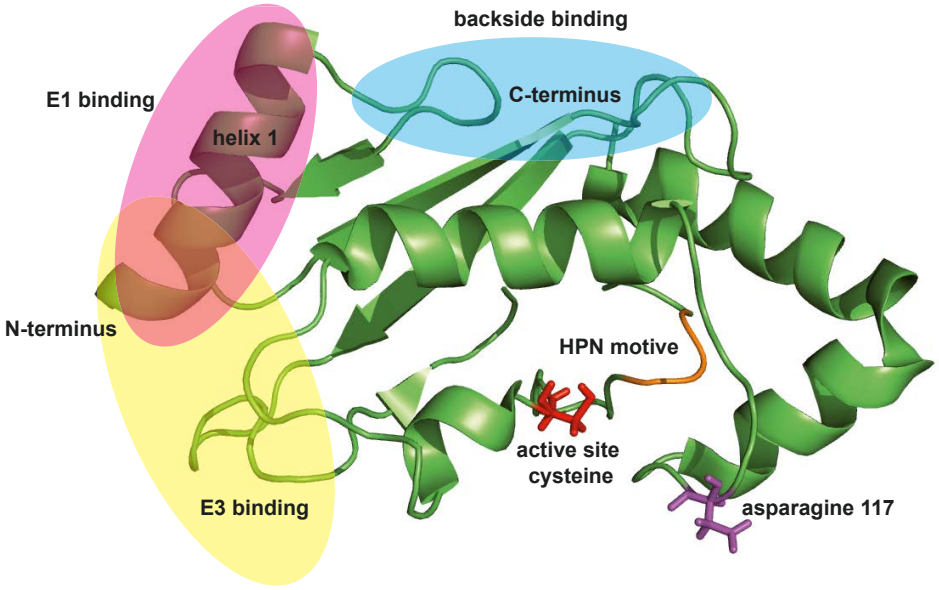

Figure 1.4 – Conserved structure of Ub conjugating enzymes. Structure of the E2 UbcH5 with highlighted binding sites (E3 binding: yellow; E1 binding: pink; Ub backside binding: cyan) and important catalytic amino acids (active site cysteine: red; HPN motive: orange; asparagine 117: purple). The figure was adapted from Stewart *et al.* [15]. Structural depictions were prepared using PyMOL [31].

The catalytic activity of E2 enzymes can be regulated in multiple ways. It was demonstrated, for example, that non-covalent binding of Ub to a backside interaction site on the E2 enhances activity towards chain synthesis (figure 1.4) [99, 100]. Paradoxically, some E2 enzymes seem to be negatively affected in their ubiquitylation activity by a similar binding event [101]. Consequently, backside binding of Ub can have different impacts on E2 functionality most likely depending on individual structural properties. Accessory factors of E2 enzymes can further regulate their activity and enhance chain assembly processivity [13]. Modulation of the activity of the E2 enzyme Ubc7 by its co-factor Cue1 is an important example for such a regulatory mechanism, which is described in detail in section 1.9. Several E2 enzymes were reported to ubiquitylate themselves and thereby modulate their activity [102, 103]. Summing up, it is evident that E2 enzymes are key players during ubiquitylation and take part in several steps of the reaction.

1.6 RING-type E3 ligases

RING (Really Interesting New Gene) domain containing E3 ligases represent the most abundant class of Ub ligases [16]. The structural characteristics, which are shared by all these ligases, comprise a cysteine residue containing domain that adopts a conserved cross brace arrangement, which is stabilized by two zinc ions (figure 1.5 a) [104]. This structure serves as a docking site for charged E2 enzymes and stimulates the transfer of Ub to client molecules [105]. Some RING domains need to dimerize to be functionally active [105–107]. Structurally and functionally related to RING domains are so-called U-box domains, which obtain their fold based on a hydrophobic core and the interaction of polar and charged amino acids, but do not rely on zinc ions for structural stabilization (figure 1.5 b) [108]. The most important feature of RING domains is their ability to bind E2 enzymes charged with Ub. This interaction is facilitated by loop 1 and 2 as well as the major α-helix 1 of the RING domain [88, 91, 109, 110]. Importantly, RING domains exhibit a much higher affinity for charged than for uncharged E2 enzymes, because the Ub molecule on the E2 is part of the interaction surface [82, 83]. Ub transfer is facilitated by the reduction of conformational freedom of the E2 bound Ub

moiety: The C-terminus of the Ub molecule is positioned by the RING domain in a conserved groove of the E2 enzyme, which presumably favorably orients it for reaction with an attacking lysine residue [111]. Consequently, the rate of thioester hydrolysis is increased by restricting the flexibility of the bound Ub moiety [112]. Some RING E3 ligases harbor additional domains, which interact with their cognate E2 enzymes and thereby manipulate their activity [113, 114].

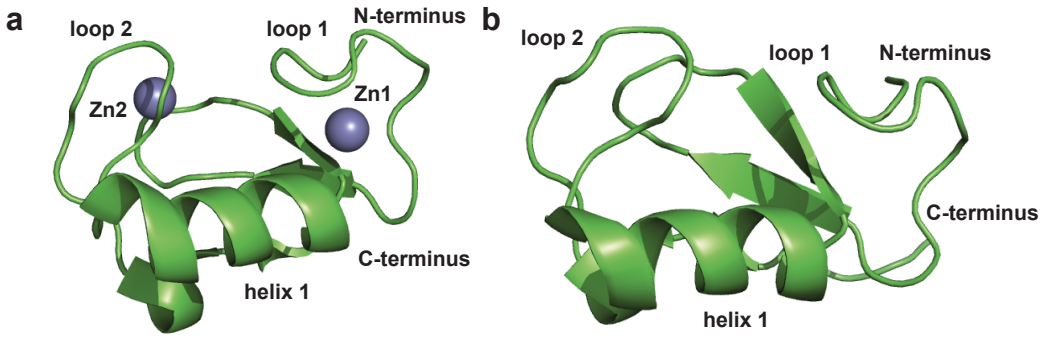

Figure 1.5 – Structures of RING and U-box domains. (a) Representation of the TRAF6 RING domain with highlighted loops and central helix 1 (PDB ID: 3HCS). Coordination of two zinc ions stabilizes the cross brace fold generating a platform for E2 binding. **(b)** U-box domain of Prp19 with highlighted loops and central helix 1 (PDB ID: 2BAY). Electrostatic interactions stabilize the conformation instead of zinc ions. Structural figures were prepared using PyMOL [31].

1.7 Protein quality control

To maintain cellular homeostasis, it is mandatory to control protein maturation by regulating translation and folding [115]. Dysfunction in this processes are associated with the onset of human disorders as Alzheimer's or Parkinson's disease, but also several other illnesses are linked to a disturbed proteome [116, 117]. Hence, cells evolved an elaborate protein quality control (PQC) apparatus to ensure the integrity of its proteome [118]. PQC processes supervise protein synthesis, assembly and disassembly of protein complexes, trafficking, transport to different cellular compartments and function of organelles [115]. During maturation, proteins fold into their native three-dimensional structure

to be functionally active. Because polypeptide chains can adopt a large number of different conformations and the native fold depends on the cooperation of lots of weak non-covalent interactions, this process is error-prone [119].

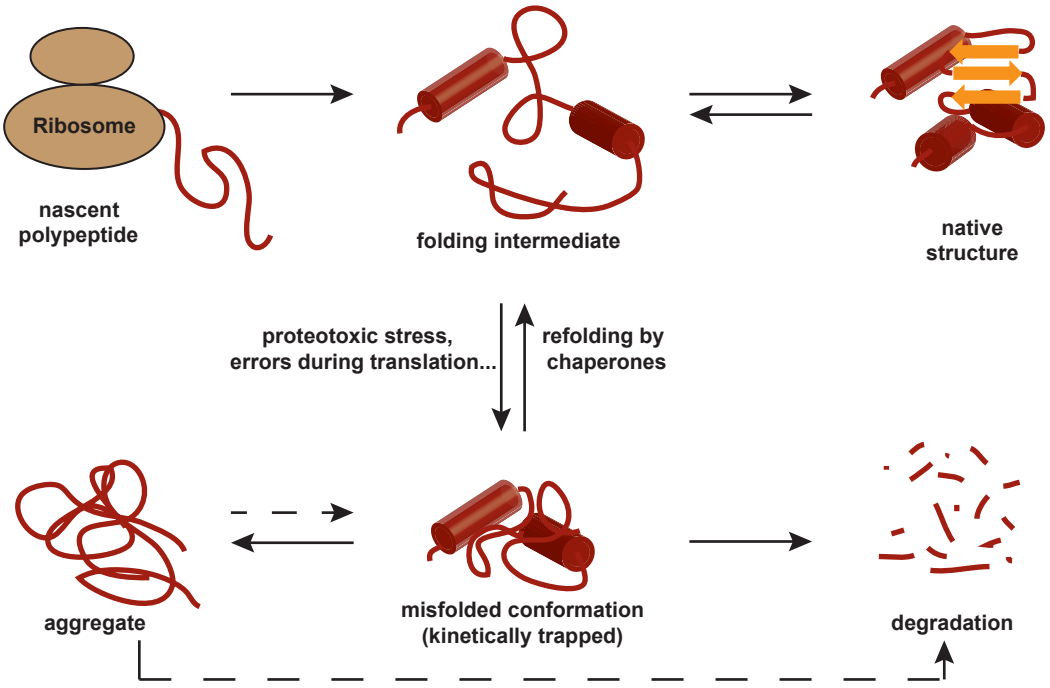

Figure 1.6 – Overview of protein folding and aggregation. Proteins fold during and after translation at the ribosome by passing through several intermediate conformations until they reach their native three-dimensional structure. Due to proteotoxic stress and errors during transcription and translation, misfolded conformations can occur. These species might be kinetically trapped and cannot reenter the productive folding pathway. Because these conformers tend to aggregate, which are potentially harmful for cells, the protein quality control systems ensure their clearance. Chaperones rescue such protein conformations by initiating their refolding and irreversibly misfolded proteins are degraded. The figure was adapted from Tyedmers *et al.* [120].

A typical protein passes several intermediate states until it reaches its final native structure (figure 1.6). In some instances such intermediates represent kinetically trapped species that cannot reenter the productive folding cycle [120]. Errors during transcription and translation, for example, might result in amino acid substitutions, which in turn cause misfolding of the protein. Additionally,

stress conditions such as reactive oxygen species, heat and radiation can also cause perturbations of native protein conformations [121]. Aberrantly folded protein species usually expose hydrophobic surfaces, which are normally buried in their native structure. Hence, these species tend to form aggregates, which eventually leads to cell death [122, 123]. To minimize the population of misfolded proteins, chaperones support newly translated polypeptides during maturation but also promote the refolding of proteins with aberrant conformations [119]. Irreversibly malfolded proteins are cleared from cells by protein degradation mechanisms [124].

1.8 Cdc48 and the 26S proteasome

A major protein degradation apparatus in eukaryotes is the Ub proteasome system. Substrates of this pathway are recognized by E3 quality control ligases and subsequently modified with K48-linked poly-Ub chains. Deubiquitylating enzymes are suggested to counteract these Ub ligases to control the amount of degraded protein species [125]. Hence, only protein conformers, which are stably recruited to E3 ligases, would be decorated with a Ub signals, which initiates their degradation. Cdc48, a AAA-ATPase, acts as segregase in the Ub proteasome pathway by extracting ubiquitylated clients from protein complexes, membranes or chromatin [126]. In complex with its co-factors Rad23 and Dsk2, Cdc48 transfers the ubiquitylated target proteins to the 26S proteasome for degradation [127, 128]. The 26S proteasome is a huge protein complex with a molecular weight of around 2.5 MDa [129, 130]. It is composed of a 20S core complex and a regulatory 19S cap unit. The core of the proteasome harbors the proteolytic activity, which cleaves peptide linkages. The catalytic center of the proteasome is shielded from the cytoplasm to prevent unspecific breakdown of proteins. Access to the catalytic core is regulated by the cap complex, which consists of a lid and a base segment. Rpn proteins of the lid recognize ubiquitylated proteins, deubiquitylating enzymes cleave the Ub moieties for recycling purposes and AAA-ATPases of the base unfold target proteins, which allows their insertion into the core subunit. K48-linked tetra Ub species were thought to be the minimal Ub signal, which is recognized by the proteasome and initiates protein degradation [131]. However, recent

findings indicate that also other chain linkage types as well as multiple mono-ubiquitylation can efficiently target client proteins for proteasomal degradation [57, 132]. Consequently, a "ubiquitylation threshold" model was proposed in which the amount of Ub molecules on a protein rather than the nature of the Ub linkage is the critical factor for recognition by the 26S proteasome [1]. Due to the activity of deubiquitylating enzymes, only stably and heavily modified proteins would be transferred to the proteasome, which would prevent degradation of falsely ubiquitylated protein species.

1.9 The Doa10 Ub ligase complex

Yeast Doa10 is a major Ub ligase of the endoplasmic reticulum and the nucleus (figure 1.7) [133, 134]. It facilitates degradation of misfolded proteins during quality control but also mediates regulated turnover of short-lived proteins such as transcription factors. The Doa10 protein is embedded into the ER- and the inner nuclear membrane by 14 trans-membrane segments and exposes an N-terminal RING-CH domain into the cytoplasm [135]. Substrates of Doa10 mainly encompass integral-membrane proteins and soluble nuclear and cytosolic proteins [136, 137]. It is not clear, how Doa10 engages substrate proteins. Recently, it was demonstrated that the cytosolic conserved C-terminus of the ligase is mandatory for ubiquitylation of a subset of clients and thus might be involved in substrate binding [138]. Furthermore, Hsp70 and Hsp40 chaperones are implicated to play a role during recruitment of target proteins but specific data on this topic are not available at the moment [137, 139, 140].

Genetic data imply that Doa10 teams up with two Ub conjugating enzymes, Ubc6 and Ubc7, for substrate ubiquitylation [141]. Ubc7 is known to catalyze the formation of K48-linked Ub chains [142]. The catalytic core domain of this soluble E2 harbors an atypical acidic loop, which presumably accounts for the catalytic propensities of this enzyme [143]. The activity of Ubc7 is tightly regulated by its binding partner Cue1. This integral protein of the ER recruits Ubc7 to the ERAD ligases Doa10 and Hrd1 [144]. In addition, binding to Cue1 initiates a structural rearrangement in Ubc7 and thereby activates its chain elongation activity [145, 146]. Furthermore, Cue1 positions Ubc7 at

the end of the Ub chain, which favors the addition of further Ub molecules to the polymer [147]. Ubc7, which is not bound to Cue1, auto-ubiquitylates itself presumably on its active site cysteine, which initiates its proteolysis [148]. This control mechanism ensures that Ubc7 is only active when recruited to the ER membrane, where it is part of three ligase complexes. Besides being a component of the Doa10 complex, Ubc7 is also found at the Hrd1 ligase, which mediates degradation of ER luminal and integral-membrane proteins, and as recently suggested at the Asi complex in the inner nuclear membrane mediating ubiquitylation of transcription factors [149, 150].

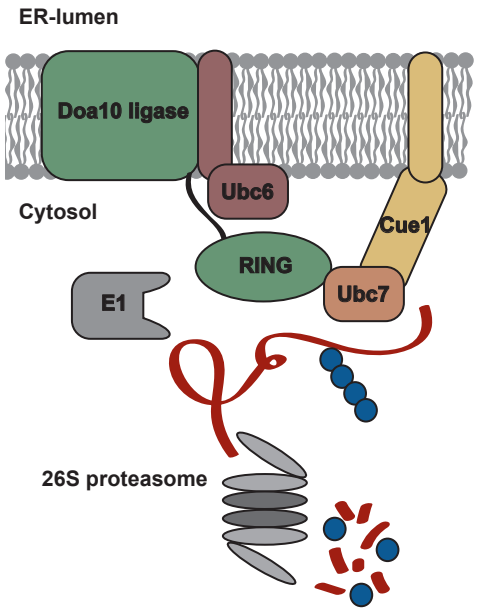

Figure 1.7 – The Doa10 ligase complex. The Doa10 Ub ligase is an integral membrane protein residing in the ER- and inner nuclear membrane with a cytosolic N-terminal RING domain. The ligase employs two E2 enzymes: Ubc6 and Ubc7. Both enzymes are required for Doa10-mediated substrate proteolysis.

In contrast to Ubc7, the ubiquitylation capacity of Ubc6 and its role during Doa10-mediated substrate ubiquitylation remain elusive to date. Knockout of *UBC6* as well as its overexpression results in diminished Doa10-mediated substrate proteolysis [151]. Ubc6 integrates into the ER-membrane through a carboxy terminal trans-membrane anchor with the UBC domain facing the cytosol [151]. The E2 is a short-lived protein, which is constantly degraded

in dependency of its own activity as well as of Ubc7 and Doa10 [152]. The region between the catalytic core domain (UBC) and the trans-membrane segment is termed linker area and transfers instability when fused to other proteins. Besides being part of the Doa10 ligases, it was reported that Ubc6 associates with the Asi complex in the inner nuclear membrane [153]. However, a specific function at this complex was not shown to date. Furthermore, Ubc6 was implicated to participate in the ubiquitylation of CPY*, an ER-luminal Hrd1 ligase substrate [154]. However, detailed data on the role of Ubc6 at the Hrd1 ligase are not available.

1.10 Aims of the thesis

In contrast to other RING-type Ub ligases, which typically co-operate with a single E2 enzyme for substrate ubiquitylation, Doa10 employs two of such enzymes, Ubc6 and Ubc7. Remarkably, only a balanced activity of both enzymes at the ligase ensures efficient substrate processing: Overexpression of *UBC6* impairs the degradation of Doa10 client proteins to a similar extent than observed in cells lacking *UBC6*. The aim of this work was the functional characterization of Ubc6 and Ubc7 and their operational interplay at the Doa10 ligase. To this end two experimental strategies were designed that in combination should reveal the mechanistic details of Doa10-mediated substrate ubiquitylation.

On the one hand a powerful *in vitro* assay should be developed to investigate the enzymatic properties of Ubc6 and Ubc7. Using purified components, each of the E2 enzymes in combination with the Doa10 RING-finger domain were to be investigated for their ability to synthesize Ub conjugation under defined conditions. By changing individual parameters, such as the variable combination of components or the employment of different Ub variants, such reactions allow the detailed investigation of the catalytic propensities of E2 enzymes. However, the significance of the *in vitro* approach is apparently limited because only the cytosolic soluble parts of the involved membrane-bound proteins could be studied.

Hence, Ubc6 and Ubc7 were also to be investigated in intact yeast cells to

review the results from the *in vitro* work. Studies on the degradation as well as the ubiquitylation pattern of selected client proteins in strains lacking individual components of the Doa10 degradation pathway would serve to characterize the function of each factor in more detail.

The results of both experimental strategies promised to reveal a comprehensive picture, on how the combined activity of two highly specialized E2 enzymes ensures the efficient poly-ubiquitylation of the highly heterogeneous substrate pool of the Doa10 Ub ligase.

2 | Material and methods

2.1 Material

2.1.1 Chemicals

Chemicals and reagents applied in this thesis, unless otherwise noted, were purchased from Sigma, VWR and Roth. Restriction enzymes were purchased from New England Biolabs (NEB). Buffer solutions were prepared with ddH_2O, which was deionized with a Milli-DI® system (Millipore).

2.1.2 Antibodies

Purchased primary and secondary antibodies as well as primary antibodies manufactured in the laboratory of Prof. Sommer are listed in table 2.1.

Table 2.1 – Antibodies applied in this thesis

Antibody	Reference
Primary antibodies	
Monoclonal α-Ub (P4D1), mouse	Santa Cruz Biotechnology
Monoclonal α-FLAG, mouse	Sigma (F3169)
Monoclonal α-HA, mouse	Sigma (H9658)
Monoclonal α-CPY, mouse	Thermo Fischer Scientific (A6428)
Monoclonal α-GFP, mouse	Living colors (JL-8)
Polyclonal α-GFP, rabbit	Life Technologies (A11122)
Polyclonal α-Myc, rabbit	CST (71D10)
Polyclonal α-Sec61, rabbit (214)	Biederer *et al.* [144]
Polyclonal α-Cue1, rabbit (259)	Biederer *et al.* [144]

Polyclonal α-Doa10, rabbit (250)	Bagola *et al.* [142]
Polyclonal α-Ubc6, rabbit (120-3)	Walter *et al.* [152]
Polyclonal α-Ubc6, rabbit (286)	Weber *et al.* [155]
Polyclonal α-Ubc7, rabbit (277)	Neuber *et al.* [156]
Polyclonal α-Cdc48, rabbit (282)	Neuber *et al.* [156]
Polyclonal α-Sbh2, rabbit (24-54)	Finke *et al.* [157]
Secondary antibodies	
Polyclonal α-mouse-IgG HRP-conjugated, rabbit	Sigma (A9044)
Polyclonal α-rabbit-IgG HRP-conjugated, goat	Sigma (A0545)
Polyclonal α-rabbit-IgG IRDye®800CW-conjugated, goat	LI-COR

2.1.3 Yeast strains

All yeast strains used in this study are haploid descendants of DF5, which has the following genotype: *MATa/alpha trp1-1(am)/trp1-1(am) his3-Δ200/his3-Δ200 ura3-52/ura3-52 lys2-801/lys2-801 leu2-3,-112/leu2-3,-112* [5]. Genotype variants of yeast strains are listed in table 2.2.

Table 2.2 – Yeast strains with relevant genotype applied in this thesis

Denotation	Genotype	Reference
YTX949	*prc1-1*	Bagola *et al.* [142]
YTX996	Δ*ubc6::HIS3, prc1-1*	Weber *et al.* [155]
YTX154	Δ*ubc7::LEU2, prc1-1*	laboratory of Prof. Sommer
YAW021	$Ubc7_{C89S}$*, prc1-1*	this study
YBM74	Δ*doa10::kanMX6*	Birgit Meusser
YTX112	Δ*ssh1::HIS3*	Weber *et al.* [155]
YTX113	Δ*ssh1::HIS3,* Δ*ubc7::LEU2*	Weber *et al.* [155]

YTX131	Δ*ssh1::HIS3,* Δ*ubc6::LEU2*	Weber *et al.* [155]
YAW032	Δ*ssh1::HIS3,* Δ*doa10::kanMX6*	Weber *et al.* [155]
YTX127	Δ*ssh1::HIS3,* Δ*sbh2::TRP1*	Weber *et al.* [155]
YTX126	Δ*ssh1::HIS3,* Δ*sbh2::TRP1,* Δ*ubc7::LEU2*	Weber *et al.* [155]
YAW065	Δ*ssh1::HIS3,* Δ*sbh2::TRP1,* Δ*ubc6::HIS3*	Weber *et al.* [155]
YAW067	Δ*ssh1::HIS3,* Δ*sbh2::TRP1,* Δ*doa10::kanMX6*	Weber *et al.* [155]
YAW073	Δ*ssh1::HIS3, rpt4R*	Weber *et al.* [155]
YAW074	Δ*ssh1::HIS3,* Δ*doa10::kanMX6, rpt4R*	Weber *et al.* [155]
YAW076	Δ*ssh1::HIS3,* Δ*ubc6::HIS3, rpt4R*	Weber *et al.* [155]
YAW077	Δ*ssh1::HIS3,* Δ*ubc7::LEU2, rpt4R*	Weber *et al.* [155]
YAW003	*TEF2-doa10::NatNT2, prc1-1*	this study
YUL26	*Doa10-13×Myc::HIS3*	Uwe Lenk
YON26	$Doa10_{C93S}$-*13×Myc::HIS3*	Oliver Neuber

2.1.4 Plasmids

Plasmids applied in this thesis are listed in table 2.1.4 with encoding insert and plasmid backbone. For yeast expression plasmids, inserts were under control

of the corresponding endogenous promoter, unless otherwise noted. Plasmids pTR990, pTR1646 and pTR1543 were gifts from Tommer Ravid [155, 158] and plasmid pTX481 from Cynthia Wolberger [159].

Table 2.3 – Plasmids applied in this thesis

Denotation	Backbone	Encoded proteins	Reference
		Bacterial expression plasmids	
pTX249	pGEX-6p1	Ubc7 (2-165)	Bagola *et al.* [142]
pTX327	pGEX-6p1	Doa10R (2-125)	Bagola *et al.* [142]
pTX352	pQE60	Ubc6ΔTM-His_6 (1-230)	Weber *et al.* [155]
pTX401	pQE60	$Ubc6_{C87S}$ΔTM-His_6 (1-230)	Weber *et al.* [155]
pTX410	pGEX-6p1	Cue1ΔTM-His_6 (24-203)	Bagola *et al.* [142]
pTX481	pET21d	Uba1-His_6	Berndsen *et al.* [159]
pAW039	pGEX-6p1	Ubc6ΔTM (2-230)	Weber *et al.* [155]
pAW040	pGEX-6p1	Ubc6ΔL (2-164)	this study
pAW128	pGEX-6p1	$Ubc6_{S196A}$ΔTM (2-230)	Weber *et al.* [155]
pAW140	pGEX-6p1	$Ubc6_{Y66A}$ΔTM (2-230)	this study
pAW133	pGEX-6p1	UBE2J2ΔTM-HA_3 (1-235)	Weber *et al.* [155]
pMD008	pGEX-6p1	Yeast Ub_{S20C}	Bagola *et al.* [142]
pAW101	pGEX-6p1	$Doa10R_{I41A}$ (2-125)	Weber *et al.* [155]
pAW102	pGEX-6p1	$Doa10R_{R43A}$ (2-125)	Weber *et al.* [155]
pAW103	pGEX-6p1	$Doa10R_{W73A}$ (2-125)	Weber *et al.* [155]
pAW074	pGEX-6p1	Ubc6ΔK11 (2-230)	this study
pAW097	pGEX-6p1	$Doa10R_{K119R}$ (2-125)	this study
pTR1543	pET14	FLAG-Ub	Cohen *et al.* [158]
		Yeast expression plasmids	
pAW123	pRS416	Sbh2	Weber *et al.* [155]
pAW124	pRS416	$Sbh2_{K48R}$	Weber *et al.* [155]
pAW125	pRS416	$Sbh2_{K15R,\ K23R,\ K25R,\ K28R}$	Weber *et al.* [155]

pTR1646	pRS414	FLAG-Sbh2	Weber *et al.* [155]
pAW135	pRS414	FLAG-$Sbh2_{K15R,\ K23R,\ K25R,\ K28R}$	Weber *et al.* [155]
pAW027	pRS416	Ubc6	Weber *et al.* [155]
pAW028	pRS426	$Ubc6_{oe}$	this study
pAW041	pRS416	$Ubc6_{C87S}$	Weber *et al.* [155]
pAW091	pRS416	Ubc6-Linker (165-251), Cup-promoter	this study
pAW136	pRS416	$Ubc6_{Y66A}$	this study
pAW047	pRS424	Myc-Ub, CUP-promoter	Weber *et al.* [155]
pTR990	pRS317	Ub, CUP-promoter	Weber *et al.* [155]
pJU267	pRS426	$Cue1_{oe}$, $Ubc7_{oe}$	Jörg Urban
pJU287	pRS426	$Ubc6_{oe}$, $Cue1_{oe}$, $Ubc7_{oe}$	Jörg Urban
pUL038	pRS414	Deg1-GFP_2	Lenk *et al.* [160]
pAW068	pRS416	$Ubc6_{K151R}$	this study
pAW070	pRS416	$Ubc6_{K132R,\ K133R}$	this study
pAW071	pRS416	Ubc6ΔK11	this study
pAW075	pRS416	$Ubc6_{K132R,\ K133R,\ K151R}$	this study

2.1.5 Oligonucleotides

Oligonucleotides were purchased from BioTez GmbH (Berlin). Oligonucleotides used for this study are listed in table 2.1.4. Katrin Bagola designed the primer pair $Ubc6_{C87S}$fw/rev. Mismatching bases of site-directed mutagenesis primer are indicated with lowercases as well as restriction sites in gene amplification primer.

Table 2.4 – Oligonucleotides applied in this thesis; fw = forward primer, rev = reverse primer

Denotation	Description	Sequence 5' to 3'
	Primer for site-directed mutagenesis	
AW85	Ubc6 (K221R	GAAAATAATTCCAgGAgAGATGGCAgA
	K222R	GAACCTAATGATAG
	K225R) fw	
AW86	Ubc6 (K221R	CTATCATTAGGTTCTcTGCCATCTcTCc
	K222R	TGGAATTATTTTC
	K225R) fw	
AW92	Ubc6 (K188R	GATGAAACAGAAGACCCTTTTACAg
	K191R	AGGCTGCGAgGGAAAgAGTCATCTC
	K193R) rev	GTTGGAGG
AW93	Ubc6 (K188R	CCTCCAACGAGATGACTcTTTCCcTCG
	K191R	CAGCCTcTGTAAAAGGGTCTTCTGT
	K193R) rev	TTCATC
AW95	Ubc6 (K167R	GTAGAGACATTAGAAAgGAGAAgATTG
	K169R) fw	GATGAGGGGGATGCGGC
AW96	Ubc6 (K167R	GCCGCATCCCCCTCATCCAATcTTCTC
	K169R) rev	cTTTCTAATGTCTCTAC
AW143	Ubc6 (K132R	CAATTACAACATCAGACCATCAGAgGA
	K133R) fw	gGACATTAGCAAGAAATTCC
AW144	Ubc6 (K132R	GGAATTTCTTGCTAATGTCcTCcTCTG
	K133R) rev	ATGGTCTGATGTTGTAATTG
AW145	Ubc6	CTTTTCAAAATGTTAGATTCAgATTGA
	(K151R) fw	TTTTTCCGGAAG
AW146	Ubc6	CTTCCGGAAAAATCAATcTGAATCTAA
	(K151R) rev	CATTTTGAAAAG
AW175	Doa10	CCTTTTTCTTTACTACTATCCAgGAGC
	(K119R) fw	ATCTTGACATTTTTC
AW176	Doa10	GAAAAATGTCAAGATGCTCcTGGATAG
	(K119R) rev	TAGTAAAGAAAAAGG

AW198	Doa10 (I41A) fw	CCGGCGCCACCTGCCGTgcTTGTCGTG GAGAAGCTACTG
AW199	Doa10 (I41A) rev	CAGTAGCTTCTCCACGACAAgcACGGC AGGTGGCGCCGG
AW200	Doa10 (R43A) fw	CCGGCGCCACCTGCCGTATTTGTgcTG GAGAAGCTACTGAGGAC
AW201	Doa10 (R43A) rev	GTCCTCAGTAGCTTCTCCAgcACAAAT ACGGCAGGTGGCGCCGG
AW202	Doa10 (W73A) fw	GCATGAATCCTGTCTGTTGGAAgcGG TAGCTTCAAAAAATATAG
AW203	Doa10 (W73A) rev	CTATATTTTTTGAAGCTACCgcTTCCA ACAGACAGGATTCATGC
AW220	Sbh2 (K15R K23R K25R K28R) fw	GCGTATCTTGCAGaGgAGAAGACAGG CACAATCCATTaGgGAAaGgCAAGCA aGaCAAACGCCCACTTCC
AW221	Sbh2 (K15R K23R K25R K28R) rev	GGAAGTGGGCGTTTGtCtTGCTTGcCtT TCcCtAATGGATTGTGCCTGTCTTC TcCtCTGCAAGATACGC
AW222	Sbh2 (K48R) fw	CGGTGGGTCTTCAAGCTCAATTTTGa GgTTATATACGGACGAAGCC
AW223	Sbh2 (K48R) rev	GGCTTCGTCCGTATATAAcCtCAAAATT GAGCTTGAAGACCCACCG
AW227	Ubc6 (S196A) fw	GCGAAGGAAAAAGTCATCgCGTTGGA GGAAATTCTAGACC
AW228	Ubc6 (S196A) rev	GGTCTAGAATTTCCTCCAACGcGATGA C TTTTTCCTTCGC
AW241	Ubc6 (Y66A) fw	CTTTCCCGTCTGATTATCCAgcCAAACC ACCGGCTATCAG
AW242	Ubc6 (Y66A) rev	CTGATAGCCGGTGGTTTGgcTGGATAA TCAGACGGGAAAG
$Ubc6_{C87S}$fw	Ubc6 (C87S) fw	CCCAACACACGATTATcgCTTTCTATGA GTGAT
$Ubc6_{C87S}$rev	Ubc6 (C87S) rev	ATCACTCATAGAAAGcgATAATCGT GTGTTGGG

Primer for gene amplification

AW111	Ubc6 fw	cgggatccGCTACAAAGCAGGCTC
AW117	Ubc6ΔTM rev	ccgctcgagtcaACTATCATTAGGTTCTTTGC
AW118	Ubc6ΔL rev	ccgctcgagtcaTGTCTCTACATTTTCCTG
AW122	1 × Myc-Ub fw	gaattcATGGAACAAAAACTTATTTCTGAAGAAGATCTGCAGATCTTCGTCAAGACG
AW123	Ub rev	atcgatTCAACCACCTCTTAGTC
AW136	Ubc6 terminator rev	ccatcgatGTTTCTTGGTCAATACATACTC
AW163	Ubc6 linker and TM fw	ggaattcatgTTAGAAAAGAGAAAATTGGATG
AW212	Sbh2 promoter fw	cggaattcGTGCTGTAACAATAAGGC
AW213	Sbh2 terminator rev	ataagaatgcggccgcCGAAGTCGAACAAGAGG
AW238	UBE2J2 fw	ggaattcATGAGCAGCACCAGC
AW233	UBE2J2ΔTM-3×HA-tag rev	ataagaatgcggccgcTCATCAGCACTGAGCAGCGTAATCTGGAACGTCATATGGATAGGATCCTGCATAGTCCGGGACGTCATAGGGATAGCCCGCATAGTCAGGAACATCGTATGGGTAAAAGATGTTCGCCAGGGCG

2.2 Molecular biological methods

2.2.1 Polymerase chain reaction (PCR)

Polymerase chain reactions were performed with the *Expand High Fidelity PCR-System* (Roche). In a first reaction step, the DNA template was denaturized for 4 min at 95 °C, followed by a cycle with 25 to 30 repetitions: first denaturation

at 95 °C for 30 s, followed by an oligonucleotide annealing step at 50 °C for 30 s and finished with an elongation step at 68 °C for 1 min/kb. The reaction ended with a final elongation step for 10 min at 68 °C. The PCR reaction mixture had a final volume of 50 µL.

2.2.2 Site-directed mutagenesis of plasmid DNA

Point mutations were integrated into plasmid DNA with the *Pfu Ultra*^{TM} *HF* DNA polymerase (Agilent Technologies) according to the manufacturers manual *QuikChange® Site Directed Mutagenesis Kit* (Aligent Technologies).

2.2.3 Cloning, DNA purification and transformation of *Escherichia coli* with plasmid DNA

Restriction digestion of DNA was conducted with restriction enzymes purchased from New England Biolabs (NEB) according to the manufactures protocol. DNA fragments were diluted with OrangeG loading dye (5 × buffer: 0.25 % (w/v) OrangeG, 50 % (v/v) glycerol, 5 mM EDTA pH 8.0) and separated by gel electrophoresis with agarose gels (0.8-2 % (w/v) agarose in TAE buffer (40 mM Tris-HCl pH 8.2, 0.14 % (v/v) acetic acid, 1 mM EDTA)). Gels contained the fluorophore *RedSafe*^{TM} (IntRON Biotechnologies) for DNA visualization. DNA fragments were purified from gels with the help of the *Wizard® SV Gel and PCR Clean-Up Systems* (Promega). Digested and purified insert and vector DNA were ligated with the T4 DNA ligase (NEB) at 16 °C over night. The newly generated plasmid DNA was transformed into *Escherichia coli XL1-blue* cells (Aligent Technologies) by electroporation. Bacterial cells were resuspended in 0.5 mL SOC medium (2 % (w/v) Bacto^{TM} tryptone, 0.5 % (w/v) Bacto^{TM} yeast extract, 10 mM NaCl, 2.5 mM KCl, 10 mM $MgCl_2$, 10 mM $MgSO_4$, 0.2 % (w/v) glucose) after transformation and incubated for 30 min at 37 °C. Afterwards, they were plated on LB-Agar (2 % (w/v) agar-agar, 1 % (w/v) Bacto^{TM} tryptone, 0.5 % (w/v) Bacto^{TM} yeast extract, 1 % (w/v) NaCl) containing the appropriate antibiotic marker (final concentration: ampicillin 50 µg/mL, kanamycin 25 µg/mL) and incubated over night at 37 °C.

2.2.4 *Escherichia coli* cultivation, plasmid DNA purification and sequencing

Single colonies of bacteria were picked from LB-plates and cultivated in 3 mL LB-medium (1 % (w/v) Bacto^{TM} tryptone, 0.5 % (w/v) Bacto^{TM} yeast extract, 1 % (w/v) NaCl) containing the appropriate antibiotic marker (final concentration: ampicillin 50 µg/mL, kanamycin 25 µg/mL) over night at 37 °C and 200 rpm. Plasmid DNA was isolated from bacterial cells with the help of the *JetStar*^{TM} *Plasmid Purification Kit* (Genome GmbH): 2 mL bacterial over night culture were pelleted (5000 × g, 3 min) and resuspended in 150 µL solution E1 (50 mM Tris-HCl pH 8.0, 10 mM EDTA, 0,1 mg/mL RNase A (Roth)). For basic cell lysis 150 µL solution E2 (0.2 M NaOH, 1 % (w/v) SDS) were added and carefully inverted. Addition of 150 µL solution E3 (3,1 M potassium acetate pH 5.5) neutralized the basic pH from solution E2. Precipitated proteins and genomic DNA were pelleted (20,000 × g, 10 min) and the supernatant was transferred into a fresh Eppendorf tube. The plasmid DNA was precipitated with addition of 1 mL cold ethanol and pelleted (21,000 × g, 4 °C, 10 min). The supernatant was removed, the pellet dried at room temperature and subsequently suspended in 50 µL ddH_2O. The final nucleic acid concentration was determined with a NanoDrop2000 (Thermo Scientific, PeqLab Biotechnologie GmbH). Samples were analyzed by the company SourceBioScience Germany GmbH to validate the sequence of the newly generated plasmid DNA.

2.2.5 Isolation of genomic DNA from yeast cells

5 to 10 OD_{600} of exponentially growing yeast cells were harvested by centrifugation (2000 × g, 3 min) and the pellet was washed with 1 mL ddH_2O before it was resuspended in 200 µL DNA preparation buffer (10 mM Tris-HCl pH 8.0, 100 mM NaCl, 1 mM EDTA, 1 % (w/v) SDS, 2 % (v/v) Triton X-100). 200 µL phenol-chloroform-isoamyl alcohol (49.5:49.5:1) were added before cells were lyzed by vigorous shacking with glass beads. The mixture was diluted with 200 µL 1 × TE buffer (10 mM Tris-HCl pH 8.0, 1 mM EDTA) and centrifuged (21,000 × g, 10 min) for phase separation. The upper, aqueous phase was harvested and mixed with 1 mL cold ethanol. Precipitated nucleic acids were centrifuged (21,000 × g, 4 °C, 5 min) and the pellet was resuspended in 400 µL

1 × TE buffer containing 30 µg RNase A (Roth). The mixture was incubated for 10 min at 37 °C to remove precipitated RNA. Ammonium acetate (final concentration 100 mM) and 1 mL ethanol were added to precipitate the remaining DNA (21,000 × g, 4 °C, 2 min). The DNA pellet was washed with 70 % (v/v) ethanol, dried at room temperature and resuspended in 100 µL ddH_2O.

2.3 Biochemical methods

2.3.1 Preparation of yeast cell lysates

5 to 10 OD_{600} logarithmic growing yeast cells were harvested (2000 × g, 2 min) and the pellet was suspended in 100 µL lysis buffer (50 mM Tris-HCl pH 7.5, 1 % (w/v) SDS). Yeast cells were lyzed by vigorous shacking with glass beads for 2 min. 100 µL 2 × SDS sample buffer (135 mM Tris-HCl pH 6.8, 20 % (v/v) glycerol, 4 % (w/v) SDS, 0.05 % (w/v) bromophenol blue, 200 mM DTT) were added and the lysate was incubated at 65 °C for 15 min. Samples were centrifuged at 1000 × g for 5 min to separate glass beads and cell debris from cell extract. The supernatant was collected and analyzed by SDS-PAGE and immunoblotting (see section 2.3.5 and 2.3.7).

2.3.2 Isolation of membranes from yeast cells

5 to 10 OD_{600} logarithmic growing yeast cells were harvested (2000 × g, 2 min) and the pellet was resuspended in 400 µL membrane preparation buffer (50 mM Tris-HCl, 5 mM EDTA, 1 mM PMSF, pH 7.5). Yeast cells were lyzed by vigorous shacking with glass beads for 2 min and the lysate was diluted with 1 mL membrane preparation buffer. To remove cell debris and glass beads, samples were centrifuged at 1000 × g for 5 min at 4 °C. The supernatant was collected and again centrifuged (20,000 × g, 10 min, 4 °C) to enrich cellular membranes. The supernatant was removed, the membrane pellet was resuspended in 50 µL 4 × urea sample buffer (200 mM Tris-HCl pH 6.8, 5 % (w/v) SDS, 0.1 mM EDTA, 8 M urea, 0.05 % (w/v) bromophenol blue, 100 mM DTT) and incubated for 20 min at 42 °C. Samples were analyzed by SDS-PAGE and immunoblotting (see section 2.3.5 and 2.3.7).

2.3.3 Non-denaturing immunoprecipitation (Co-IP) of Doa10-13×Myc variants

60 to 80 OD_{600} logarithmically growing yeast cells were harvested (2000 × g, 2 min) and washed in 4 mL cold ddH_2O containing 1 mM PMSF for protease inhibition. The following steps were all performed on ice and all used solutions contained 1 mM PMSF. The cell suspension was transferred to 15 mL *Falcon®* *tubes* and centrifuged (2000 × g, 2 min). The pellet was suspended in 1 mL Doa10 IP buffer (50 mM Tris-HCl pH 7.5, 200 mM sodium acetate, 1 mM EDTA, 10 % (w/v) glycine, 10 mM DTT) and cells were lyzed by vigorous shacking with glass beads for 3 min. The lysate was diluted with 2 mL Doa10 IP buffer and centrifuged at 1000 × g for 5 min to remove cell debris. The supernatant was again centrifuged (20,000 × g, 10 min, 4 °C) to pellet membranes. The membrane pellet was then solubilized in 500 µL solubilization buffer (Doa10 IP buffer + 5 % (v/v) digitonin) and incubated for 1 h at 4 °C under constant stirring. Afterwards, samples were centrifuged (20,000 × g, 10 min, 4 °C) to remove remaining membrane parts. The supernatant was collected and 35 µL were taken as input control and mixed with 15 µL 4 × urea sample buffer (200 mM Tris-HCl pH 6.8, 5 % (w/v) SDS, 0.1 mM EDTA, 8 M urea, 0.05 % (w/v) bromophenol blue, 100 mM DTT) and incubated at 42 °C for 20 min. The remaining supernatant was diluted 1:1 with Doa10 IP-buffer to reduce the digitonin concentration to 0.5 %. 15 µL *ProteinA-Sepharose^{TM}4FastFlow* (GE Healthcare) and 1 µL α-Myc antibody (M5546, SIGMA) were added to the mixture for Doa10-Myc precipitation and incubated over night at 4 °C under constant stirring. In a next step Sepharose^{TM} was washed 3 times with 500 µL wash buffer (50 mM Tris-HCl pH 7.5, 200 mM sodium acetate, 1 mM EDTA, 10 % (w/v) glycine, 0.5 % digitonin). After washing, 50 µL 4 × urea sample buffer were added to the dried Sepharose^{TM} and incubated for 20 min at 42 °C to elute proteins. 10 µL input as well as 10 µL eluate were analyzed by SDS-PAGE and subsequent immunoblotting (see section 2.3.5 and 2.3.7).

2.3.4 Immunoprecipitation of ubiquitylated proteins from yeast cell lysates

Doa10 substrates as FLAG-Sbh2 variants and Ubc6 variants were isolated from yeast cells overexpressing wt Ub or Myc-tagged Ub. 80 to 100 OD_{600} cells in exponential growth phase were harvested (2000 × g, 2 min, 4 °C) and washed in 4 mL cold ddH_2O containing 1 mM PMSF and 20 mM NEM. Cells were lyzed by vigorous shacking in 1 mL urea lysis buffer (6 M urea, 50 mM Tris-HCl pH 7.5, 150 mM NaCl, 1 % (v/v) SDS, 1 mM PMSF, 20 mM NEM) with glass beads for 3 min. The lysate was diluted with 9 volumes of IP dilution buffer (55 mM Tris-HCl pH 7.5, 165 mM NaCl, 5.5 mM EDTA, 1.1 % (v/v) Triton X-100, 1 mM PMSF, 20 mM NEM) and cleared from remaining cell debris by centrifugation (20,000 × g, 10 min, 4 °C). For input controls, 75 µL sample were mixed with 25 µL 4 × SDS sample buffer (250 mM Tris-HCl pH 6.8, 40 % (v/v) glycerol, 8 % (w/v) SDS, 0.05 % (w/v) bromophenol blue, 100 mM DTT) and incubated at 65 °C for 15 min. FLAG-tagged proteins were precipitated with 50 µL *ANTI-FLAG® M2 Affinity Gel* (Sigma) which was added to the lysate and incubated over night at 4 °C under constant stirring. Other proteins such as Ubc6 were isolated from cell lysate with 40 µL *ProteinA-Sepharose™ 4FastFlow* (GE Healthcare) and 2 µL specific antibody. In a next step, beads were washed 3 times with IP dilution buffer, which was followed by protein elution with 50 µL 4 × SDS sample buffer without DTT for 15 min at 42 °C. Finally, the supernatant was collected and DTT (final concentration 25 mM) was added and incubated for 15 min at 65 °C. Samples were analyzed by SDS-PAGE and subsequent immunoblotting (see section 2.3.5 and 2.3.7). When IP samples were incubated with NaOH, experiments were performed with double amount of yeast cells. The eluted protein mixture was split after the first incubation step with 4 × SDS sample buffer and NaOH (final concentration 150 mM) or the equivalent amount of ddH_2O was added together with DTT to the samples. Incubating the samples for 15 min at 65 °C removed the ubiquitylation on hydroxylated amino acids.

2.3.5 SDS polyacrylamide gel electrophoresis (SDS-PAGE)

Proteins were separated based on their molecular weight with a discontinuous SDS polyacrylamide gel electrophoresis in LRB buffer (50 mM Tris-HCl pH, 383 mM glycine, 0.1 % (w/v) SDS) based on a protocol published by Lämmli *et al.* [161]. In a first step, proteins were concentrated in a 3 % stacking gel (3 % (v/v) acrylamide, 0.15 % (v/v) bis-acrylamide, 125 mM Tris-HCl pH 6.8, 0.1 % (v/v) SDS, 0.25 % (v/v) TEMED, 2.5 % (v/v) APS) with a voltage of 80 V for approximately 30 min. In a second step, proteins were separated in a 9 to 18 % separating gel (9-18 % (v/v) acrylamide, 0.06-0.09 % (v/v) bis-acrylamide, 500 mM Tris-HCl pH 8.8, 0.1 % (v/v) SDS, 0.25 % (v/v) TEMED, 2.5 % (v/v) APS) with a voltage between 100 V and 140 V for approximately 90 min. For direct protein detection, gels were incubated with a Coomassie staining solution (45 % (v/v) methanol, 10 % (v/v) acetic acid, 0.25 % (w/v) Coomassie Brilliant Blue R-250) for 30 min and destained with ddH_2O over night. For specific protein detection gels were applied to protein immunoblotting. Protein markers were purchased from Thermo Fisher Scientific (*PageRuler^{TM} Prestained Protein Ladder*) and New England Biolabs (*Color Protein Standard, broad range*).

2.3.6 Fluorescence scanning

Alexa488 fluorophore labeled proteins were visualized directly from SDS-PAGE gels with a fluorescence scanner (Typhoon FLA9500 Biomolecular Imager, GE Healthcare). The fluorescent dye was excited at 473 nm and emission was detected with a LBP filter (510LP).

2.3.7 Western blotting (protein immunoblotting)

For specific protein detection, separated proteins from SDS-PAGE gels were transferred on a PVDF membrane (Roth, pore size 0.45 µm) with a wet electroblotting system (tank blotting) from Hoefer®. Gels were blotted with 250 mA for 1 h to 1.5 h in western blot buffer (1.1 % (w/v) glycine, 0.24 % (w/v) Tris-Base, 25 % (v/v) methanol, 0.01 % (w/v) SDS). Membranes were incubated in 10 % skimmed milk suspended in 1 × TBT buffer (10 × TBT: 0.5 M

Tris-HCl pH 7.5, 1.5 M NaCl, 1 % (v/v) Tween 20) to reduce unspecific antibody binding to the membranes. Next, membranes were incubated with the specific antibody for the target protein in 5 % skimmed milk in 1 × TBT solution over night at 4 °C. Membranes were washed 3 times with 1 × TBT and 1 time with 1 × PBS (137 mM NaCl, 2.7 mM KCl, 10.1 mM Na_2HPO_4, 1.8 mM KH_2PO_4). Afterwards, membranes were incubated with a secondary antibody, coupled to the horseradish peroxidase (HRP), which binds to the constant part of the primary antibody, in 5 % skimmed milk in 1 × TBT for 1 h at room temperature. Membranes were again washed 3 times with 1 × TBT and 1 time with 1 × PBS. Detection of target proteins was facilitated by either using *Western Lightning® Plus-ECL* (PerkinElmer) with x-ray films (Biomax, Kodak®) or *WesternSure® ECL Substrate* (LI-COR®) with a LI-COR® Odyssey system. For protein quantification membranes were incubated with a fluorescently labeled secondary antibody and visualized with a LI-COR® Odyssey system or a Typhoon FLA9500 Biomolecular Imager (GE Healthcare). Signal intensities were analyzed with the ImageStudioLite software (LI-COR®) or the ImageQuant TL software (GE Healthcare).

2.3.8 Purification of GST-fusion proteins from *Escherichia coli* cells

GST epitope tagged proteins were expressed in *Escherichia coli BL21 Rosetta 2* cells (Novagen), which were grown in TB medium (1.2 % (w/v) Bacto^{TM} tryptone, 2.4 % (w/v) Bacto^{TM} yeast extract, 0.4 % (v/v) glycerol, 17 mM KH_2PO_4, 72 mM K_2HPO_4) at 37 °C and 150 rpm until they reached an OD_{600} of 1 to 1.5. Cultures were then cooled to 16 °C for 1 h and protein expression was induced with 0.5 mM IPTG (Roth) over night for 16 to 18 h. Cells were harvested (Sorvall RC 6+, rotor FiberLite F10-4 × 1000 LEX or rotor FiberLite F10-6 × 500y, 5000 × g, 15 min, 4 °C) and washed with cold ddH_2O. Cells were either stored at -80 °C or lyzed with high-pressure homogenization (EmulsiFlex-C5, AVESTIN Europe GmbH) in 1 × PBS buffer (137 mM NaCl, 2.7 mM KCl, 10.1 mM Na_2HPO_4, 1.8 mM KH_2PO_4) containing *cOmplete^{TM} EDTA-free* protease inhibitor (Sigma). The lysate was centrifuged (Sorvall RC 6+, SS34 rotor, 20,000 × g, 30 min, 4 °C) to remove remaining cell debris and the supernatant

was incubated with an appropriate amount of *Glutathione Sepharose^{TM} 4Fast-Flow* for 2.5 h at 4 °C under constant stirring. Afterwards, the Sepharose^{TM} was washed 6 times (10 times the volume of the used Sepharose^{TM}) with 1 × PBS buffer to remove unbound material and protease inhibitor. To elute the bound protein without the GST-tag, the Sepharose^{TM} was incubated with 3 mL 1 × PBS buffer and *PreScission Protease* (GE Healthcare) over night at 4 °C under constant stirring. The supernatant was collected and the Sepharose^{TM} was washed another 2 times with 3 mL 1 × PBS buffer to gain high amounts of cleaved protein. The supernatant was concentrated with *Amicon® Ultra Centrifugal Filters* (Merck Millipore) and stored at -80 °C. Doa10R variants were additionally purified by gelfiltration with a Superdex 75 size exclusion column (GE Healthcare) in 20 mM HEPES buffer (pH 7.5). Fractions were analyzed by SDS-PAGE and Coomassie staining and were pooled according to their content of pure Doa10R.

2.3.9 Purification of proteins with hexa histidine tags from *Escherichia coli* cells

Hexa histidine epitope tagged proteins were expressed in *Escherichia coli M15* (QIAGEN), which were grown in LB medium (1 % (w/v) Bacto^{TM} tryptone, 0.5 % (w/v) Bacto^{TM} yeast extract, 1 % (w/v) NaCl) at 37 °C and 150 rpm until they reached an OD_{600} of 1. Protein expression was induced with 0.5 mM IPTG (Roth) for 3 h at 37 °C and 150 rpm. Subsequently, cells were harvested (Sorvall RC 6+, rotor FiberLite F10-4 × 1000 LEX or rotor FiberLite F10-6 × 500y, 5000 × g, 15 min, 4 °C). The pellet was washed with cold ddH_2O and either stored at -80 °C or lyzed with high-pressure homogenization (EmulsiFlex-C5, AVESTIN Europe GmbH) in lysis buffer (50 mM NaH_2PO_4, 300 mM NaCl, 10 mM imidazole, pH 7.5) containing *cOmplete^{TM} EDTA-free* protease inhibitor (Sigma). The lysate was centrifuged (Sorvall RC 6+, SS34 rotor, 20,000 × g, 30 min, 4 °C) to remove remaining cell debris and the supernatant was incubated with an appropriate amount of *TALON® Metall Affinity Resin* (Clontech Laboratories Inc.) for 2.5 h at 4 °C under constant stirring. Afterwards, the resin was washed 3 times with cold wash buffer (50 mM NaH_2PO_4, 300 mM NaCl, 20 mM imidazole, pH 7.5). The protein was eluted with elution buffer

(50 mM NaH_2PO_4, 300 mM NaCl, 300 mM imidazole, pH 7.5) and dialyzed over night at 4 °C in dialysis buffer (50 mM Tris-HCl pH 7.5, 200 mM NaCl, 5 % (v/v) glycerin). The protein solution was concentrated with *Amicon® Ultra Centrifugal Filters* (Merck Millipore) and stored at -80 °C.

2.3.10 Lowry protein assay for protein concentration determination

Concentration of purified proteins was determined using the *DC Protein Assay* (Bio-Rad), which is based on the protein detection method by Lowry [162]. A BSA concentration gradient served as calibration series for absorption at 750 nm to determine unknown protein concentrations.

2.3.11 Absorption measurements

Cell density of bacterial and yeast liquid cultures was determined by measuring the absorption at 600 nm with a spectrometer (Ultrospec 3100 pro, Amersham Bioscience). Protein or fluorophore concentrations were determined by measuring the extinction at an appropriate wavelength (proteins: 280 nm, Alexa488: 490 nm) and by employing the Beer-Lambert law. Absorption measurements were performed at room temperature with ultra micro cuvettes for the UV spectrum (105.202-QS, Hellma) or disposable plastic cuvettes for the visible spectrum (REF 67.742, Sarstedt).

2.3.12 Circular dichroism spectroscopy (CD)

CD measurements were performed with a Chirascan spectropolarimeter (AppliedPhotophysics). A total amount of 40 µg Doa10R variant was diluted in CD buffer (100 mM NaF, 10 mM K_2HPO_4/KH_2PO_4, pH 8.5). Wavelength scans were performed at 20 °C and were repeated 3 times for each sample. Emission was recorded between 260 nm and 190 nm with a band-pass of 0.5 nm in a quartz cuvette (Hellma) with a diameter of 0.1 cm. Wavelength scans with CD buffer alone served as background control and were subtracted from all sample measurements. Obtained values were corrected with the software provided by dichroweb [163] by employing the following equation calculating the mean

residue ellipticity:

$$[\theta]_{MRE} = \frac{\theta \cdot 100}{c \cdot d \cdot N}$$

$[\theta]_{MRE}$ is the mean residue ellipticity with cm^2dmol^{-1} as unit, θ are the measured ellipticity values, c the protein concentration, d the path length of the used cuvette and N the number of amino acid residues of the measured protein.

2.3.13 Fluorescence labeling of Ub cysteine variants

The Ub variant S20C, carrying a single cysteine residue, was labeled with the Alexa488 fluorophore connected to a C5 maleimide backbone (Life Technologies). The thiol group of Ub_{S20C} was reduced with 120 nmol TCEP (Life Technologies) in 400 µL 1 × PBS (137 mM NaCl, 2.7 mM KCl, 10.1 mM Na_2HPO_4, 1.8 mM KH_2PO_4) for 10 min at room temperature. Afterwards, the reaction mixture was incubated with 4 times excess of fluorescent dye for 90 min at room temperature in the dark. The reaction was stopped with addition of β-mercaptoethanol (final concentration 10 mM). Excess amount of fluorescent dye and remaining reduction reagent were removed with 2 size exclusion purification steps using *NAP™-5 columns* (GE Healthcare) with buffer containing 50 mM Tris-HCl (pH 8.0). The eluate was concentrated with *Amicon® Ultra Centrifugal Filters* (Merck Millipore). The labeling efficiency was determined by calculating the ratio of fluorescent dye concentration (see section 2.3.11) and protein concentration, which was determined with the Lowry protein assay (see section 2.3.10).

2.3.14 *In vitro* ubiquitylation reaction

Equal amounts (3.5 µM) of purified soluble Doa10 ligase components (Ubc6ΔTM varaints, Ubc7/Cue1ΔTM, Doa10R variants) were incubated with 7.5 µM Ub and 150 nM human E1 enzyme (Uba1) in ubiquitylation reaction buffer (50 mM HEPES pH 7.5, 2.5 mM magnesium acetate, 0.5 mM DTT). The ubiquitylation reaction was started with the addition of ATP (final concentration: 4 mM,

Sigma (A9187)) and incubated for 20 min at 30 °C. Addition of 4 × SDS sample buffer (250 mM Tris-HCl pH 6.8, 40 % (v/v) glycerol, 8 % (w/v) SDS, 0.05 % (w/v) bromophenol blue, 100 mM DTT) stopped the reaction and samples were analyzed by SDS-PAGE, fluorescence scanning and immunoblotting. For time course experiments: Samples for time point 0 were collected before the addition of ATP. Ub lysine mutants Ub_{K11R}, Ub_{K48R}, Ub_{K63R} and Ub_{K0} were purchased from Boston Biochem Inc., and His_6-Ub from ENZO® life science GmbH.

2.3.15 Immunoprecipitation of Doa10R from *in vitro* ubiquitylation reactions

The ubiquitylation reaction mixture was diluted with 15 volumes of IP buffer (50 mM Tris-HCl pH 7.5, 150 mM NaCl, 5 mM EDTA, 1 % (v/v) Triton X-100, 0.1 % (w/v) SDS), which contained 15 µL *ProteinA-Sepharose^{TM}4FastFlow* (GE Healthcare) and 0.5 µL specific Doa10 antibody to precipitate Doa10R. The suspension was incubated over night at 4 °C under constant stirring. In a next step, Sepharose^{TM} was washed 3 times with 500 µL IP buffer and the Sepharose^{TM} was incubated with 25 µL 4 × SDS sample buffer (250 mM Tris-HCl pH 6.8, 40 % (v/v) glycerol, 8 % (w/v) SDS, 0.05 % (w/v) bromophenol blue, 100 mM DTT) to elute bound protein. Input samples were collected before Sepharose^{TM} was added to the reaction mixture. Samples were analyzed by SDS-PAGE and immunoblotting.

2.3.16 Purification of ubiquitylated Ubc6ΔTM from *in vitro* assays

Ubc6ΔTM was incubated with human E1 (Uba1) and N-terminal hexa histidine tagged Ub as described in section 2.3.14 in a total reaction volume of 300 µL for 16 h at 30 °C. The total reaction mixture was applied to a 1 mL *HisTrap HP column* (GE Healthcare). Bound proteins were extensively washed with 30 column volumes of wash buffer (50 mM NaH_2PO_4, 300 mM NaCl, 20 mM imidazole, pH 7.5) and eluted with an imidazole gradient (20 to 300 mM imidazole in 30 min, flow rate 1 mL/min). Fractions were analyzed by SDS-PAGE and Coomassie staining. Samples containing His_6-Ub-Ubc6ΔTM were pooled and applied to a Superdex 200 size exclusion column (GE Healthcare) in gelfiltration

buffer (20 mM HEPES pH 7.5, 150 mM NaCl) to separate His_6-Ub-Ubc6ΔTM from free His_6-Ub. Fractions containing pure His_6-Ub-Ubc6ΔTM were pooled, concentrated with *Amicon® Ultra Centrifugal Filters* (Merck Millipore) and stored at -80 °C.

2.3.17 Sample preparation for mass spectrometry analysis

Mass spectrometry sample preparation was performed by Dr. Oliver Popp from the mass spectrometry core facility (Dr. Gunnar Dittmar) of the Max Delbrück Center for molecular medicine. Proteins separated on SDS-PAGE gels were processed based on a protocol developed by Shevchenko *et al.* [164]. SDS-PAGE gel pieces were washed with 50 % ethanol in 50 mM ammonium bicarbonate and 50 mM ammonium bicarbonate in an alternating fashion. Disulfide bonds were reduced with 2.5 pmol TCEP and alkylated with 12.5 pmol chloroacetamide for 30 min at room temperature. Subsequently, samples were digested with 5 µg sequencing grade Trypsin (Promega) for 10 h at room temperature. Originated peptides were isolated with extraction buffer (80 % (v/v) acetonitrile, 20 mM acetic acid) and dried with a SpeedVac (Savant). To preserve Ub ester bonds, C18 stage tips [165] were purified under mild acidic conditions with 20 mM acetic acid and dried in a SpeedVac. Finally, peptides were dissolved in 3 % (v/v) acetonitrile in 20 mM acetic acid.

2.3.18 Liquid chromatography tandem mass spectrometry (LC-MS/MS)

Mass spectrometry analysis was performed by Dr. Oliver Popp and Dr. Gunnar Dittmar from the mass spectrometry core facility (Dr. Gunnar Dittmar) of the Max Delbrück Center for molecular medicine. Samples were measured with an LTQ^{TM} orbitrap VELOS mass spectrometer (Thermo Scientific) combined with a Proxeon nano-LC^{TM} system (Thermo Scientific). A nano-LC column (0.074 mm × 250 mm, 3 µm Reprosil C18, Dr. Maisch GmbH) was loaded with 5 µL sample and peptides were separated with a gradient (4 to 76 % acetonitrile) for 155 min applying a flow rate of 0.25 µL/min. Peptides were ionized on the proxeon and directly sprayed into the mass spectrometer. The acquisition

was done at a resolution of 60,000 with a scan range from 200 to 1700 m/z in FTMS mode to select the top 20 peaks for CID fragmentation. MS/MS scans were measured in IT mode with an isolation width of 2, the collision energy was normalized to 40 eV and the dynamic exclusion was set to 60 s. The MaxQuant software package version 1.5.2.8 was used for data analysis [166]. Carbaminomethylation was set as a fixed modification and oxidized methionine as well as acetylated amino acid termini as a variable one. To identify ubiquitylation sites a variable modification was defined including a monoisotopic mass-shift of 114.042927 Da, which corresponds to an addition of a double glycine (tryptic carboxy-terminal Ub fragment) on defined amino acids (lysine, serine, threonine and cysteine residues). An FDR of 0.01 was applied for peptides as well as proteins and the database search was performed with *Saccharomyces cerevisiae (S288c)* Uniprot database (August 2014).

2.3.19 Quantification of Ub chains by mass spectrometry

Mass spectrometry analysis for Ub chain quantification was performed by Dr. Oliver Popp and Dr. Gunnar Dittmar from the mass spectrometry core facility (Dr. Gunnar Dittmar) of the Max Delbrück Center for molecular medicine. Ub chains were quantified as published by Mirzaei *et al.* [167]. Heavily labeled peptides (Spiketides, JPT peptide technology), which are designed to resemble tryptic digested products of Ub branched peptides of certain chain linkages, were added to ubiquitylation reactions. The reactions were digested with endopeptidase LysC and Trypsin under denaturing conditions [168]. Peptides were separated on a 20 cm in-house packed C18 column (75 µm inner diameter, 3 µm Reprosil, Dr. Maisch GmbH) with a 5 % to 50 % acetonitrile gradient applying a flow rate of 250 nL/min and directly sprayed into a Q-TRAP 5500 mass spectrometer (AB Sciex). Signals of branched peptides were recorded in NRM mode and analyzed with the MultiQuant software package (AB Sciex). Statistical analysis was performed with the R software package [169].

2.4 Cytological methods

2.4.1 Cell culture of *Escherichia coli*

Bacterial cells were grown in liquid culture LB medium (1 % (w/v) Bacto^{TM} tryptone, 0.5 % (w/v) Bacto^{TM} yeast extract, 1 % (w/v)NaCl). Solid culture medium was generated by adding 2 % (w/v) agar-agar to the liquid LB medium. For plasmid selection antibiotics were added to the medium (final concentration: ampicillin 50 µg/mL, kanamycin 25 µg/mL).

2.4.2 Cell culture of *Saccharomyces cerevisiae*

Yeast cells were grown in either complete medium YPD (2 % (w/v) Bacto^{TM} peptone, 1 % (w/v) Bacto^{TM} yeast extract, 2 % (w/v) glucose, pH 5.5 adjusted with HCl) or synthetic minimal medium SD (0.67 % (w/v) yeast nitrogen base without amino acids, 2 % glucose, 20 mg/L L-Histidine, 30 mg/L L-Leucine, 30 mg/L L-Lysine, 20 mg/L L-Tryptophan, 20 mg/L adenine sulfate, 20 % uracil) at 30 °C and 200 rpm. Solid culture medium was generated by adding 2 % (w/v) agar-agar to the liquid medium.

2.4.3 Yeast cell transformation with plasmid DNA

0.5 OD_{600} logarithmic growing yeast cells were centrifuged (2000 × g, 2 min) and the pellet was suspended in 100 µL 100 mM lithium acetate and 1 × TE buffer (10 mM Tris-HCl pH 7.4, 1 mM EDTA) containing 0.2 µg herring sperm DNA and 0.5-1 µg/µL plasmid DNA. After addition of 500 µL 40 % PEG, 100 mM lithium acetate and 1 × TE buffer, cells were incubated for 30 min at 30 °C and heat shocked at 42 °C for 15 min. Cells were pelleted, resuspended in ddH_2O and platted on SD selection medium.

2.4.4 Sporulation and tetrad dissection

Haploid yeast strains with differing mating type were grown in 3 mL YPD medium over night. 500 µL of each culture were combined in an Eppendorf tube and incubated for 5 to 8 h at room temperature under constant stirring. Cell aggregates were sedimented and platted on SD selection medium, which allowed

only diploid cells with combined auxotrophy markers from both initial haploid strains to grow. Diploid cells were grown over night at 30 °C in 3 mL YPD medium. 200 µL of this culture was used to inoculate 3 mL of presporulation medium (0.3 % (w/v) Bacto^{TM} peptone, 0.8 % (w/v) Bacto^{TM} yeast extract, 10 % (w/v) glucose), which was cultured for 6 to 8 h at 30 °C and 200 rpm. 2 mL of this cell suspension were pelleted (2000 × g, 2 min), washed 2 times with 1 mL ddH_2O and transferred into 3 mL sporulation medium (0.1 % (w/v) Bacto^{TM} yeast extract, 0.05 % (w/v) glucose, 1 % (w/v) potassium acetate). Diploid cells sporulated 2 to 4 days at 30 °C and 200 rpm and sporulation efficiency was controlled with a light microscope (Zeiss). For separation of yeast tetrads, 1 mL of the sporulation culture was centrifuged (2000 × g, 2 min) and the pellet was resuspended in 1 mL SED medium (18.2 % (w/v) sorbitol, 25 mM EDTA). 200 µL of this suspension were mixed with DTT (final concentration 50 mM) and 200 µg Zymolyase (MB Biomedicals) and incubated at room temperature for 20 min to digest the ascus wall. Tetrads were dissected on a YPD plate using a micromanipulator (Singer Instruments). Individual spores were analyzed by replica plating on appropriate selection plates to determine their genotype.

2.4.5 Cycloheximide decay experiment

20 OD_{600} logarithmic growing yeast cells (5 OD_{600} for each time point of the experiment) were harvested (2000 × g, 2 min) and the pellet was resuspended in 4.5 mL SD medium. In a next step, 0.33 mg/mL cycloheximide were added to the cell suspension and immediately 1 mL of the mixture was transferred into an Eppendorf tube containing 0.5 mL cold 50 mM NaN_3 and 1 mM PMSF and placed on ice. The rest of the sample was incubated at 30 °C and at the given time points aliquots were removed and treated as described above. Aliquots were centrifuged (20,000 × g, 1 min) and the cell pellet was suspended in 100 µL lysis buffer (50 mM Tris-HCl pH 7.5, 1 % (w/v) SDS, 1 mM PMSF). After lysis of the cells by vigorous shacking with glass beads, 100 µL 2 × SDS sample buffer (135 mM Tris-HCl pH 6.8, 20 % (v/v) glycerol, 4 % (w/v) SDS, 0.05 % (w/v) bromophenol blue, 200 mM DTT) were added and the lysate was incubated at 65 °C for 15 min. Samples were centrifuged at 1000 × g for 5 min to separate glass beads and cell debris from cell extract. The supernatant was collected and analyzed by SDS-PAGE and immunoblotting (see section 2.3.5 and 2.3.7).

3 | Results

3.1 Characterization of the ubiquitylation capacity of Ubc6 and Ubc7

3.1.1 Ubc6 and Ubc7 are required for Doa10 dependent substrate degradation *in vivo*

Genetic data imply that degradation of Doa10 client proteins depends on activity of two E2 enzymes, Ubc6 and Ubc7 [136, 141, 170]. Deg1-GFP_2 is a model substrate of the Doa10 ligase and the influence of the different ligase components on its proteolysis was investigated (figure 3.1). Deg1 is comprised of a 68 amino acid long stretch of the Matα transcription factor, which confers degradation through the Doa10 ligase pathway when fused to stable proteins [133]. As shown in figure 3.1, degradation of Deg1-GFP_2 was impaired in yeast cells lacking Ubc6 and Doa10 or expressing a catalytically inactive Ubc7 variant ($Ubc7_{C89S}$). Disruption of the *UBC6* gene in combination with an inactive Ubc7 mutant had no further impact on Deg1-GFP_2 degradation, which implies that both enzymes act in the same pathway. Obviously, the enzymatic activities of Ubc6 and Ubc7 are required for Doa10-mediated substrate degradation.

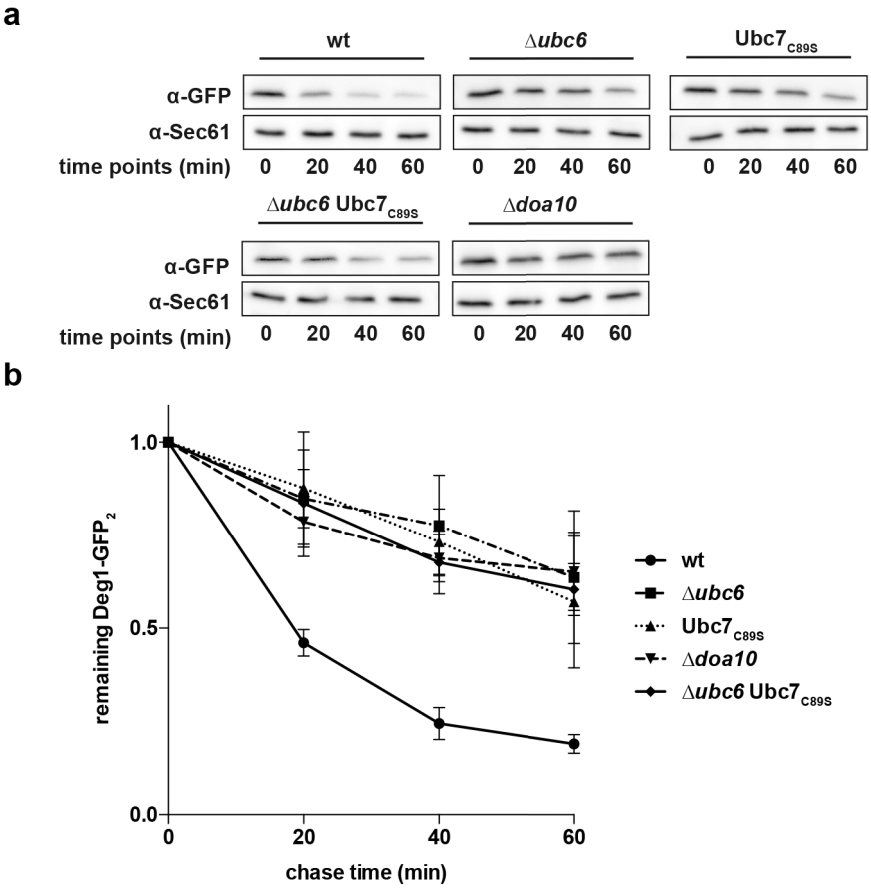

Figure 3.1 – Ubc6 and Ubc7 are both required for degradation of Deg1-GFP$_2$. (a) Cycloheximide decay assay monitoring turnover of Deg1-GFP$_2$ in given yeast strains. Samples were analyzed by SDS-PAGE and immunoblotting against GFP and Sec61 (loading control). **(b)** Quantified GFP signals of cycloheximide experiments as exemplary presented in (a). Error bars represent the standard deviation of mean from at least 3 independent experiments.

3.1.2 Ubc6 and Ubc7 exhibit distinct ubiquitylation activities *in vitro*

To study the catalytic propensities of Ubc7 and Ubc6 in detail, an *in vitro* ubiquitylation assay was established based on a protocol developed by Bagola *et al.* [142]. This approach allows the detailed analysis of the formed Ub reaction products with regard to their abundance, length and Ub linkage composition. Such information cannot be obtained by *in vivo* studies due to the high amount of Ub products within cells and the disruptive activities of the deubiquitylating system and the proteasome. To this end, the cytoplasmatically exposed parts of Ubc6 (Ubc6ΔTM), Cue1 (Cue1ΔTM) as well as the Doa10 RING domain (Doa10R) were expressed in *E.coli* and purified. The Ubc6ΔTM and Cue1ΔTM constructs lack the trans-membrane anchors, which represent only minor parts of the full-length proteins. The Doa10R construct is composed of the N-terminal region of the ligase that contains the RING domain and neighboring elements until the first trans-membrane domain. However, it omits the 14 trans-membrane segments and the connecting ER-luminal and cytoplasmatically exposed loops of Doa10. Thus, the Doa10R construct represents only 10 % of the total protein. The substrate recognition domains of Doa10 are not identified yet, but it is speculated that they are not part of Doa10R. Hence, incorporation of known substrates into the *in vitro* ubiquitylation assay might prove to be difficult. Other cytoplasmic components of the Doa10 ubiquitylation machinery as Ubc7, Uba1 (E1) and Ub were purified as full-length proteins. The final products of the purified proteins are depicted in

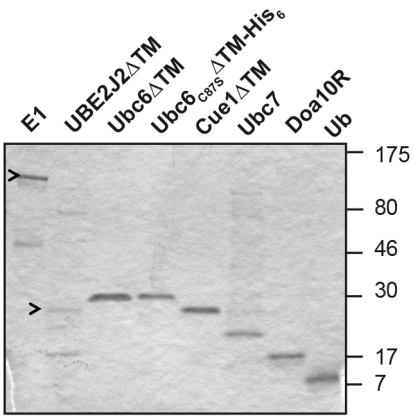

Figure 3.2 – Purified proteins for the *in vitro* ubiquitylation assay. Exemplary presentation of purified proteins expressed in *E.coli*, separated on a SDS-PAGE and stained with Coomassie. Signals corresponding to E1 enzyme (Uba1) and UBE2J2ΔTM are marked with an arrowhead. Numbers on the right indicate migration of standard proteins and their corresponding molecular weight in kDa.

figure 3.2.

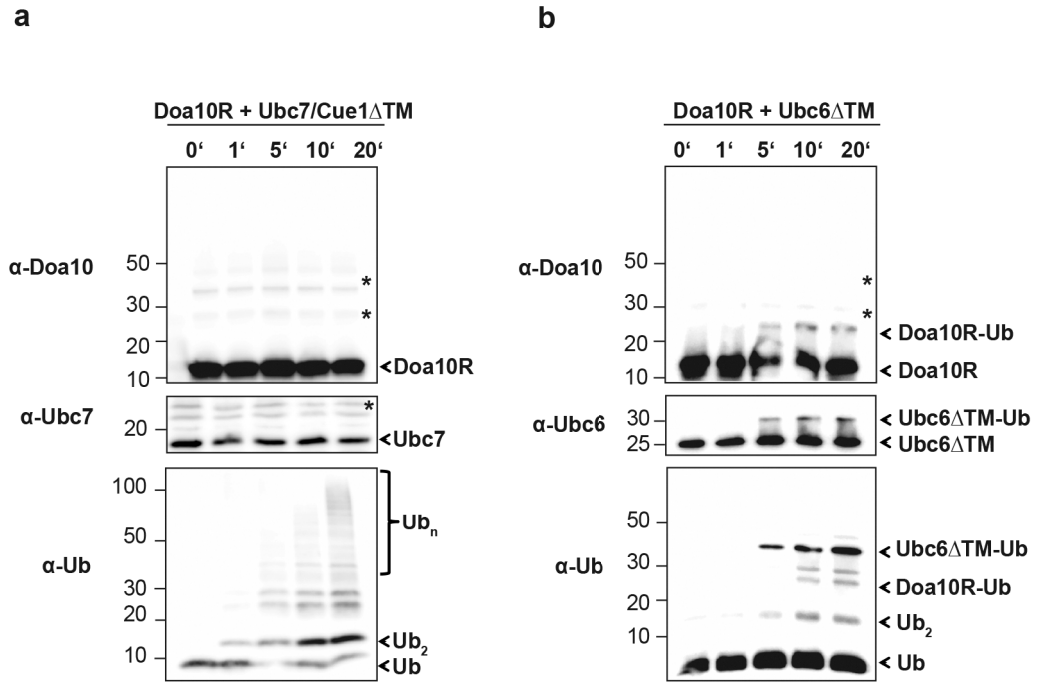

Figure 3.3 – Individual *in vitro* ubiquitylation properties of Ubc6ΔTM and Ubc7. (a, b) Time course experiments containing (a) Doa10R and Ubc7/Cue1ΔTM and (b) Doa10R and Ubc6ΔTM. Samples were analyzed by SDS-PAGE and immunoblotting. Ub blots depict overall levels of Ub species including free unanchored Ub chains as well as chains attached to substrate molecules. Asterisks indicate cross-reaction signals of the corresponding antibody. The figure was adapted from Weber *et al.* [155].

For the *in vitro* ubiquitylation assay equimolar amounts of the given proteins were incubated as described in section 2.3.14. The reaction was started by the addition of Ub variants and ATP. In a first setup each E2 enzymes was separately incubated with Doa10R. Ubc7 in presence of its co-factor Cue1ΔTM and Doa10R readily catalyzed the formation of free unanchored Ub chains as shown in figure 3.3 a. This is in agreement with results from Bagola *et al.* [142]. Notably, Ubc7 did not attach Ub molecules to itself or other proteins in the assay. On the contrary, Ubc6 was barely able to form poly-Ub chains when incubated with Doa10R (figure 3.3 b). Only tiny amounts of di or tri-Ub species were detected in the Ub blots in figure 3.3 b. Strikingly, Ubc6ΔTM attached

single Ub moieties to itself and Doa10R in the course of the reaction. Both *in vitro* ubiquitylation events can serve as reliable read-out of the enzymatic properties of Ubc6ΔTM. Ubc6 is a well-established substrate of the Doa10 ligase and its degradation depends on its own activity [152]. Furthermore, RING domains, which interact with E2 enzymes [14], are known to serve as artificial substrates in *in vitro* assays in the absence of other potential substrates [105, 171].

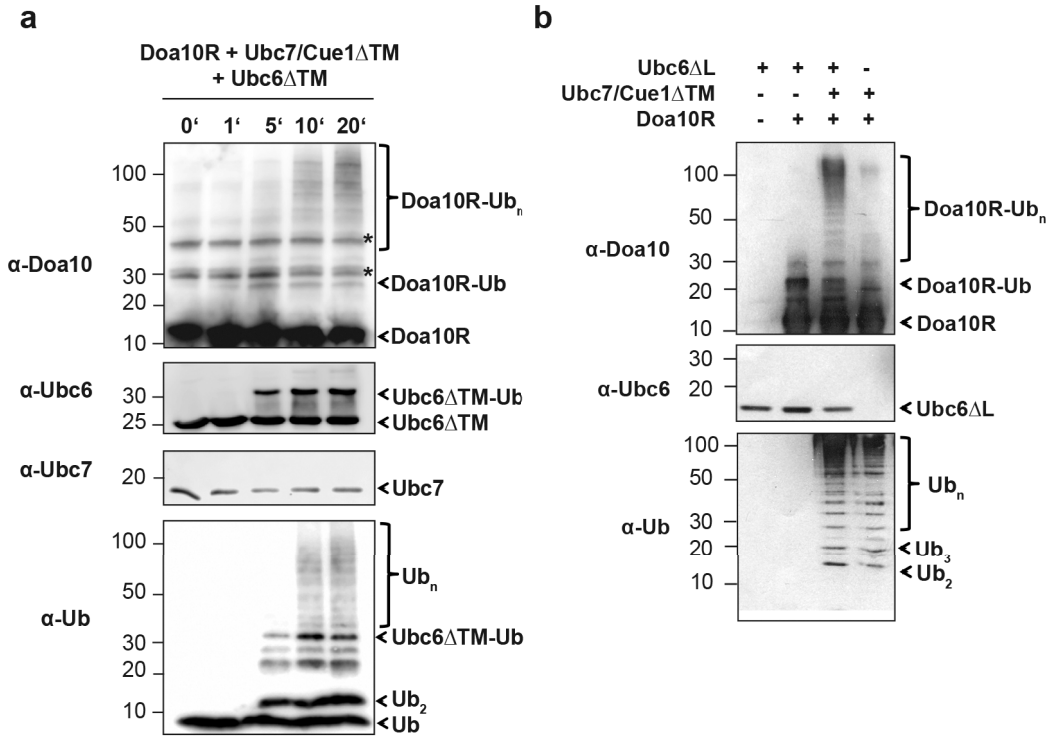

Figure 3.4 – Ubc6ΔTM and Ubc7 act in a consecutive manner on Doa10R *in vitro*. **(a)** Time course experiment containing Doa10R, Ubc6ΔTM and Ubc7/Cue1ΔTM. Samples were analyzed by SDS-PAGE and immunoblotting with indicated antibodies. Ub blots depict overall levels of Ub species including free unanchored Ub chains as well as chains attached to substrate proteins. Asterisks mark cross-reaction signals of the corresponding antibody. **(b)** Ubc6ΔL, a Ubc6 variant lacking linker and trans-membrane region, was incubated with Doa10R and Ubc7/Cue1ΔTM in varying combinations. Samples were analyzed by SDS-PAGE and immunoblotting. The figure was adapted from Weber *et al.* [155].

Since Ubc6ΔTM and Ubc7 display different enzymatic properties in the

in vitro assay, it became interesting how both enzymes operate together at the Doa10 RING domain. Consequently, the E2 enzymes were incubated together with Doa10R in an experimental setup. Remarkably, Doa10R was poly-ubiquitylated under those conditions over time (figure 3.4 a). This was not observed when Doa10R was incubated with each E2 enzyme separately. This indicates that a concerted action of both enzymes is required *in vitro* to decorate Doa10R with poly-Ub chains. Poly-ubiquitylation of Ubc6ΔTM was not detected in the same experimental setup and was further studied as described in section 3.1.7.

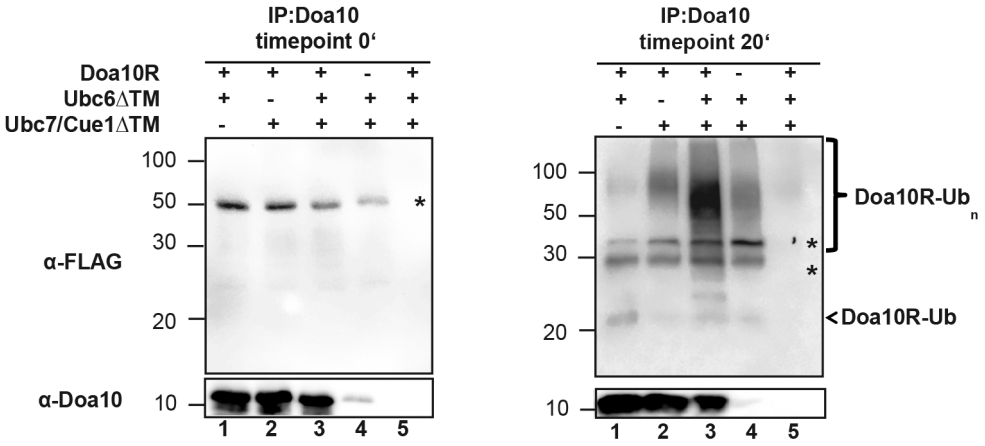

Figure 3.5 – Ub moieties are covalently attached to Doa10R. Doa10R was immunoprecipitated from *in vitro* ubiquitylation reactions containing FLAG-Ub at time points 0 and 20 min. Samples were analyzed by SDS-PAGE and immunoblotting with specific antibodies for Doa10 and FLAG. The negative control in lane 5 did not contain Doa10 antibody. Asterisks mark cross-reaction signals of the corresponding antibody. The figure was adapted from Weber *et al.* [155].

To test whether the UBC core domain of Ubc6 is sufficient to mediate Doa10R mono-ubiquitylation, a truncated Ubc6 variant (Ubc6ΔL) was studied. The Ubc6ΔL construct lacks the linker and trans-membrane region of the wt protein. The minimal Ubc6 construct was incubated with Doa10R in presence and absence of Ubc7/Cue1ΔTM (figure 3.4 b). Strikingly, the variant was still capable to conjugate Ub molecules to Doa10R, which in turn initiated Doa10R poly-ubiquitylation in presence of Ubc7/Cue1ΔTM. However, Ubc6ΔL did not attach Ub moieties to itself in contrast to the Ubc6ΔTM construct which still contains the linker region (compare Ubc6 blots in figure 3.3 a,b). Thus, the

ubiquitylation site of Ubc6 should be located within its linker region.

Immunoprecipitation (IP) experiments were performed to verify that Ub moieties were indeed covalently conjugated to the Doa10R protein (figure 3.5). For this purpose, Doa10R was incubated with N-terminal FLAG-tagged Ub and precipitated at time points 0 and 20 min from *in vitro* reactions. Poly-Ub signals were only detected in IPs from reactions containing both E2 enzymes Ubc6ΔTM and Ubc7 after 20 min. This experiment supports the necessity of a collective action of Ubc6ΔTM and Ubc7 to decorate Doa10R with poly-Ub chains. Ubiquitylated full-length Doa10 was never detected when precipitated from yeast cell extract (data not shown). Thus, it can be assumed that Doa10R *in vitro* ubiquitylation is an artificial event, which takes place due to the absence of other available substrates in the assay.

3.1.3 The enzymatic properties of Ubc6 are conserved in human

Two orthologues of Ubc6 were identified in human: UBE2J1 and UBE2J2 [172, 173]. A multiple sequence alignment of all three proteins displays high degree of similarity in their UBC domain located at the N-terminus (figure 3.6 a). The linker region between the UBC domain and the trans-membrane anchor is less conserved. Especially UBE2J1 exhibits a much longer linker region when compared to Ubc6 and UBE2J2. UBE2J2 is closer related to the yeast protein and was chosen for further investigations *in vitro*. UBE2J2ΔTM, a truncated version lacking the trans-membrane anchor, was purified from *E.coli* and assayed in *in vitro* ubiquitylation reactions (figure 3.6 b). The human Ubc6 orthologue was able to conjugate mono-Ub to Doa10R as already observed for Ubc6ΔTM (section 3.1.1). The modification of Doa10R initiated poly-ubiquitylation in presence of Ubc7/Cue1ΔTM. In contrast to Ubc6ΔTM, UBE2J2ΔTM did not mount Ub molecules on itself in the course of the reaction, which is in line with previous observations [174]. Results from this experiment clearly demonstrate that the enzymatic properties of E2 enzymes belonging to the Ubc6 family are highly conserved in evolution.

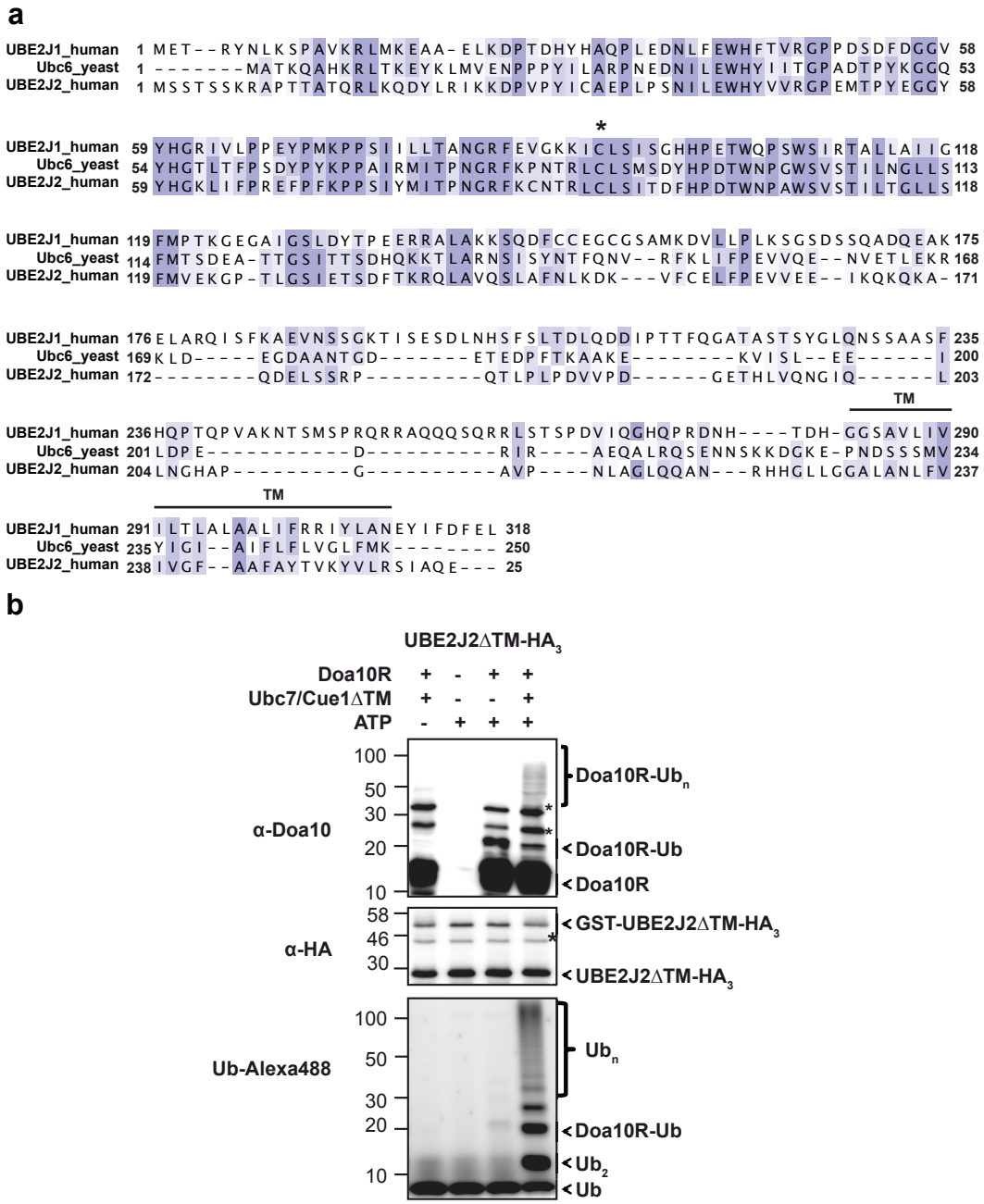

Figure 3.6 – UBE2J2ΔTM mono-ubiquitylates Doa10R *in vitro*. **(a)** Clustal Omega multiple sequence alignment [175] of Ubc6 and its human orthologues UBE2J1 and UBE2J2. The alignment was edited with Jalview and colored according to BLOSUM62 (BLOcks SUbstitution Matrix) [176]. The trans-membrane region (TM) and the active site cysteine (*) are highlighted. **(b)** UBE2J2ΔTM-HA_3 was incubated with Doa10R in presence and absence of Ubc7/Cue1ΔTM. Samples were analyzed by SDS-PAGE and immunoblotting or fluorescence scanning. Asterisks mark unspecific cross-reaction signals of the corresponding antibody. The figure was adapted from Weber *et al.* [155].

3.1.4 Ubc6ΔTM ubiquitylates Doa10R at several lysine residues

Ubc6ΔTM was shown to label Doa10R with mono-Ub moieties *in vitro*. Consequently, the question was raised whether Ubc6 attaches the Ub molecules to a specific lysine residue or to various sites within Doa10R. All nine lysine residues in Doa10R were independently mutated to arginine (table 3.1) and tested in *in vitro* ubiquitylation experiments to identify potential ubiquitylation sites.

Table 3.1 – List of analyzed Doa10R lysine mutants. MS - Mass spectrometry; ND - not determined

Mutation	Ubiquitylation	Identified by MS	pH sensitive
K18R	yes	no	no
K57R	yes	yes	no
K63R	ND	no	ND
K77R	yes	no	no
K83R	yes	yes	no
K89R	ND	yes	ND
K100R	yes	yes	no
K110R	yes	no	no
K119R	yes	yes	no

Single lysine mutations did not result in diminished Doa10R *in vitro* ubiquitylation as exemplary shown for the Doa10R variant K119R in figure 3.5 b. Previously, it was reported that Ub moieties could be conjugated to hydroxylated amino acids during protein quality control [75, 177]. Ester bonds, as formed between the hydroxyl group of serine or threonine residues and the C-terminus of Ub, are susceptible to elevated pH levels. To exclude that hydroxylated amino acids were modified in Doa10R, samples from *in vitro* reactions were incubated with 100 mM NaOH (exemplary shown for $Doa10R_{K119R}$ in figure 3.7 b). However, the Ub modification on Doa10R was not removed upon elevation of pH levels (figure 3.7 b, lane 4 and 6). Thus, it can be assumed that Doa10R ubiquitylation takes place mostly on lysine residues.

In a next step, mass spectrometry analysis was employed to investigate if multiple lysine residues in Doa10R are ubiquitylated by Ubc6ΔTM (Mass spectrometry measurements and analysis were performed by Oliver Popp and Gunnar Dittmar). Several ubiquitylation sites were identified with this method (table 3.1). Remarkably, all lysine residues clustered in the region of loop 2, which encompasses the second zinc coordination site (figure 3.7 a). Supposedly, Ubc6ΔTM, when bound to the RING domain, is able to access this area. Multiple mono-ubiquitylated Doa10R species were not detected in the course of the experiments. This is most likely due to steric restrictions of the first conjugated Ub moiety, which prevents further attachments of Ub moieties to other sites. Summing up, Ubc6ΔTM is able to ubiquitylate several lysine residues within Doa10R, which indicates that the E2 is flexible in selecting ubiquitylation sites in a target protein.

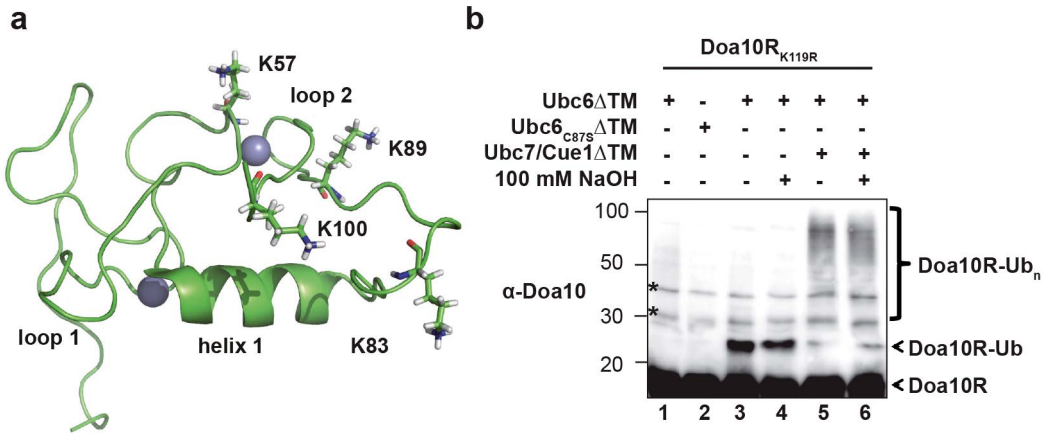

Figure 3.7 – Ubiquitylation sites in Doa10R. (a) In solution NMR structure of the Doa10 RING domain covering amino acid residues from 19 to 101 (PDB ID: 2M6M) [178]. Ubiquitylation sites, which were identified by mass spectrometry, are highlighted. Structural depictions were prepared using PyMOL [31]. **(b)** Doa10R$_{K119R}$ was incubated with Ubc6ΔTM alone (lane 3 and 4) and with both enzymes Ubc6ΔTM and Ubc7/Cue1ΔTM (lane 5 and 6). 100 mM NaOH was added to samples to probe for ubiquitylation of hydroxylated amino acids (lane 4 and 6). Negative controls were incubated without ATP (lane 1) or inactive Ubc6$_{C87S}$ΔTM (lane 2). Samples were analyzed by SDS-PAGE and immunoblotting against Doa10. Asterisks mark unspecific cross-reaction signals of the antibody.

3.1.5 Characterization of Ub chain types involved in Doa10R *in vitro* ubiquitylation

Ub variants lacking individual lysine residues (Ub_{K11R}, Ub_{K48R}, Ub_{K63R}) were incorporated into the experimental setup of the ubiquitylation assay to analyze the Ub chain linkages involved in Doa10R poly-ubiquitylation. Ubc6ΔTM was able to attach all of these Ub variants equally well to itself and Doa10R (figure 3.8 a).

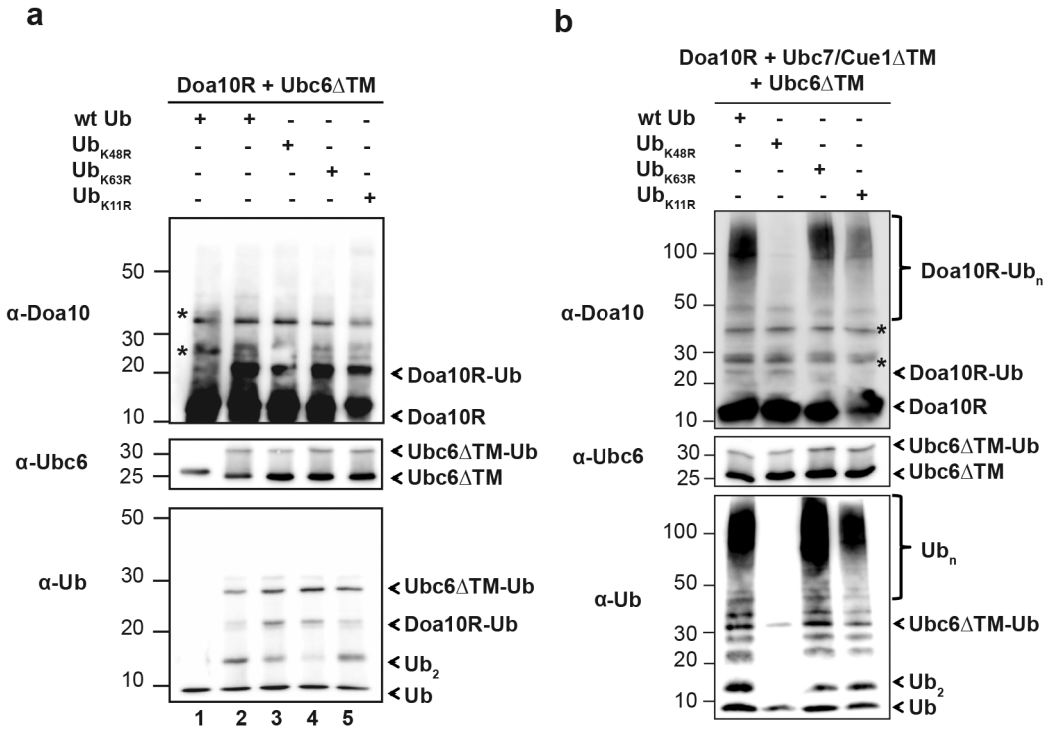

Figure 3.8 – Ubc6ΔTM and Ubc7 decorate Doa10R with K48-linked poly-Ub chains. (a) *In vitro* ubiquitylation reactions containing Ubc6ΔTM, Doa10R and different Ub variants (Ub, Ub_{K11R}, Ub_{K48R}, Ub_{K63R}). The negative control (lane 1) was incubated with inactive $Ubc6_{C87S}$ΔTM. Samples were analyzed by SDS-PAGE and immunoblotting with indicated antibodies. **(b)** *In vitro* ubiquitylation reactions containing Ubc6ΔTM, Ubc7/Cue1ΔTM, Doa10R and different Ub variants (Ub, Ub_{K11R}, Ub_{K48R}, Ub_{K63R}). Samples were analyzed by SDS-PAGE and immunoblotting with indicated antibodies. Asterisks mark cross-reaction signals of the corresponding antibody. The figure was adapted from Weber *et al.* [155].

Additionally, the formation of di-Ub species was observed in all reactions containing active Ubc6ΔTM. This suggests that Ubc6ΔTM is able to conjugate Ub donor moieties to different lysine residues within the Ub acceptor molecule. In contrast, Ubc7 is known to exclusively synthesize K48-linked poly-Ub chains [142]. This characteristic was confirmed for Doa10R *in vitro* poly-ubiquitylation (figure 3.8 b). Ubc7 decorated Doa10R with poly-Ub chains in presence of Ub_{K11R} and Ub_{K63R} to a similar extent as when incubated with wt Ub. The mono-ubiquitylated form of Doa10R accumulated when Ub_{K48R} was incorporated in the *in vitro* reactions, because Ubc6ΔTM conjugated single Ub moiety to Doa10R but Ubc7 was not able to attach further Ub molecules to it due to the absence of lysine 48 on the acceptor Ub.

Observations of Xu *et al.* suggest that Ubc6 favors the assembly of K11-linked Ub chains [28]. The results shown in figure 3.8 a question these findings and thus Ub-Ub conjugates generated by the E2 were analyzed by mass spectrometry. Ub chain type quantification demonstrated that Ubc6ΔTM forms very low amounts of Ub chains *in vitro* (80 fmol in 20 min) (figure 3.9). In contrast, Ubc7 was shown to be much more active in synthesizing unanchored K48-linked Ub chains (80 pmol in 15 min) in a similar reaction setup [142]. Furthermore, Ubc6ΔTM mainly attached the donor Ub moiety to lysine 48 and 63 within the Ub acceptor molecule (figure 3.9). Other linkage types were not identified in a significant portion. Thus, Ubc6 is not specialized on poly-Ub chain formation but rather on attaching single Ub moieties to lysine residues in client proteins.

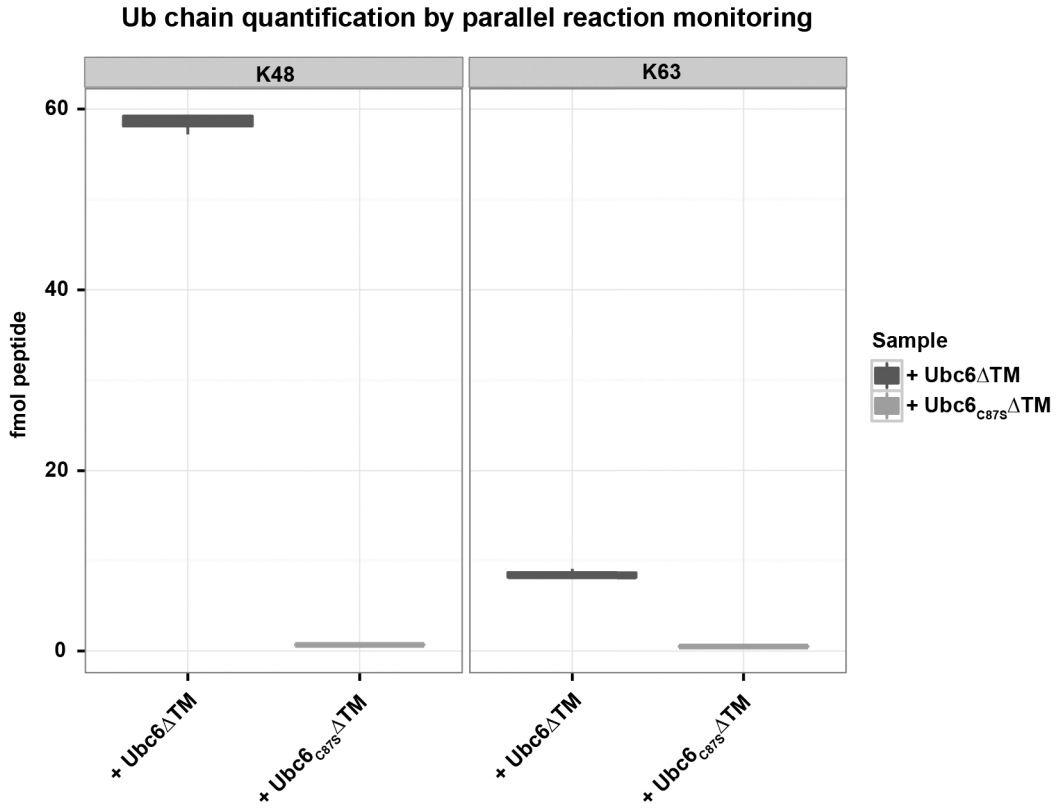

Figure 3.9 – Ubc6ΔTM catalyzes minor amounts of K48- and K63-linked Ub chains *in vitro*. Quantitative analysis of formed Ub linkages from *in vitro* ubiquitylation experiments containing Ubc6ΔTM or inactive $Ubc6_{C87S}$ΔTM with mass spectrometry. Samples were measured in selected reaction monitoring (SRM) and were compared to human Ub standards as described in detail in section 2.3.19. Mass spectrometry measurements and analysis were performed by Oliver Popp and Gunnar Dittmar.

To test how the attachment of Ub by Ubc6ΔTM labels Doa10R for subsequent Ubc7-mediated poly-ubiquitylation, *in vitro* experiments were split into two reactions to monitor the priming and elongation steps separately (figure 3.10). First, Doa10R was incubated with Ubc6ΔTM-His_6 and mutant Ub (either Ub_{K48R} or Ub_{K63R}). In this reaction step Ubc6ΔTM catalyzed the conjugation of mono-Ub to Doa10R. Subsequently, Ubc6ΔTM-His_6 was removed from the assay to prevent further modification of Doa10R. Next, mono-ubiquitylated Doa10R was incubated with Ubc7/Cue1ΔTM and excess amounts of wt Ub. Doa10R was poly-ubiquitylated only when it had been labeled with Ub_{K63R}

but not with Ub_{K48R} (figure 3.10). Summing up, this experiment demonstrates that Ubc7 directly elongates the Ub moieties on Doa10R, which were attached beforehand by Ubc6ΔTM.

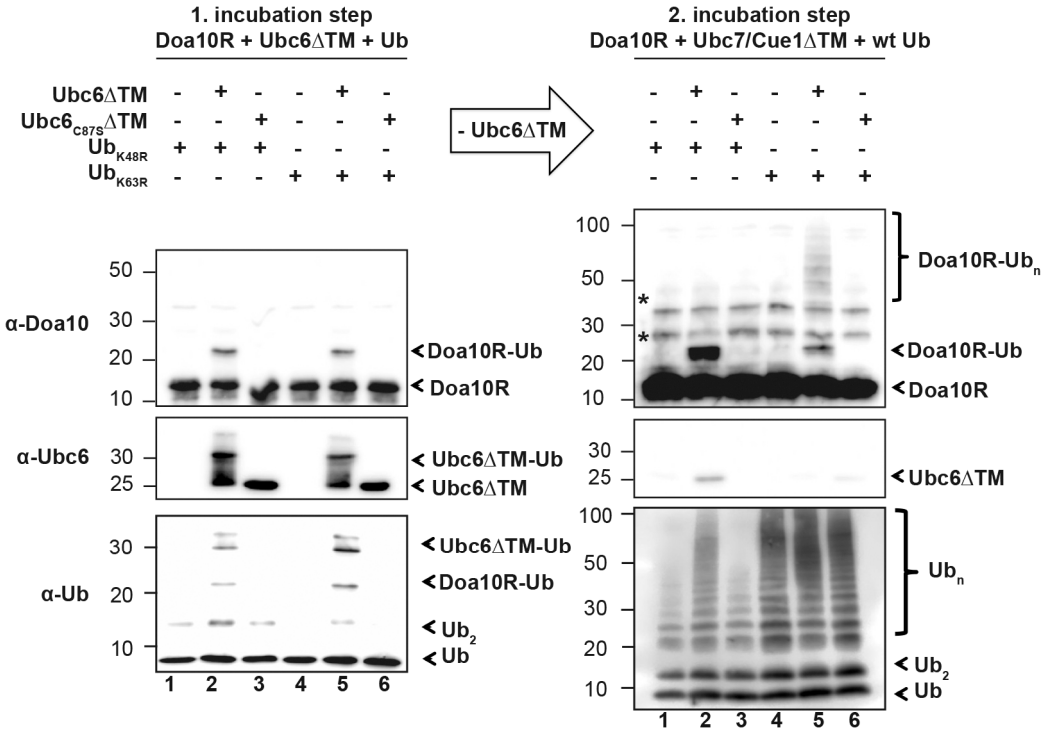

Figure 3.10 – Ubc7 attaches K48-linked Ub chains directly to Ub moieties conjugated to Doa10R by Ubc6ΔTM. Doa10R was incubated with Ub_{K48R} or Ub_{K63R} in presence of Ubc6ΔTM-His_6 or $Ubc6_{C87S}$ΔTM-His_6 or no E2. Subsequently, Ubc6 variants were removed with TALON® resin from the reactions and wt Ub as well as Ubc7/Cue1ΔTM were added. Samples were analyzed by SDS-PAGE and immunoblotting. Asterisks indicate unspecific cross-reaction signals of the corresponding antibody. Of note, commercially available Ub_{K48R} and Ub_{K63R} already contained small amounts of di-Ub. The figure was adapted from Weber *et al.* [155].

Ub blots in figure 3.10 show that Ubc7 was active in all reactions since it catalyzed the formation of unanchored Ub chains. However, overall levels of Ub chains were reduced in reactions containing Ub_{K48R}, probably because residual amounts of this Ub variant were incorporated into Ub conjugates. Furthermore, Doa10R-Ub stimulated Ubc7 activity to a higher extent when compared to unmodified Doa10R (compare lane 2 with lane 1 and 3 in Ub blots of the second

incubation step in figure 3.10). This phenomenon was observed before for other E2 enzymes due to binding of Ub to a backside interaction site in the UBC domain, which further stimulates Ub chain elongation activity [179, 180].

3.1.6 Ubc6ΔTM and Ubc7 interact with Doa10R through a conserved binding site

It was shown that Doa10R ubiquitylation depends on the successive action of Ubc6 and Ubc7. How both enzymes functionally interact with a single RING domain remains elusive. Previous studies on the Anaphase Promoting Complex (APC), which also engages two E2 enzymes during substrate ubiquitylation, showed that initiating and elongating E2 enzymes interact differently with the APC RING protein (APC11) [181]. The activity of the human chain initiating E2 enzymes, UBCH5 and UBCH10, relies on a conserved binding site in the RING domain. In contrast, the chain elongation activity of UBE2S requires a different, non-conserved interaction site. To evaluate if Ubc6 and Ubc7 cooperate in a similar manner with Doa10R, a multiple sequence alignment was conducted to identify conserved amino acids in APC11 and Doa10R (figure 3.11 a). Strikingly, the binding site of human APC11, which regulates chain elongation, is not preserved in yeast APC11 or Doa10R (figure 3.11 a, green dots). However, 3 amino acids, which are allocated to the chain initiating E2 binding site of APC11 are conserved in Doa10R (figure 3.11 a, red dots). All three residues; isoleucine 41, arginine 43 and tryptophan 73, are part of the major helix 1 and loop 1 of the Doa10 RING domain (figure 3.11 b). This area is known to be a general docking site for E2 enzymes on E3 RING domains [16].

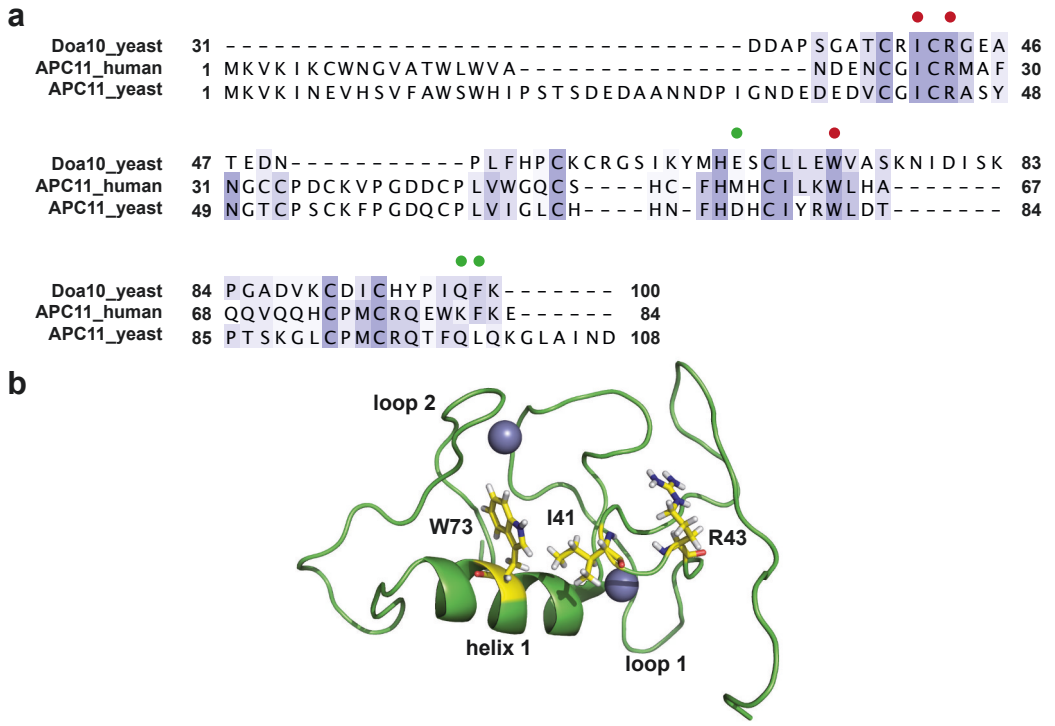

Figure 3.11 – Multiple sequence alignment of APC11 and Doa10R. (a) Clustal Omega sequence alignment [175] of the Doa10 RING domain with human and yeast APC11. The alignment was edited with Jalview and colored according to BLOSUM62 (BLOcks SUbstitution Matrix) [176]. Conserved residues related to canonical E2 binding are marked with red dots; non-conserved amino acids of human APC11 allocated with Ub-chain elongation are marked with green dots. **(b)** In solution NMR structure of the Doa10 RING domain (PDB ID 2M6M) with highlighted amino acids, which are implicated in E2 binding [178]. Structural depictions were prepared using PyMOL [31].

The conserved amino acids isoleucine 41, arginine 43 and tryptophan 73 were substituted to alanine in Doa10R to test whether the putative E2 interaction site regulates the enzymatic activities of Ubc6 and Ubc7. In a first reaction setup, the impact of these mutations on Ubc7 activity was assessed (figure 3.12 a). The catalysis of unanchored Ub-chains by Ubc7/Cue1ΔTM is significantly stimulated by addition of wt Doa10R. In contrast, $Doa10R_{I41A}$ did not enhance Ubc7-mediated chain formation at all. $Doa10R_{R43A}$ and $Doa10R_{W73A}$ displayed an intermediate phenotype with $Doa10R_{W73A}$ enhancing Ubc7 activity moderately better than $Doa10R_{W73A}$. Ubc6ΔTM activity was also signifi-

cantly affected by the Doa10R variants as shown in figure 3.12 b. Doa10R$_{I41A}$ completely abolished mono-ubiquitylation by Ubc6ΔTM. Doa10R$_{R43A}$ was mono-ubiquitylated to a similar extent as wt Doa10R and Doa10R$_{W73A}$ was barely mono-ubiquitylated. Remarkably, Ubc6ΔTM self-ubiquitylation was unaffected by the Doa10R variants. This is in line with the observation that Ubc6ΔTM can modify itself *in vitro* independently of E3 activation (figure 3.15, lane 3). Poly-ubiquitylation of the Doa10R variants was impaired in presence of Ubc6ΔTM and Ubc7 most likely because every mutation at least restricts the enzymatic activity of one E2 (figure 3.12 c). Doa10R$_{I41A}$ affects both enzymes strongly and therefore this variant was not modified in the course of the reaction. Mono-ubiquitylated Doa10R$_{R43A}$ accumulated because it was not efficiently modified by Ubc7 with poly-Ub chains. Doa10R$_{W73A}$ failed to recruit Ubc6ΔTM to initiate mono-ubiquitylation.

All Doa10R variants were analyzed by circular dichroism to exclude that structural perturbations disturb the interplay between Doa10R and the E2 enzymes. They displayed similar CD spectra when compared to wt Doa10R (figure 3.13), which resembled the typical spectra of an E3 RING domain [182]. This indicates that the Doa10R variants did fold properly. Summing up, the presented results suggest that both E2 enzymes functionally interact with Doa10R through a conserved E2 binding site. Slight divergences could be observed for the variants Doa10R$_{R43A}$ and Doa10R$_{W73A}$, which propose that Ubc6ΔTM and Ubc7 engage in a distinct manner with Doa10R most likely to fulfill their individual function during ubiquitylation.

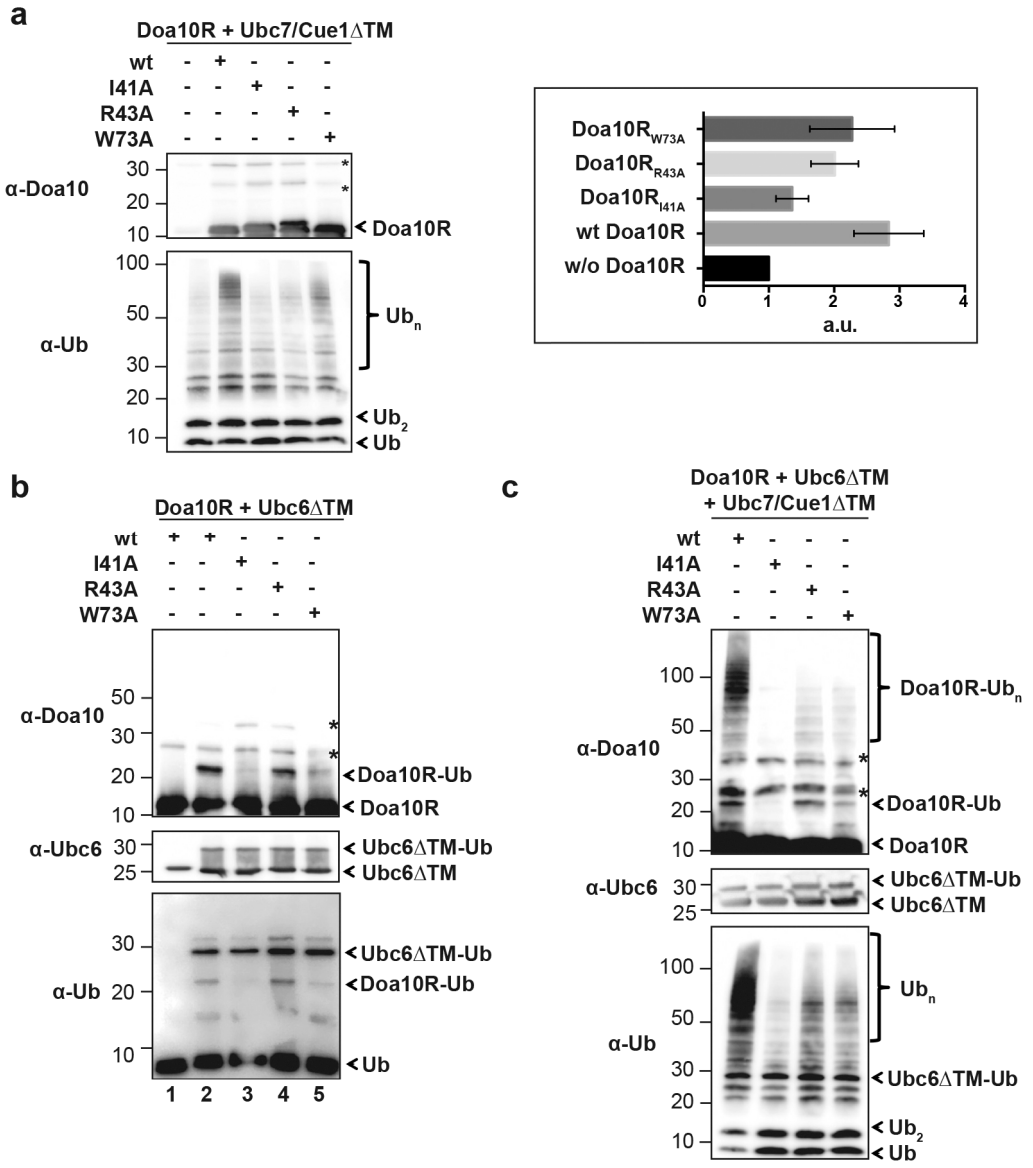

Figure 3.12 – Mutation of a conserved E2 binding site in Doa10R affects the enzymatic activities of Ubc6ΔTM and Ubc7. (a-c) *In vitro* ubiquitylation reactions containing Doa10R variants (wt, $Doa10R_{I41A}$, $Doa10R_{R43A}$, $Doa10R_{W73A}$) with (a) Ubc7/Cue1ΔTM, (b) Ubc6ΔTM and (c) both E2 enzymes. The negative control was incubated with inactive $Ubc6_{C87S}$ΔTM (b, lane 1). Samples were analyzed by SDS-PAGE and immunoblotting. Asterisks mark cross-reaction signals of the corresponding antibody. (a) Quantification of unanchored Ub chain formation catalyzed by Ubc7/Cue1ΔTM normalized to basal reaction levels in absence of Doa10R. Error bars represent standard deviation of mean from at least 3 independent experiments. The figure was adapted from Weber *et al.* [155]. a.u. - arbitrary unit; w/o - without

Questions were raised whether Ubc6 and Ubc7 compete for interaction with Doa10R during ubiquitylation, because both E2 enzymes occupy the same docking site. However, *in vitro* ubiquitylation experiments with different Ubc6:Ubc7 ratios did not indicate that high amounts of Ubc6 can prevent poly-ubiquitylation of Doa10R or *vice versa* (data not shown). Thus, it can be speculated that even when one E2 enzymes is added in excess to the reaction, the other one has still access to Doa10R. This is in line with observations, which showed that E2 interactions with RING domains are extremely dynamic and transient [13, 92].

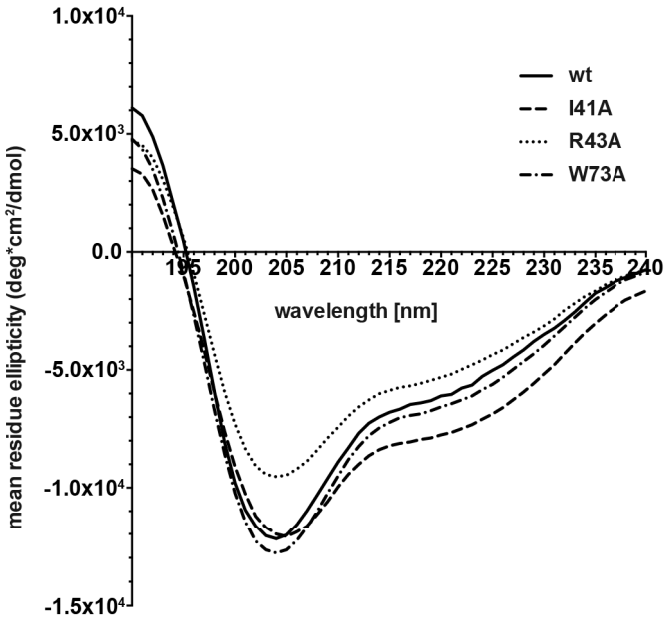

Figure 3.13 – Circular dichroism spectra of Doa10R variants in comparison to the wt protein. Wavelength scans were performed at 20 °C for Doa10R$_{I41A}$, Doa10R$_{R43A}$, Doa10R$_{W73A}$ and wt Doa10R (for experimental details see section 2.3.12). The figure was adapted from Weber *et al.* [155].

3.1.7 Characterization of Ubc6 auto-ubiquitylation

Ubc6 itself is a target of the Doa10 ligase. Its turnover depends on its own enzymatic activity and on that of Ubc7 (figure 3.14) [152]. In agreement with these genetic data, Ubc6ΔTM conjugated mono-Ub moieties to itself in the course of *in vitro* ubiquitylation experiments (figure 3.3 b). It was shown earlier that *in vivo* Ubc6 ubiquitylates itself in *cis* [152]. This was validated *in vitro*

with an inactive His-tagged Ubc6ΔTM variant ($Ubc6_{C87S}$ΔTM-His_6) and an active non-tagged Ubc6ΔTM, which were incubated together in one reaction set-up (figure 3.15). The active Ubc6ΔTM variant was modified during the reaction whereas the inactive variant was not (figure 3.15 lane 6 and 7). These observations suggest that the Ubc6 molecule, which is ubiquitylated, initiates its own turnover without the aid of another Ubc6 protein.

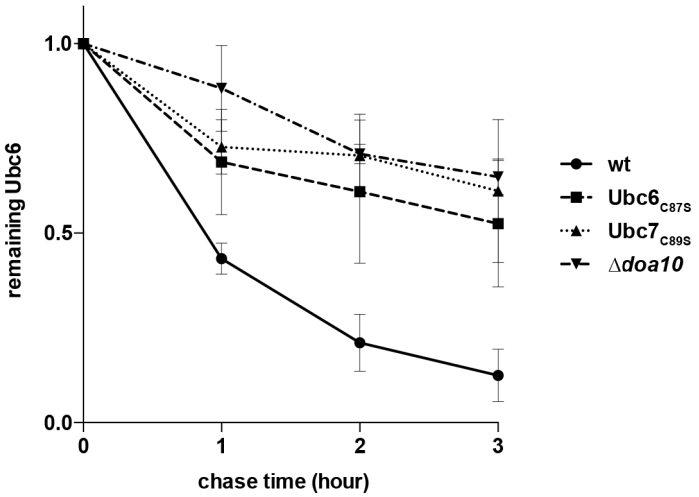

Figure 3.14 – Ubc6 is a Doa10 substrate. Quantification of Ubc6 signals from cycloheximide experiments monitoring endogenous Ubc6 turnover in indicated yeast strains. Error bars represent standard deviation of mean from at least 3 independent experiments.

In *in vitro* experiments two modified Ubc6 species were detected, which could account for mono- and di-ubiquitylated Ubc6 or a double mono-ubiquitylated form (figure 3.15, Ubc6 blot). To assess whether Ubc6ΔTM was ubiquitylated at several sites with mono-Ub or at one position with di-Ub, a Ub variant lacking all lysine residues was incorporated into the *in vitro* ubiquitylation assay (Ub_{K0}) (figure 3.15, lane 9). This Ub variant allows single conjugation through its C-terminus to target proteins but no chain formation through internal lysine residues. Indeed, Ubc6ΔTM readily attached this Ub variant to itself. Furthermore, Ubc6ΔTM-Ub_2 conjugates were still generated in these experiments, proposing that Ubc6ΔTM is able to mono-ubiquitylate itself simultaneously at several positions.

To exclude that Ubc6 attaches Ub molecules to the N-terminus of Ub_{K0}, the experiment was repeated with N-terminal GST-tagged Ub (data not shown).

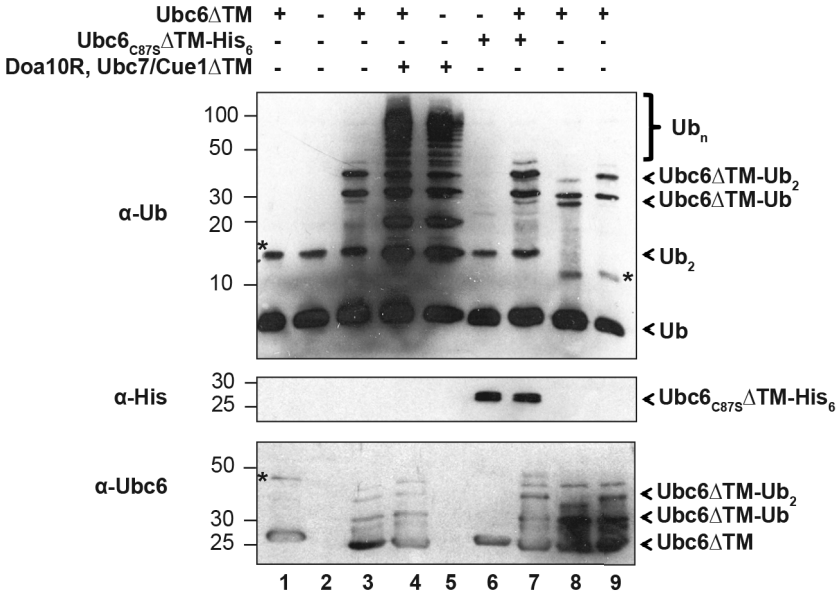

Figure 3.15 – Characterization of the self-ubiquitylation capacity of Ubc6ΔTM *in vitro*. Ubc6 variants (Ubc6ΔTM and $Ubc6_{C87S}$ΔTM-His_6) were incubated with Doa10R, Ubc7 and Cue1ΔTM in different experimental setups. In lane 9, Ub_{K0} (Ub variant without lysine residues) was incorporated into the assay. The negative control was incubated without ATP (lane 1). Samples were analyzed by SDS-PAGE and immunoblotting. Asterisks mark non-specific cross-reaction signals of the respective antibody.

Ubc6-Ub_2 species were also observed in such reactions, which strengthen the assumption that Ubc6 attaches several single Ub moieties to different sites within itself. Interestingly, Ubc6ΔTM conjugated Ub moieties to itself also in absence of Doa10R to a similar extent as in presence of the RING domain (compare lane 3 and 4 in figure 3.15). This suggests that self-modification of Ubc6ΔTM *in vitro* is not dependent on the stimulation by an E3 enzyme.

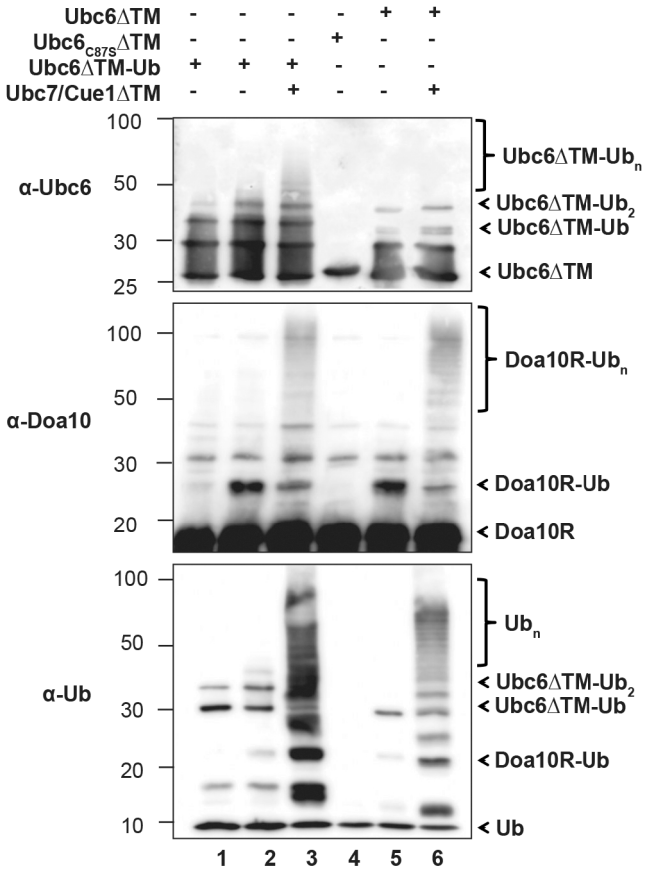

Figure 3.16 – Ubc7 decorates Ubc6ΔTM-Ub with poly-Ub chains. Enriched Ubc6ΔTM-Ub was incubated with Ubc7/Cue1ΔTM and Doa10R (lane 3) to allow its poly-ubiquitylation. The negative control was incubated without ATP (lane 1). All reactions contained Doa10R.

Ubc6ΔTM poly-ubiquitylation could not be detected in reactions containing Ubc7 and Cue1ΔTM (figure 3.15 lane 4 and figure 3.4). Even in experiments, in which Ubc6ΔTM was first mono-ubiquitylated and Ubc7/Cue1ΔTM were added thereafter, poly-Ub-Ubc6 conjugates were not observed (data not shown). Possible explanations for this phenomenon could be the absence of the E2 recruitment platform of the Doa10 ligase. Consequently, Ubc6ΔTM and Ubc7 might not get into close proximity. This limitation would not account for Doa10R poly-ubiquitylation since it was shown that both E2 enzymes interact with the RING domain (section 3.1.6). Additionally, it could be envisioned that Ub molecules attached to Ubc6ΔTM are not accessible for Ubc7/Cue1ΔTM due to steric hindrances. To overcome these constrains,

ubiquitylated Ubc6ΔTM was purified in high quantities and subjected to ubiquitylation reactions in excess (figure 3.16). Of note, not all unmodified Ubc6ΔTM could be separated from ubiquitylated species, because the protein tented to stick to metal affinity raisin. However, experiments with enriched Ub-Ubc6ΔTM proteins showed tiny amounts of poly-ubiquitylated Ubc6ΔTM species in the presence of Ubc7/Cue1ΔTM and Doa10R (figure 3.16, lane 3). Thus it can be assumed that Ubc6ΔTM poly-ubiquitylation takes place in the *in vitro* ubiquitylation assay with low efficiency, which hinders detection. Doa10R was mono-ubiquitylated in reactions containing high amounts of Ubc6ΔTM-Ub (figure 3.16, lane 2 and 5). This observation suggests that modified Ubc6ΔTM is still catalytically active. However, it cannot be excluded that low amounts of unmodified Ubc6ΔTM species account for the observed basal Ub priming activity at Doa10R.

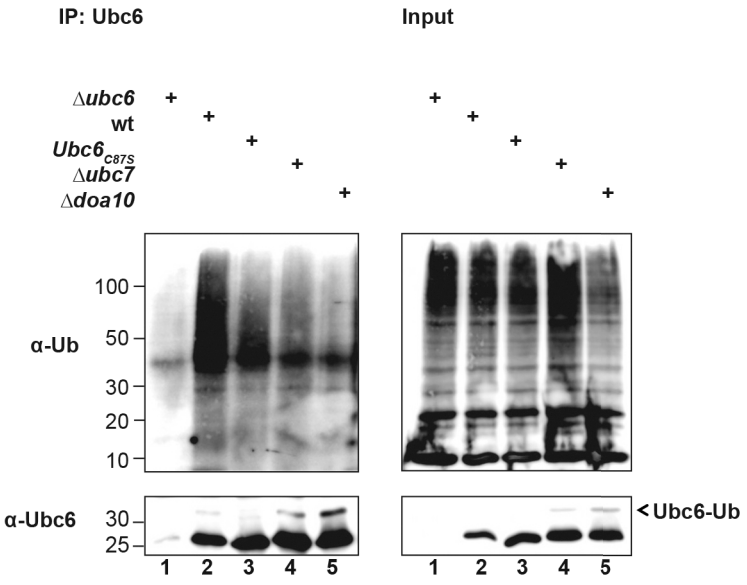

Figure 3.17 – Ubc6 is mono-ubiquitylated *in vivo* in dependency on its own enzymatic activity. Ubc6 was precipitated from yeast cell extract devoid of components of the Doa10 complex. All strains overexpressed wt Ub from plasmid. Samples were analyzed by SDS-PAGE, immunoblotting and probed for Ubc6 and Ub. The control strain in lane 1 did not contain *UBC6*.

To validate the *in vitro* findings on the self-ubiquitylation of Ubc6ΔTM, the protein was immunoprecipitated from cell extract prepared from strains, which lacked components of the Doa10 ligase complex (figure 3.17). Ubc6

was mono-ubiquitylated in wt, Δ*ubc7* and Δ*doa10* cells (Ubc6 blots in figure 3.17). In contrast, the active site mutant $Ubc6_{C87S}$ was not modified, which is in line with observations from *in vitro* experiments (figure 3.16, lane 3). Mono-ubiquitylated Ubc6 accumulated in Δ*ubc7* and Δ*doa10* yeast cells when compared to the wt situation. This can be explained by the absence of Ubc7. At an intact E3 ligase Ubc7 would act on these primed Ubc6 species and attach poly-Ub chains to mono-ubiquitylated Ubc6. Ub blots of the IP experiment are of poor quality most likely due to low abundance of poly-ubiquitylated Ubc6. Nevertheless, Ubc6 appears to be poly-ubiquitylated in wt cells. In contrast, Ubc6 seems to be modified to a significant lesser extent in cells lacking components of the Doa10 ligase. Thus, the IP experiment of Ubc6 supports the proposed model in which Ubc6 primes Doa10 target proteins and Ubc7 elongates these moieties with poly-Ub chains.

Summing up, it can be stated that mono-ubiquitylation of Ubc6ΔTM is a very robust event *in vitro* and *in vivo*, which does not depend on the presence of the Doa10 ligase. This is most likely due to easily accessible ubiquitylation sites close to the active center of Ubc6ΔTM. Generally, this phenomenon has been observed for several other E2 enzymes before [174]. On the contrary, Ubc6ΔTM poly-ubiquitylation is inefficient *in vitro* as well as *in vivo* in the absence of the Doa10 ligase. This confirms the necessity of a recruitment platform, which brings together target proteins and active components at the ligase to start the ubiquitylation reaction.

3.1.8 Interaction of Ubc6 with the Doa10 RING domain is mandatory for Doa10 substrate degradation

Investigation of Ubc6 auto-ubiquitylation showed that this phenomenon occurs independently of the Doa10 ligase *in vitro* as well as *in vivo* (section 3.1.7). Whether Ubc6 is also able to mono-ubiquitylate Doa10 target proteins autonomously of the Doa10 RING domain remains elusive. To address this question, a Ubc6 variant, $Ubc6_{Y66A}$, which does not interact with the Doa10 RING domain was characterized in detail. Tyrosine 66 is located in loop 4 of the UBC domain of Ubc6 (figure 3.18 a). Substitution of aromatic amino acids

in this area is known to interfere with E3 RING interaction [183, 184]. *In vitro* experiments confirmed that the amino acid substitution from tyrosine to alanine at position 66 abolished Doa10 mono-ubiquitylation (figure 3.18 b). In contrast, Ubc6ΔTM self-modification was only slightly reduced by the mutation, which indicates that the amino acid substitution does not interfere with the enzymatic activity of Ubc6ΔTM.

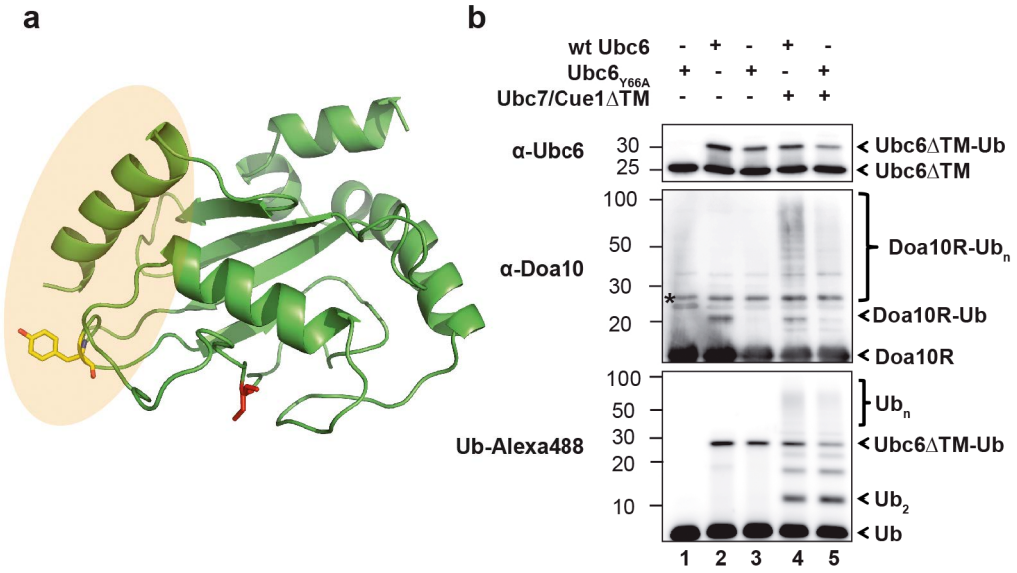

Figure 3.18 – Ubc6$_{Y66A}$ΔTM does not attach Ub moieties to Doa10R *in vitro*. **(a)** Structure of Ubc6 generated by homology modeling with SWISS-MODEL covering amino acids from 5 to 164 [185]. Tyrosine 66 (yellow) and the active site cysteine (red) are highlighted as well as the area, which is implicated in E3 interaction (orange) [13, 186]. Structural depictions were prepared using PyMOL [31]. **(b)** Ubc6$_{Y66A}$ΔTM and wt Ubc6ΔTM were incubated with Doa10R, fluorescently labeled Ub, E1 enzyme and Ubc7/Cue1ΔTM where indicated. The negative control in lane 1 did not contain ATP. Samples were analyzed by SDS-PAGE, immunoblotting and fluorescence scanning. Asterisks mark non-specific cross-reaction signals of the respective antibody.

Cycloheximide decay assays clearly demonstrated that turnover of Ubc6$_{Y66A}$ is only modestly delayed when compared to wt Ubc6 (figure 3.19 c). However, proteolysis of the Doa10 model substrate Deg1-GFP$_2$ was significantly diminished when Ubc6$_{Y66A}$ was expressed (figure 3.19 d). Thus, interaction of Ubc6 with the Doa10 RING domain is mandatory for degradation of Doa10

clients. However, it remains unclear if the Doa10 RING domain activates the ubiquitylation capacity of Ubc6 or if it positions the E2 favorably towards substrates and initiates thereby the turnover of target proteins. Nevertheless, the necessity for Doa10R binding might also prevent Ubc6 from ubiquitylating randomly proteins in the ER membrane when it is not bound to the Doa10 ligase complex. Additionally, the presented data suggest that the self-initiated turnover of Ubc6 represents an exception from general substrate ubiquitylation at the ligase maybe due to the close proximity of available ubiquitylation sites close to the active site.

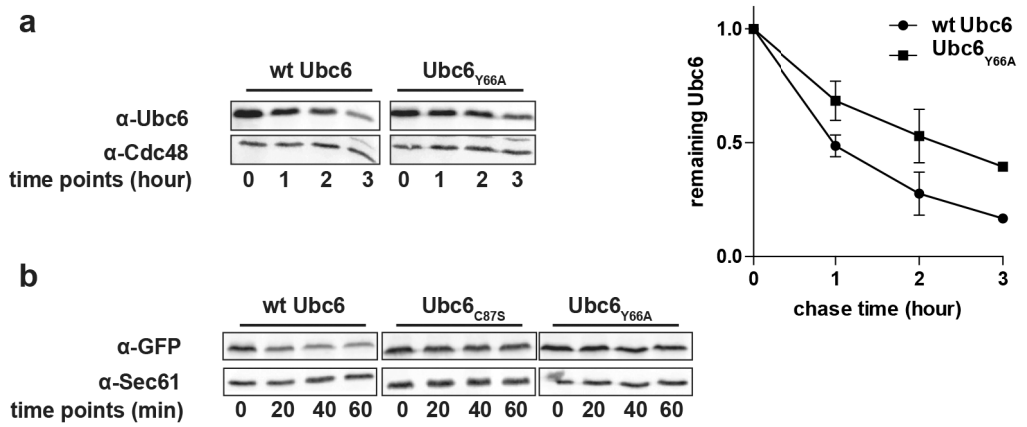

Figure 3.19 – Expression of Ubc6$_{Y66A}$ diminishes proteolysis of the Doa10 model substrate Deg1-GFP$_2$. (a,b) Cycloheximide decay assay monitoring turnover of (a) Ubc6 and (b) Deg1-GFP$_2$ in Δ*ubc6* yeast cells, which harbored plasmids expressing either wt Ubc6, Ubc6$_{Y66A}$ or Ubc6$_{C87S}$ (negative control). Samples were probed for Ubc6 and Cdc48 (loading control) or GFP and Sec61 (loading control). Ubc6 signals in (a) were quantified to emphasize small differences between degradation kinetics of the Ubc6 variants. Error bars represent standard deviation of mean of 2 independent experiments.

3.2 Investigation of non-canonical ubiquitylation events catalyzed by Ubc6

3.2.1 Identification of ubiquitylated lysine residues within Ubc6ΔTM

As demonstrated before, Ubc6 itself is a short-lived protein, which is degraded in dependency on the Doa10 ligase components (figure 3.14). On the one hand, Ubc6 turnover could be a regulatory element to control Doa10 function. On the other hand, it might be a coincidental event, which happens due to the robust self-ubiquitylation activity of Ubc6, which starts the ubiquitylation cascade at the ligase. To distinguish between these two scenarios, it was the aim to generate and subsequently characterize a stable Ubc6 variant. For this purpose, ubiquitylation sites within Ubc6 were determined to mutate them and thereby preventing Ubc6 turnover. The linker region of Ubc6 was reported to be required for its continuous turnover [152]. This observation was supported by *in vitro* experiments showing that a truncated Ubc6 variant Ubc6ΔL, lacking the linker region, is not ubiquitylated *in vitro* (figure 3.4 b). Thus, it seems plausible that Ub acceptor sites are located within this linker area. Ubc6 contains around 11 lysine residues in the region connecting the catalytically core domain and the trans-membrane anchor (figure 3.20 a). Hence, mass spectrometry analysis was employed to identify potential ubiquitylation sites in Ubc6ΔTM. In a first analysis two ubiquitylated lysine residues at position 133 and 151 were detected. To test their relevance *in vitro* and *in vivo* these residues were mutated to arginine. Because lysine 133 is directly neighbored by another lysine residue at position 132, both amino acids were exchanged to ensure the complete disruption of this ubiquitylation site. However, cycloheximide decay experiments showed that the individual as well as the combined mutations (Ubc6ΔK3) did not diminish Ubc6 proteolysis (figure 3.20 b).

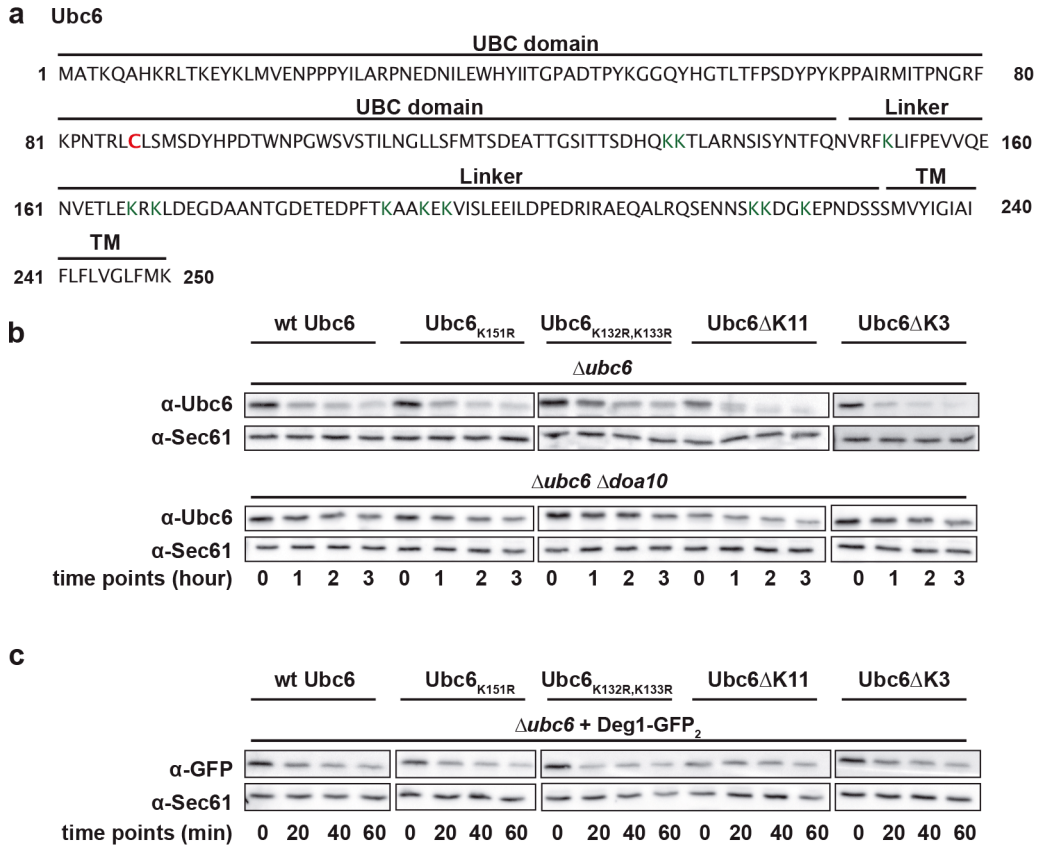

Figure 3.20 – Mutation of several lysine residues in the linker region of Ubc6 does not affect its proteolysis. (a) Protein sequence of Ubc6 with highlighted catalytically core domain (UBC), the linker region (Linker) and the transmembrane anchor (TM). Lysine residues, which were substituted to arginine, are depicted in green. **(b,c)** Cycloheximide decay experiments monitoring (b) Ubc6 or (c) Deg1-GFP_2 turnover in yeast strains expressing differing Ubc6 variants (wt Ubc6, $Ubc6_{K132R,K133R}$, $Ubc6_{K151R}$, $Ubc6_{K132R,K133R,K151R}$ (Ubc6ΔK3) and Ubc6ΔK11). The mutant Ubc6ΔK11 harbors lysine to arginine substitutions at following positions: 132, 133, 151, 167, 169, 188, 191, 193, 221, 222 and 225. Ubc6 turnover was additionally analyzed in yeast cells devoid of *DOA10*. Samples were analyzed by SDS-PAGE and immunoblotting and probed for Ubc6 or GFP and Sec61 (loading control).

The stability of the Ubc6 mutants was tested in yeast strain deleted for *DOA10*. All Ubc6 variants displayed diminished proteolysis under these conditions, which indicates that they are still degraded through the Doa10 pathway. This was supported by cycloheximide decay assays monitoring the turnover of the Doa10 model substrate Deg1-GFP_2, which did not display any perturbations due to the expression of the different Ubc6 variants (figure 3.20 c). Additionally, *in vitro* ubiquitylation experiments demonstrated that all Ubc6ΔTM variants were similarly ubiquitylated when compared to wt Ubc6ΔTM (data not shown). Summing up, the experiments suggest that both identified ubiquitylation sites do not substantially contribute to Ubc6 turnover. Additionally, the observations provide further evidence for Ubc6 being extremely versatile in choosing ubiquitylation sites within its linker region. This phenomenon was already observed for Doa10R *in vitro* ubiquitylation, where Ubc6 did not target a specific lysine residue (section 3.1.4). Further mass spectrometric analysis identified additional ubiquitylation sites in Ubc6ΔTM. Mutation of these sites alone as well as combinations of these mutations did not impact Ubc6 turnover (data not shown). Even substitution of all 11 lysine residues to arginine in the linker area (Ubc6ΔK11) had no influence on the half-life of the protein *in vivo* (figure 3.20 b). However, steady-state levels of this Ubc6 variant were diminished, which explains a slower turnover of Deg1-GFP_2 in these cells (figure 3.20 c). Ubc6ΔK11 is still degraded by the Doa10 pathway because it accumulates in Δ*doa10* yeast cells, which suggests that this variant is at least partially active.

For further characterization, Ubc6ΔK11ΔTM was expressed in *E.coli* and purified. *In vitro* ubiquitylation experiments showed that the variant still auto-ubiquitylated itself to a similar extent as wt Ubc6ΔTM (figure 3.21). The variant mono-ubiquitylated Doa10R only moderately. The reasons for this behavior are unknown. However, it can be speculated that the severe manipulation of the Ubc6 linker region might affect the interaction with Doa10R. To test if the prominent ubiquitylation on Ubc6ΔTM is located on lysine residues or if it involves the modification of other amino acids such as serine or threonine residues, samples were incubated with 100 mM NaOH. Oxyester linkages between the C-terminus of Ub and the hydroxyl-group of amino acid are susceptible to changes in the pH [177]. In contrast, isopeptide linkages between

the ε-amino group of a lysine residue and the carboxyl-group of the C-terminus of Ub are not cleaved upon elevation of pH levels. Additionally, ubiquitylation was also reported to occur on cysteine residues. Thioester linkages between cysteine residues and the C-terminus of Ub can be cleaved by adding reducing agents as β-mercaptoethanol [59].

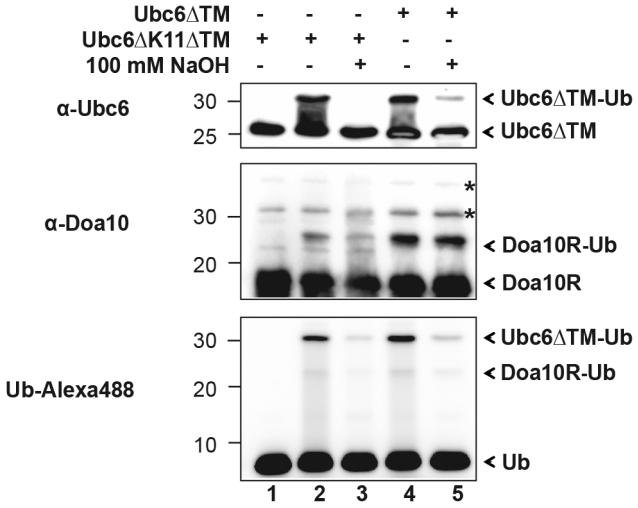

Figure 3.21 – Ubc6ΔTM is ubiquitylated at hydroxylated amino acids *in vitro*. Ubc6ΔK11ΔTM and wt Ubc6ΔTM were incubated with Doa10R, fluorescently labeled Ub and E1 enzyme. Samples were incubated with 100 mM NaOH when indicated. The sample in lane 1 did not contain ATP (negative control). Asterisks mark cross-reaction signals of the corresponding antibody.

Surprisingly, most of the ubiquitylation signals on Ubc6ΔK11ΔTM and Ubc6ΔTM were removed upon treatment with NaOH. This observation indicates that Ubc6ΔTM is primarily ubiquitylated at serine or threonine residues but not on lysine residues. The ubiquitylation signal on Ubc6ΔTM was not cleaved off upon the addition of β-mercaptoethanol, which argues against cysteine ubiquitylation of Ubc6ΔTM *in vitro* (data not shown). However, the general analysis of reaction products was conducted in presence of the reducing agent DTT, which might already remove such linkages. Thus, further experiments are required to fully exclude ubiquitylation of cysteine residues within Ubc6ΔTM. Ubiquitylation of lysine residues seems to play a minor role in Ubc6ΔTM self-modification *in vitro*. This becomes evident by the small amount of Ubc6ΔTM-Ub, which is detectable after the NaOH treatment. Of note, Ub was fully removed from Ubc6ΔK11ΔTM in NaOH treated samples,

which demonstrates that some lysine residues are modified within the linker region. These results imply that Ubc6 is able to target various sites within its linker area. Additionally, the E2 does not only mount Ub on lysine residues but also on hydroxylated amino acids.

3.2.2 Ubc6ΔTM is ubiquitylated at hydroxylated amino acids *in vitro*

Experiments presented in the previous section 3.2.1 gave some evidence for ubiquitylation of serine or threonine residues on Ubc6ΔTM *in vitro*. However, dissociation of putative oxyester linkages with high pH is by no means a direct proof for such an activity. To determine if Ubc6 is able to ubiquitylate hydroxylated amino acids, mass spectrometry analysis was employed, using an adapted protocol to preserve oxyester linkages (sections 2.3.17 and 2.3.18). Several amino acids including lysine but also serine and threonine residues were identified as potential ubiquitylation sites (table 3.2).

Table 3.2 – List of potentially ubiquitylated amino acids within Ubc6ΔTM identified by MS.

Amino acid	Position	Unambiguous identification	Experimentally investigated
Lysine	15	no	no
Lysine	67	no	no
Lysine	151	no	yes
Lysine	169	no	yes
Lysine	188	no	yes
Lysine	193	yes	yes
Serine	139	no	no
Serine	196	yes	yes
Threonine	139	no	no
Threonine	164	no	no
Threonine	178	no	no
Threonine	187	no	no

Interestingly, the majority of these residues clustered in the linker region, the putative ubiquitylation "hot spot" of Ubc6. However, most of these positions could not be definitely identified as Ub acceptor sites in the mass spectrometric analysis because the corresponding fragments of the tryptic peptides were not detected. Nevertheless it can be assumed that some of them are indeed ubiquitylated. The ubiquitylation of one serine residue was clearly assigned to position 196 in Ubc6 with mass spectrometry (figure 3.22 a,b).

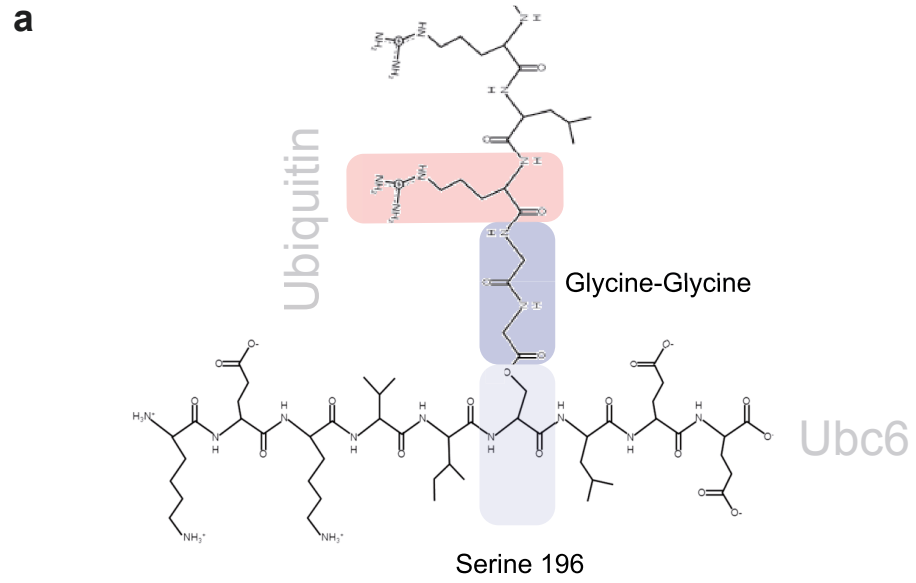

Figure 3.22 – Ubc6ΔTM is ubiquitylated at serine 196. (a) Schematic representation of the chemical structure of an oxyester bond between the C-terminus of a Ub molecule and a hydroxyl-group of the serine side chain in Ubc6 at position 196. **(b)** Ubc6ΔTM was incubated with E1, Ub and ATP for 20 min and subsequently separated on SDS-PAGE gels and Commassie stained. Ubc6ΔTM-Ub was isolated and processed as described in section 2.3.17. The b and γ-fragmentation pattern of the tryptic peptide covering amino acids from 194 to 206 shows a Gly-Gly site on serine 196 (page 75). Mass spectrometry measurements and analysis were performed by Oliver Popp and Gunnar Dittmar. The figure was adapted from Weber *et al.* [155].

b

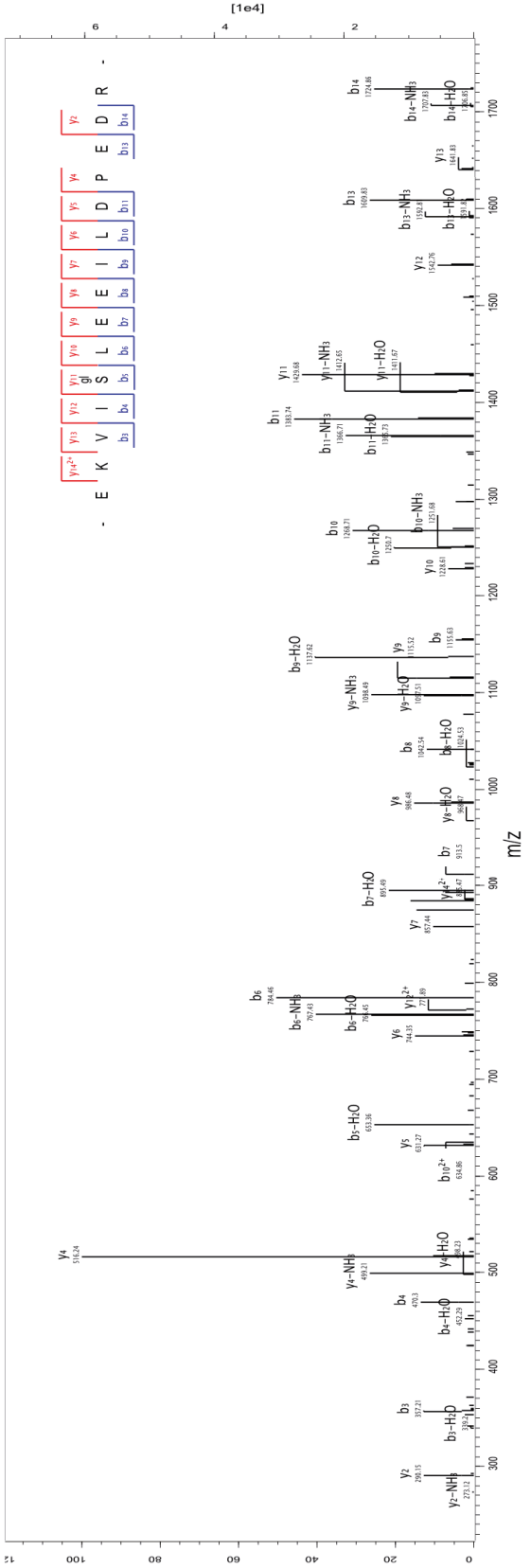

To determine any relevance of serine 196 ubiquitylation for Ubc6 function or turnover, it was substituted to alanine and the resulting Ubc6 variant was analyzed *in vitro* and *in vivo*. Remarkably, Ubc6$_{S196A}$ΔTM was significantly less ubiquitylated *in vitro* when compared to wt Ubc6ΔTM (figure 3.23). Still, the Ubc6$_{S196A}$ΔTM-Ub signal decreased slightly upon NaOH treatment, which suggests that serine 196 is the most important but not the only hydroxylated amino acid in Ubc6 that can be ubiquitylated. Ubc6$_{S196A}$ΔTM mono-ubiquitylated Doa10R to a similar extent as wt Ubc6ΔTM, which demonstrates that the amino acid substitution does not interfere with the enzymatic activity of the E2.

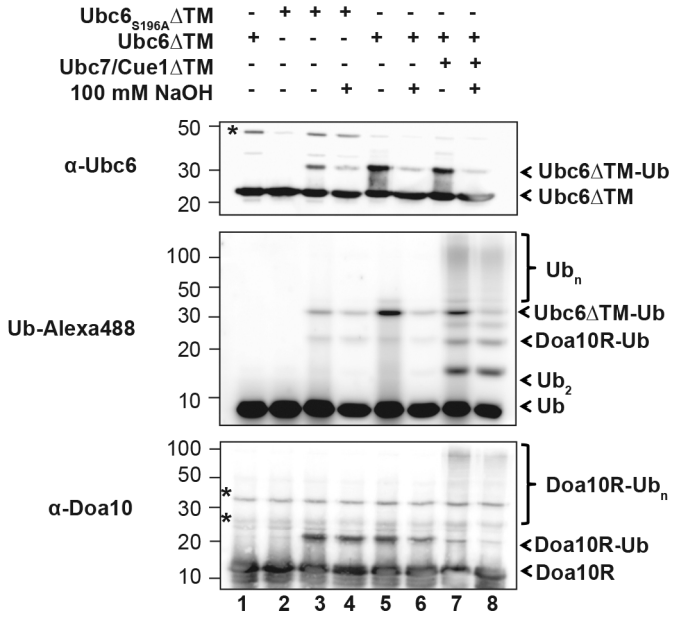

Figure 3.23 – Mutation of serine 196 significantly reduces Ubc6 auto-ubiquitylation *in vitro*. wt Ubc6 and Ubc6$_{S196A}$ΔTM were incubated with Doa10R, fluorescently labeled Ub and E1 as well as Ubc7/Cue1ΔTM (lane 7 and 8). 100 mM NaOH was added when indicated (lane 4, 6 and 8). Negative controls are displayed in lane 1 and 2, which were devoid of ATP. Asterisks mark non-specific cross-reaction signals of the respective antibody. The figure was adapted from Weber *et al.* [155].

Doa10R ubiquitylation was preserved upon addition of NaOH (figure 3.23 lane 4, 6 and 8) as well as unanchored K48-linked Ub chains formed by Ubc7 (figure 3.23, lane 8). This shows that the elevated pH levels do not dissipate

lysine-linked Ub conjugates in the *in vitro* assay.

To test if Ubc7 is able to elongate Ub moieties, which are attached to hydroxylated amino acids, wt Ubc6ΔTM-Ub and $Ubc6_{S196A}$ΔTM-Ub conjugates were purified and incubated with Ubc7 and Cue1ΔTM in presence of Ub and E1 enzyme. Ub-Ubc6ΔTM as well as Ub-$Ubc6_{S196A}$ΔTM were poly-ubiquitylated by Ubc7 in the course of this reaction (figure 3.24, lane 3 and 7). However, poly-Ub chains showed an increased sensitivity to elevated pH levels when they were attached to wt Ubc6ΔTM as when conjugated to the mutant (figure 3.24, lane 4 and 8). Thus, it can be assumed that in wt Ubc6ΔTM serine 196 is predominantly mono-ubiquitylated and serves as template for subsequent Ub-chain elongation by Ubc7. In absence of serine 196 other amino acids especially lysine residues are mono-ubiquitylated and thus elevated pH level do not affect these modifications. However, *in vivo* experiments are absolutely required to confirm these *in vitro* observations to ensure that no artifacts are analyzed in the *in vitro* setup.

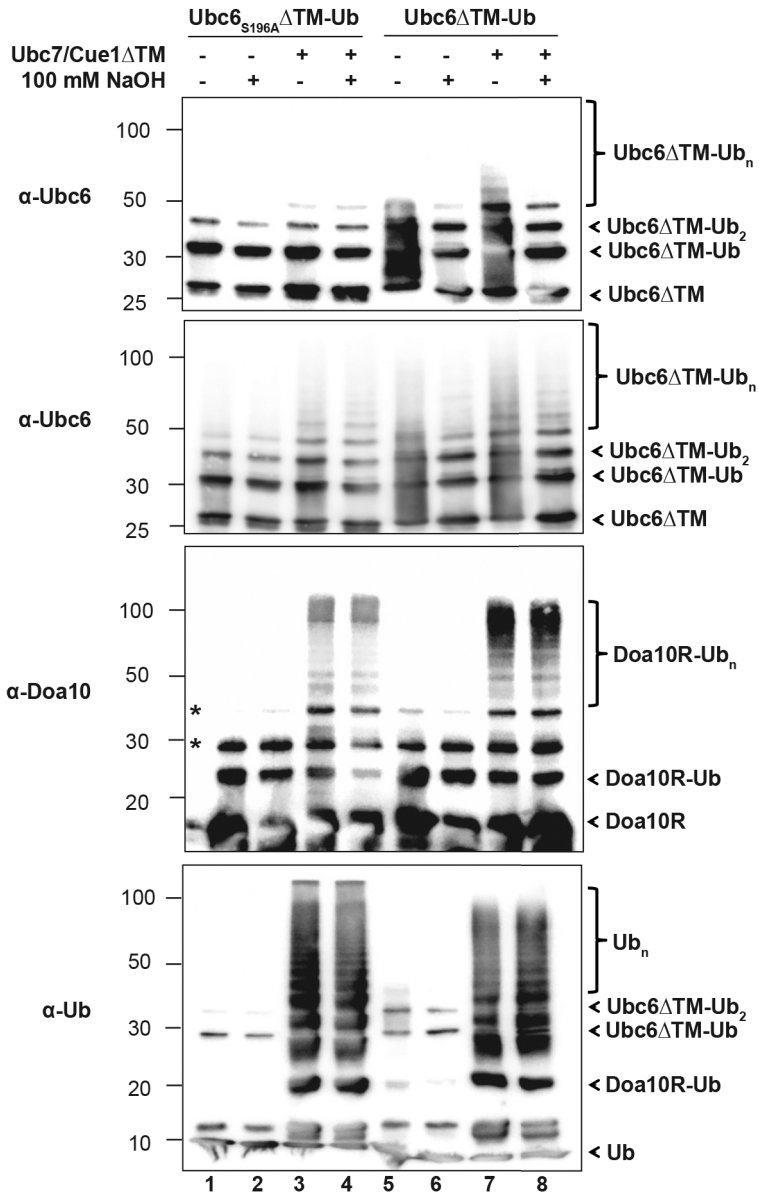

Figure 3.24 – Ubc7 is able to conjugate Ub chains to Ub moieties attached to hydroxylated amino acids. Enriched wt Ubc6ΔTM-Ub and $Ubc6_{S196A}$ΔTM-Ub species were incubated with Ubc7/Cue1ΔTM to initiate their poly-ubiquitylation (lane 3, 4 and lane 7, 8). Samples were incubated with 100 mM NaOH where indicated (lane 2, 4 and lane 6, 8). SDS-PAGE and immunoblotting were applied. Two images of the same Ubc6 blot are presented with differences in contrast and brightness to emphasize signals for weak Ubc6 poly-ubiquitylation. Asterisks mark non-specific cross-reaction signals of the respective antibody.

3.2.3 Ubc6 catalyzes non-conventional ubiquitylation events *in vivo*

In vitro experiments implicate non-canonical ubiquitylation of hydroxylated amino acids by Ubc6. Cycloheximide decay assays were employed to assess the impact of the serine to alanine substitution at position 196 on Ubc6 degradation *in vivo* (figure 3.25 a,b). The turnover of the $Ubc6_{S196A}$ variant was not diminished when compared to wt Ubc6 (figure 3.25 a).

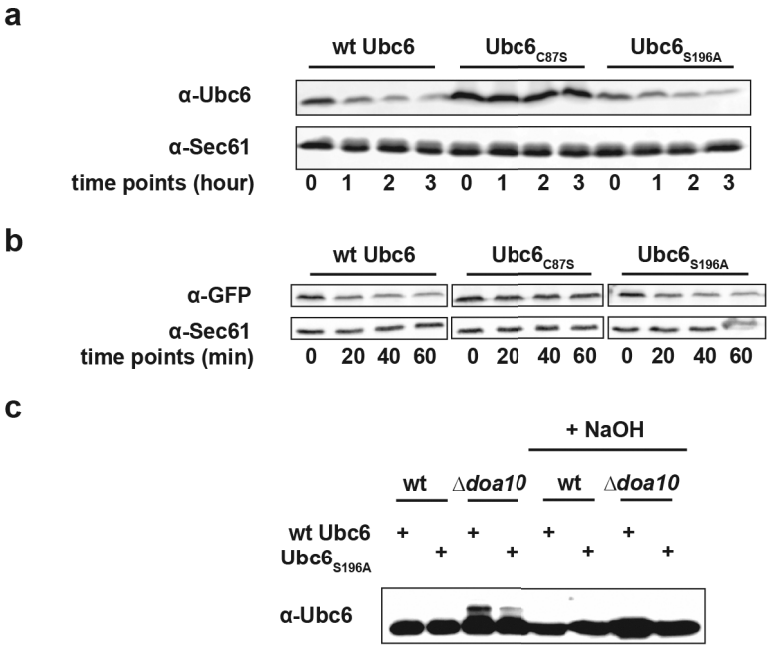

Figure 3.25 – $Ubc6_{S196A}$ does not display a degradation defect *in vivo*. **(a,b)** Cycloheximide decay assays monitoring the turnover of (a) Ubc6 and (b) Deg1-GFP_2 in Δ*ubc6* yeast cells expressing different Ubc6 variants (wt Ubc6, $Ubc6_{C87S}$ and $Ubc6_{S196A}$) from plasmid. Inactive Ubc6 ($Ubc6_{C87S}$) served as negative control. Samples were probed for Ubc6 or GFP and Sec61 (loading control).**(c)** Total cell extract was prepared from Δ*ubc6* yeast cells with and without disruption of the *DOA10* gene, which carried plasmids encoding for wt Ubc6 or $Ubc6_{S196A}$ as well as an overexpression plasmid for wt Ub. Samples were incubated with 150 mM NaOH when indicated and were probed for Ubc6. The figure was adapted from Weber *et al.* [155].

Consequently, degradation of the Doa10 model substrate Deg1-GFP_2 was neither affected (figure 3.25 b). These observations suggest that serine 196 is

not solely responsible for the initiation of Ubc6 degradation *in vivo*. It can be assumed that other amino acids in the linker are ubiquitylated, which then serve as priming template for Ubc7. This is in agreement with previous studies on the non-secreted immunoglobulin light chain NS-1, whose turnover was only efficiently diminished by mutating all putative ubiquitylation sites within the protein [75]. To study the relevance of non-conventional ubiquitylation events *in vivo*, ubiquitylation of wt Ubc6 and $Ubc6_{S196A}$ was determined when subjected to elevated pH levels (figure 3.25 c). In absence of Doa10, both Ubc6 variants were mono-ubiquitylated, but $Ubc6_{S196A}$ to a lesser extent as the wt protein. This is in line with results from *in vitro* experiments presented in figure 3.23. Both Ub modifications were susceptible to elevated pH levels, which implies that non-canonical ubiquitylation of hydroxylated amino acids plays a major role in Ubc6 proteolysis. Summing up, serine 196 indeed participates in Ubc6 ubiquitylation *in vivo*, however it is not the only amino acid, which can serve as priming site for poly-ubiquitylation. This observation adds another evidence for the flexibility of Ubc6 in choosing ubiquitylation sites in client proteins.

3.2.4 Ubc6 facilitates degradation of the Doa10 substrate Sbh2 in absence of accessible lysine residues

Sbh2 is a tail-anchored protein of the endoplasmic reticulum (figure 3.26 a), which in absence of its binding partner Ssh1 is degraded via the Doa10 ligase complex (figure 3.26 b,c) [187]. Interestingly, turnover of Sbh2 was only mildly affected in cells devoid of *UBC6* but strongly affected in Δ*ubc7* strains [187]. This suggests, that Ubc7 is able to initiate proteolysis of this protein, through in a less efficient manner as Ubc6. Sbh2 exhibits a prominent cluster of lysine residues in its cytosolic domain (figure 3.26 a, red dots). Interestingly, a Sbh2 variant Sbh2Δ4K, which harbors amino acid substitutions to arginine at these positions, was still degraded with the same half-life as the wt protein. However, the turnover of Sbh2Δ4K depends strongly on Ubc6 (figure 3.26 b,d). In contrast, mutation of lysine 48 in Sbh2, which is located downstream from the lysine cluster, did not interfere with Sbh2 proteolysis (data not shown).

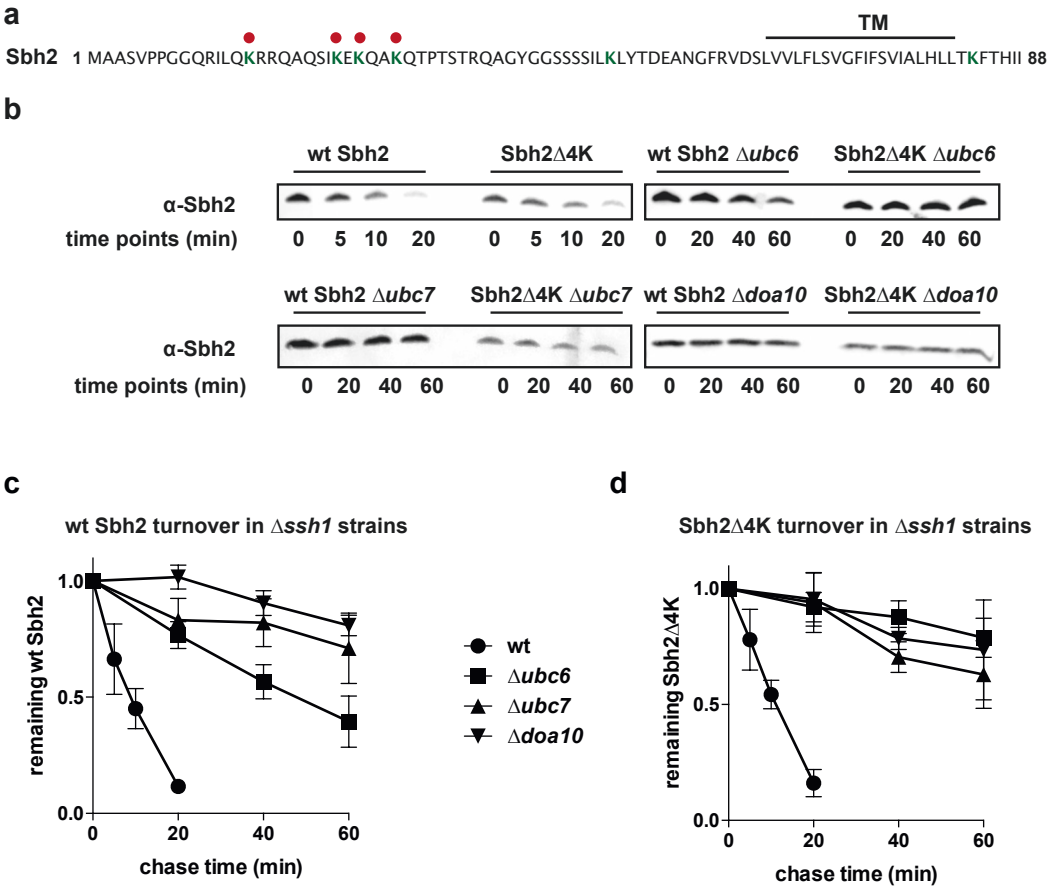

Figure 3.26 – Sbh2 turnover can be driven into Ubc6 dependency by mutating cytosolic lysine residues. **(a)** Sequence of Sbh2 with highlighted lysine residues at position 15, 23, 25, 28, 48 and 83 (green). Lysine residues substituted to arginine in the Sbh2 variant Sbh2Δ4K are marked with a red dot. **(b)** Cycloheximide decay assay monitoring turnover of wt Sbh2 and Sbh2Δ4K in yeast cells devoid of *SSH1* combined with different gene knockouts of Doa10 ligase components. **(c,d)** Quantification of Sbh2 signals from cycloheximide experiments of (c) wt Sbh2 and (d) Sbh2Δ4K as exemplary presented in (b). Error bars represent standard deviation of mean of at least 3 independent experiments. The figure was adapted from Weber *et al.* [155].

Immunoprecipitation of FLAG-tagged Sbh2 variants demonstrates that wt Sbh2 is significantly stronger ubiquitylated in Δ*ubc6* cells when compared to Sbh2Δ4K (figure 3.27). Thus, it can be assumed that Ubc7 is able to attach Ub moieties directly to wt Sbh2 to one or several sites in its cytosolic lysine cluster.

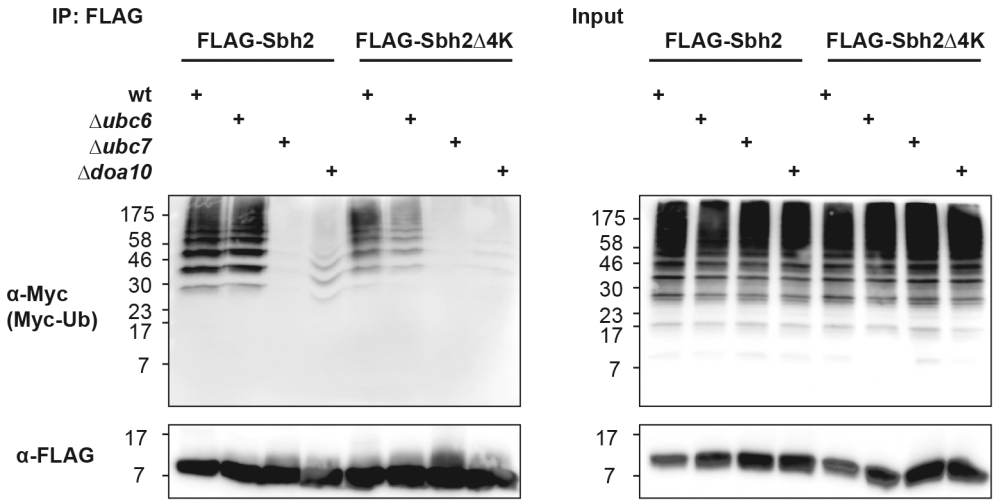

Figure 3.27 – Sbh2 is ubiquitylated in yeast cells devoid of *UBC6*. FLAG-tagged wt Sbh2 and Sbh2Δ4K were immunoprecipitated from yeast cell extract prepared from strains devoid of proteins of the Doa10 ligase complex as well as *SSH1*. All cells were overexpressing Myc-tagged Ub from plasmid. Additionally, all strains harbored a proteasomal mutant *rpt4R* to diminish proteolytic turnover, which in turn enriched ubiquitylated protein species within the cells. Samples were analyzed by SDS-PAGE and immunoblotting and probed for Myc and FLAG. The figure was adapted from Weber *et al.* [155].

Ubc6 seems to be flexible in choosing ubiquitylation sites in Sbh2, since Sbh2Δ4K, which lacks cytosolic lysine residues, was degraded with a similar kinetic as wt Sbh2 (figure 3.26). To test whether Ubc6 ubiquitylates hydroxylated amino acids in absence of suitable lysine residues, FLAG-tagged wt Sbh2 and Sbh2Δ4K were immunoprecipitated and the samples were treated with NaOH prior to loading on SDS-gels. As expected, ubiquitylation of Sbh2Δ4K was removed upon elevation of pH levels, whereas ubiquitylated species of wt Sbh2 were stable under these conditions (figure 3.28). This suggests that Sbh2Δ4K is ubiquitylated at hydroxylated amino acids. Ubiquitylation signals for mutant Sbh2Δ4K were weaker when compared to wt Sbh2 (compare lane 2

and 3 in figure 3.28). Either Sbh2Δ4K is less ubiquitylated as the wt protein or ubiquitylated material is lost during the experimental procedure due to the fragile nature of the oxyester bonds between substrate and Ub moieties. The second assumption would also explain why Ubc6 ubiquitylation, which mostly depends on a non-canonical serine ubiquitylation, is hardly detectable in immunoprecipitation experiments (figure 3.17). Summing up, it becomes evident that Ubc6 ubiquitylates hydroxylated amino acids in absence of accessible lysine residues, which ensures efficient degradation of Doa10 client proteins during protein quality control.

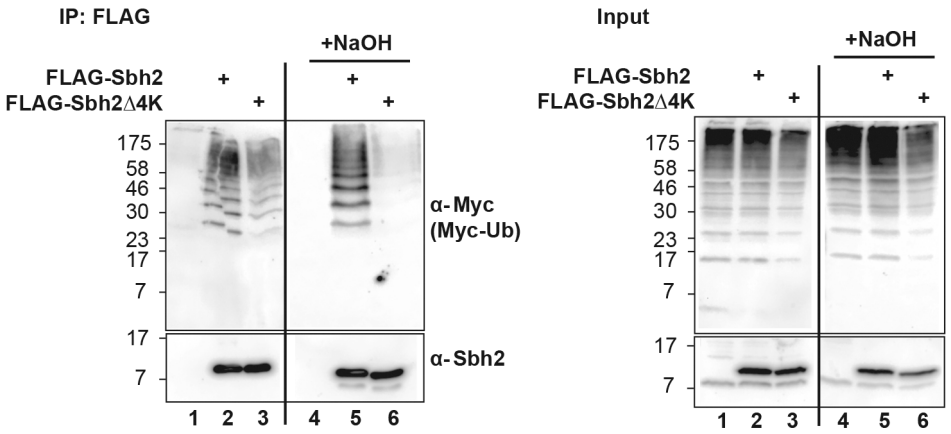

Figure 3.28 – Ubiquitylation of Sbh2Δ4K is susceptible to elevated pH levels. FLAG-tagged wt Sbh2 and Sbh2Δ4K were immunoprecipitated from cell extract prepared from yeast strains devoid of *SSH1*. All strains overexpressed Myc-tagged Ub from plasmid. Samples were treated with 150 mM NaOH when indicated. Samples generated from strains, which did not contain FLAG-tagged protein, served as negative control (lane 1 and 4). The here presented experiment was performed by Ernst Jarosch. The figure was adapted from Weber *et al.* [155].

3.3 Characterization of the Ubc6 overexpression phenotype

3.3.1 Ubc6 overexpression impairs Doa10 dependent substrate degradation

Initially, the Ub conjugating enzyme Ubc6 was identified as a high copy number suppressor of the temperature sensitive growth phenotype in yeast strains that harbor the *sec61-2* mutation [151]. The Sec61 mutant protein is selectively degraded at elevated temperatures, which results in reduced protein levels [188, 189]. Because Sec61 is part of the essential protein translocation apparatus of the ER, these cells fail to grow under these conditions [157]. Deletion of components of either the Doa10 ligase or the Hrd1 ligase can partially rescue growth due to a diminished degradation of the mutant protein, which results in elevated protein levels within the cells (figure 3.29) [189].

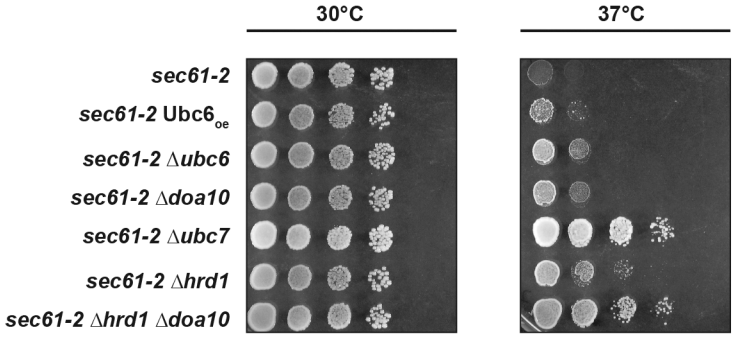

Figure 3.29 – The *sec61-2* growth phenotype is suppressed in cells devoid of *UBC6* as well as in cells overexpressing the E2 enzyme. Suppression of the *sec61-2* growth defect in yeast strains carrying gene disruptions of Doa10 and Hrd1 ligase components. *UBC6* overexpression was induced with a high copy plasmid encoding for Ubc6 under its endogenous promoter. All other strains were transformed with an empty vector control. Cells were plated on appropriate selection medium and incubated at 30 °C and 37 °C.

Because the Hrd1 and the Doa10 pathway are both involved in the degradation of Sec61-2, deletion of *UBC7* showed a similar degree of suppression as the double knockout of the ligases (figure 3.29). Remarkably, the overproduction

of Ubc6 suppressed the *sec61-2* phenotype to a similar extent as a *UBC6* or *DOA10* loss-of-function mutant (figure 3.29) [151]. Thus, it can be assumed that elevated Ubc6 protein levels negatively impact the proteolysis of Doa10 client proteins. To evaluate if *UBC6* overexpression generally affects Doa10 substrate turnover, cycloheximide decay assays were performed. Degradation of Ubc6 was impaired when overexpressed (figure 3.30 a,b). Since the E2 enzymes Ubc6 and Ubc7 act at the same ligase, elevated Ubc6 levels might displace Ubc7 from the complex and thereby affecting Doa10 dependent protein degradation. However, the observed *UBC6* overexpression phenotype could not be rescued by the simultaneous overproduction of Ubc7 and Cue1. Further elevation of Doa10 protein levels also did not rescue the phenotype. These observations suggest that *UBC6* overexpression has a dominant negative effect on Doa10-mediated protein turnover. On the contrary, elevated levels of Ubc7 and Cue1 did not display any influence on endogenous Ubc6 turnover. Notably, overproduction of a Ubc6 variant, which lacked its catalytic core domain (Ubc6ΔUBC) but was stably recruited to the Doa10 ligase (figure 3.34 lane 6), did not result in a diminished proteolysis of endogenous Ubc6. This shows that the dominant negative effect of *UBC6* overexpression depends on its enzymatic activity.

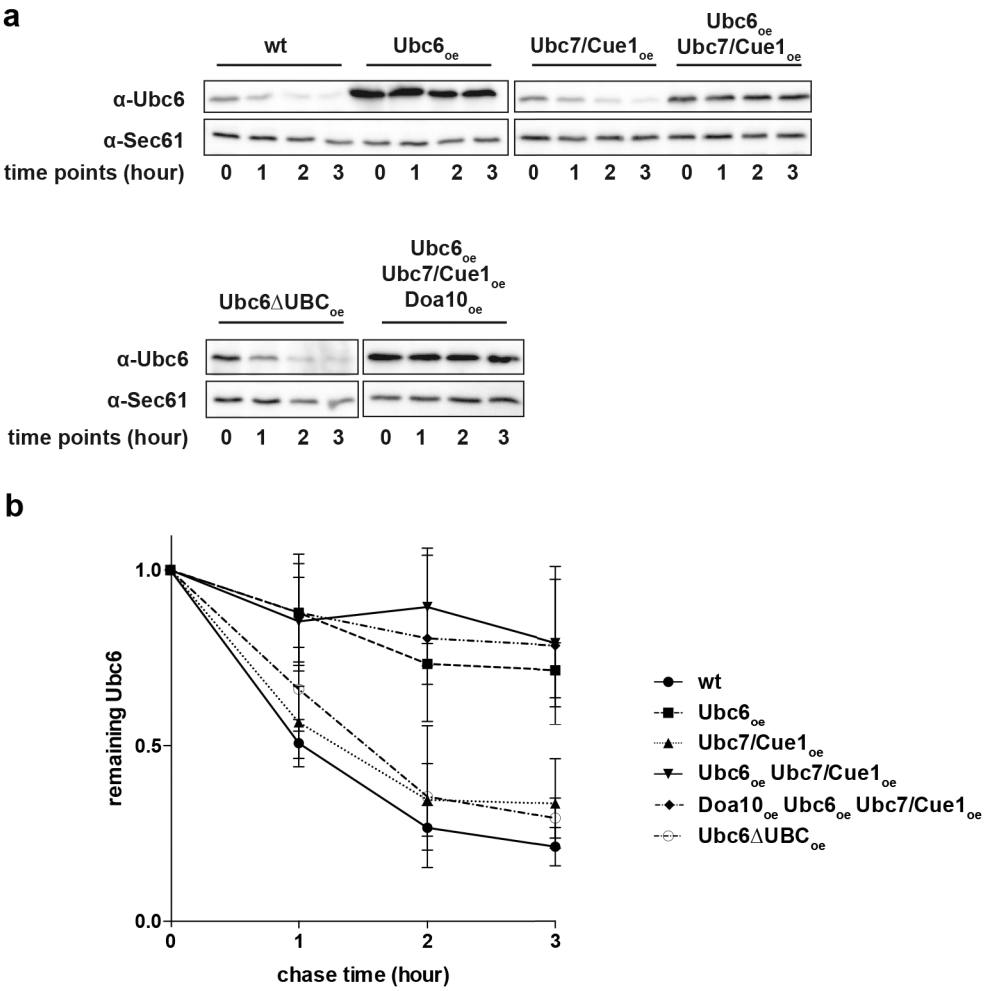

Figure 3.30 – Proteolysis of Ubc6 is diminished when the protein is overproduced. (a) Cycloheximide decay assay monitoring Ubc6 turnover under wt and different overexpression conditions of Doa10 ligase components as well as a Ubc6 variant lacking the UBC core domain (Ubc6ΔUBC). Increased expression levels of Ubc6 variants, Ubc7 and Cue1 were induced with high copy plasmids. Elevated Doa10 protein levels were generated by substitution of the Doa10 promoter with the TEF-promoter. Samples were analyzed by SDS-PAGE and immunoblotting and probed for Ubc6 and Sec61 (loading control). Overexpression of Doa10 components was validated by immunoblotting (data not shown). **(b)** Quantification of Ubc6 signals from cycloheximide experiments as exemplary shown in (a). Error bars represent standard deviation of mean from at least 3 independent experiments.

The turnover of Deg1-GFP_2 was monitored to investigate the impact of *UBC6* overexpression on other Doa10 substrates (figure 3.31 a,b). Deg1-GFP_2 proteolysis was significantly diminished when Ubc6 protein levels were elevated, despite the parallel overexpression of other Doa10 ligase components. Again, the overproduction of a truncated Ubc6 variant lacking the UBC core domain (Ubc6ΔUBC) did not influence the degradation of Deg1-GFP_2. Of note, quantification of GFP signals from cycloheximide experiments indicates that the *UBC6* overexpression effects on Deg1-GFP_2 turnover are rather variable (huge standard deviation of mean for different time points). Generally, expression levels of proteins induced by 2-micron plasmids are rather fluctuating, possibly because of variations in the copy number of plasmids within individual cells [190]. Hence, Ubc6 levels might vary between independent experiments, which results in a differing level of suppression of the Deg1-GFP_2 proteolysis.

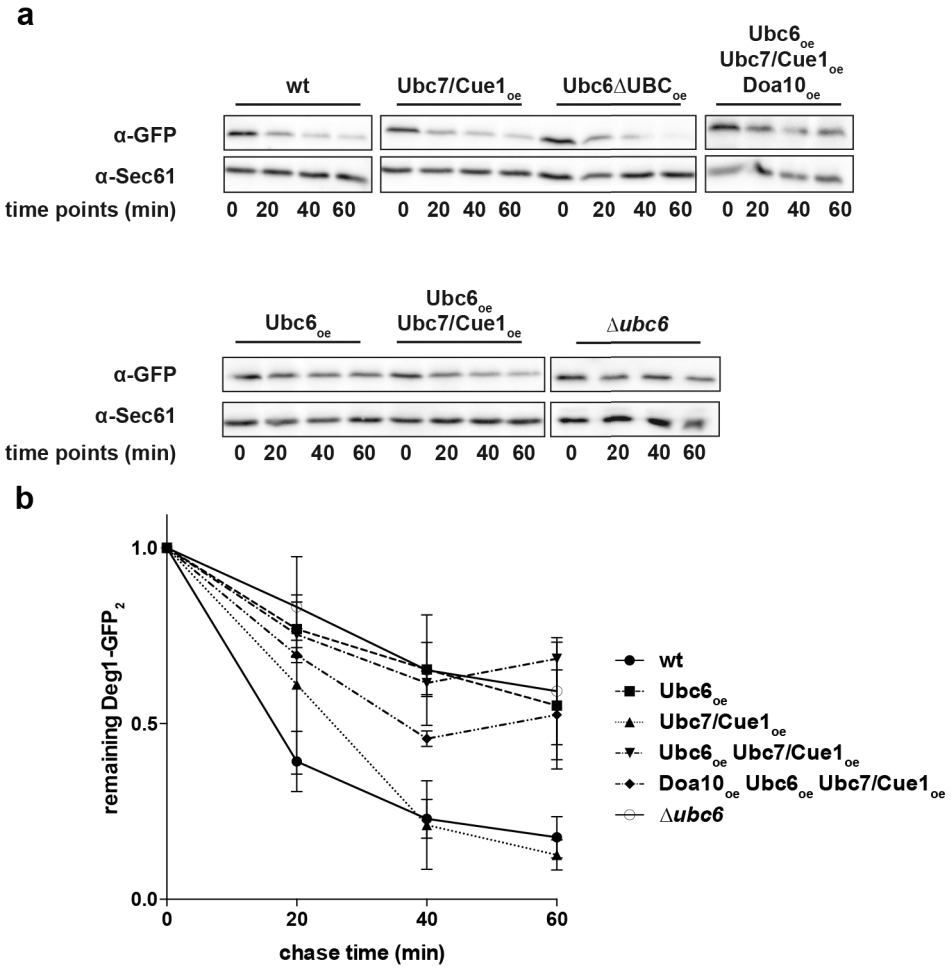

Figure 3.31 – Increased Ubc6 protein levels impair degradation of Deg1-GFP$_2$. (a) Cycloheximide decay assay monitoring Deg1-GFP$_2$ turnover under wt and different overexpression conditions of Doa10 ligase components as well as a Ubc6 variant lacking the UBC core domain (Ubc6ΔUBC). Increased expression levels of Ubc6 variants, Ubc7 and Cue1 were induced with high copy plasmids. Elevated Doa10 protein levels were generated by substitution of the Doa10 promoter with the TEF-promoter. Turnover of Deg1-GFP$_2$ in Δ*ubc6* cells served as negative control. Samples were analyzed by SDS-PAGE and immunoblotting and probed for GFP and Sec61 (loading control). **(b)** Quantification of GFP signals from cycloheximide experiments as exemplary shown in (a) (except for Ubc6ΔUBC$_{oe}$). Error bars represent standard deviation of mean from at least 3 independent experiments.

Turnover of another Doa10 substrate Sbh2, which is degraded with a half-life of less than 10 min, appears to be only moderately affected by elevated Ubc6 levels (figure 3.32 a,b). Because proteolysis of Sbh2 is only partially dependent on Ubc6, questions were raised if *UBC6* overexpression only affects Doa10 substrates, which absolutely require this E2 for degradation. However, proteolysis of Sbh2Δ4K, a Sbh2 variant whose turnover fully dependents on Ubc6 (figure 3.26), was impaired to an extent as the wt protein when Ubc6 was overproduced (data not shown). Therefore, special characteristics of this substrate must account for the robustness of its degradation under Ubc6 overproduction conditions.

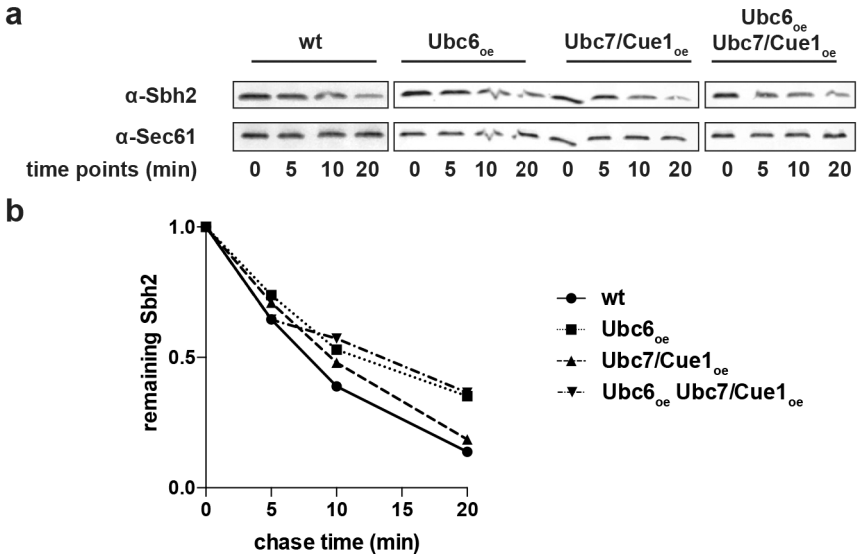

Figure 3.32 – Sbh2 turnover is only marginally affected by elevated Ubc6 levels. (a) Cycloheximide decay assay monitoring Sbh2 turnover in cells devoid of *SSH1*. Overexpression of *UBC6*, *UBC7* and *CUE1* was induced with high copy plasmids. Samples were analyzed by SDS-PAGE and immunoblotting and probed for Sbh2 and Sec61 (loading control). **(b)** Quantification of Sbh2 signals from cycloheximide experiment presented in (a).

UBC6 overexpression was shown to have a significant impact on degradation of a large number of Doa10 target proteins. To exclude that the overproduction of a membrane anchored protein affects general ER homeostasis, the turnover of CPY* was monitored (figure 3.33). CPY* is an instable variant of the vacuolar carboxypeptidase yscY with a glycine to arginine substitution at position 255 [191]. The mutant protein is unable to fold correctly within

the ER compartment and is consequently degraded by the Hrd1 but not by the Doa10 ligase. CPY* proteolysis was slightly impaired when Ubc6 was overproduced but not as strongly as in Δ*ubc7* cells (figure 3.33). This is in line with the results from the *sec61-2* growth assay, in which *UBC6* overexpression allowed the growth of cells to a similar extent as *UBC6* or *DOA10* knockout strains (figure 3.29). Furthermore, the stability of Doa10 was assed during *UBC6* overexpression (figure 3.33, Doa10 blot). Ubc6 overproduction did not cause changes in the amount of Doa10 within cells. Thus diminished Doa10 levels cannot account for the observed degradation defect. Summing up, it can be assumed that elevated Ubc6 levels have an exclusive impact on the turnover of Doa10 substrates.

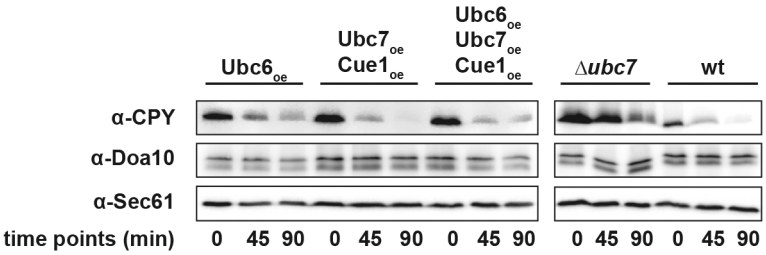

Figure 3.33 – CPY* turnover is not significantly influenced by *UBC6* overexpression. (a) Cycloheximide decay assay monitoring CPY* turnover. Overexpression of *UBC6*, *UBC7* and *CUE1* was induced with high copy plasmids. Degradation of CPY* in Δ*ubc7* cells served as negative control. Samples were analyzed by SDS-PAGE and immunoblotting and probed for CPY, Doa10 and Sec61 (loading control).

3.3.2 Ubc6 and Ubc7 do not compete for binding to Doa10

In section 3.3.1 it was demonstrated that elevated *UBC6* expression impairs proteolysis of Doa10 client proteins. This observation indicates that Ubc6 and Ubc7 might compete for recruitment to the Doa10 ligase. To verify this assumption, native immunoprecipitation experiments were performed to study the level of both E2 enzymes under different overexpression conditions (figure 3.34). Strikingly, Ubc6 levels were extremely low under wt conditions at the Doa10 ligase but strongly elevated when overproduced (compare lane 1 with lane 4 in figure 3.34). However, overproduction of Ubc6 did not diminish

the amount of Ubc7 and Cue1, which co-precipitated with the Doa10 ligase (compare lane 1 with lane 4 in figure 3.34). Of note, residual amounts of Ubc6 bound unspecifically to the sepharose but co-precipitated amounts were still significantly increased in presence of the ligase (compare lane 2 with lane 3 or 4 in figure 3.34).

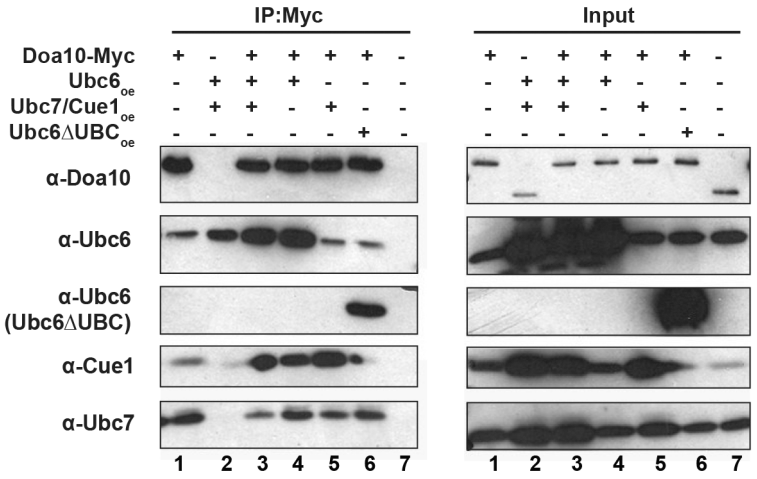

Figure 3.34 – Overproduction of Ubc6 does not deplete Ubc7 from the Doa10 ligase. Immunoprecipitation experiments of C-terminal Myc-tagged Doa10 were performed under native conditions. Ubc6 or/and Ubc7/Cue1 as well as a truncated Ubc6 variant lacking its catalytically UBC domain (Ubc6ΔUBC) were overproduced with high copy plasmids. Negative controls in lane 2 and 7 did not contain Myc-tagged Doa10. Samples were analyzed by SDS-PAGE and immunoblotting and were probed for Doa10, Ubc6, Cue1 and Ubc7. The here presented experiment was performed by Jasmin Schlotthauer.

An overexpressed truncated Ubc6 variant (Ubc6ΔUBC), which consists of the linker and trans-membrane region but omits the catalytic UBC domain, was stably recruited to the Doa10 ligase (figure 3.34 lane 6). Interestingly, the amount of endogenous Ubc6, which bound to the Doa10 ligase, did not change upon this increased presence of a Ubc6 fragment at the ligase complex. This observation indicates, that Ubc6 binding to the Doa10 ligase is not saturated under wt conditions, which in turn allows the increased recruitment of this E2 enzyme to the ligase when overproduced within cells. Summing up, it becomes evident, that Ubc6 levels seem to be tightly controlled at the Doa10 ligase. In turn, manipulating *UBC6* expression disturbs this fine balance and results in

elevated levels of the E2 enzyme at the ligase complex.

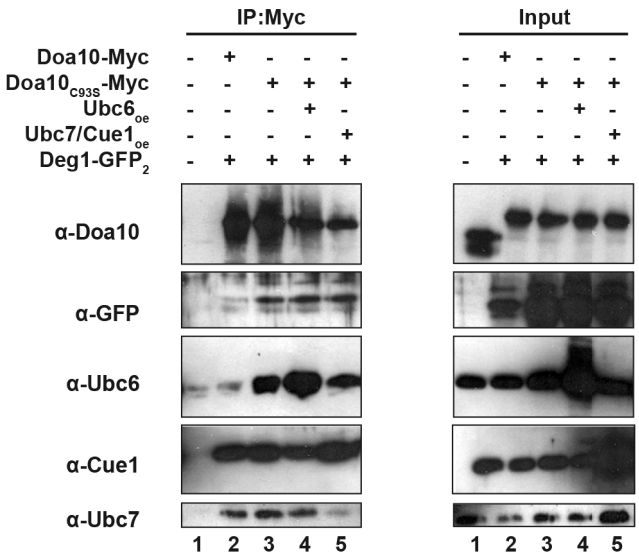

Figure 3.35 – Overexpression of Ubc6 does not influence substrate recruitment to the Doa10 ligase. Immunoprecipitation experiments of C-terminal Myc-tagged wt Doa10 and an inactive RING mutant $Doa10_{C93S}$ were performed under native conditions. Ubc6 or/and Ubc7/Cue1 were overexpressed with high copy plasmids and the model substrate Deg1-GFP_2 was expressed from an ARS/CEN plasmid. The negative control in lane 1 did not contain Myc-tagged Doa10. Samples were analyzed by SDS-PAGE and immunoblotting and were probed for Doa10, GFP, Ubc6, Cue1 and Ubc7.

Ubc6 is a substrate of the Doa10 ligase and its overexpression could influence the recruitment of other client proteins to the complex. To investigate this possibility, Doa10 was precipitated under overexpression conditions of *UBC6* or *UBC7/CUE1* in presence of the model substrate Deg1-GFP_2. Co-precipitated amounts of the substrate under different overexpression conditions were studied. Because Deg1-GFP_2 is a short-lived protein and cannot be easily detected at the ligase under wt conditions (figure 3.35, lane 2), a Doa10 RING mutant was employed to stall the substrate at the complex (figure 3.35, lane 3, 4 and 5). This RING mutation did not interfere with the recruitment of the E2 enzymes to the ligase complex. Thus, it can be assumed that both proteins form stable interactions with the Doa10 protein besides the RING domain. This assumption is supported by the observation that a Ubc6 fragment just containing the linker and trans-membrane region of Ubc6 (Ubc6ΔUBC) accumulates at the ligase

(figure 3.34, lane 6). Overexpression of either one of the E2 enzymes did not influence the amount of Deg1-GFP_2, which co-precipitated with the ligase. Thus it can be assumed, that Ubc6 levels do not influence the binding of cytosolic clients to the Doa10 ligase. However, influences of *UBC6* overexpression on recruitment of integral-membrane clients to Doa10 should be also evaluated in future.

3.3.3 Doa10 substrates are ubiquitylated when *UBC6* is overexpressed

It was demonstrated that overproduction of Ubc6 influences the ligase composition by elevating levels of the E2 enzyme at the Doa10 complex. Hence, the ubiquitylation status of substrates should be studied to understand the consequences of increased amounts of Ubc6 at the ligase. Immunoprecipitation of overexpressed Ubc6 clearly indicates, that Ubc6 is mono-ubiquitylated under these conditions (figure 3.36, Ubc6 and Ub blot). Since such a modification was observed even in absence of the Doa10 ligase (figure 3.17), it does not serve as an indicator for the ubiquitylation capacity of the ligase. Poly-ubiquitylated Ubc6 species could not be reliably identified from the Ub blots (see also figure 3.17). It appears, that higher molecular weight Ub signals are present under *UBC6* overexpression conditions. If these signals are generated by poly-Ub species or multiple mono-Ub moieties attached to Ubc6 remains elusive. Summing up, Ubc6 is not a suitable Doa10 substrate to study changes in the ubiquitylation pattern upon *UBC6* overexpression at the ligase.

Vma12-*DegAB* is a Doa10 model substrate, which is an excellent tool to study the ubiquitylation capacity of the Doa10 ligase [155, 192]. Initial immunoprecipitation experiments indicate that Vma12-*DegAB* is still ubiquitylated when Ubc6 is overproduced to a similar extent in wt, but the Ub chain composition is not studied so far (Tommer Ravid and Itamar Cohen unpublished data). This indicates that Ubc6 overexpression somehow disturbs the proteolytic signal on Doa10 target proteins, which prevents their subsequent processing by the proteasome. Further experiments addressing this problem are mandatory to understand the mechanistic fundamentals of the *UBC6* overexpression

phenotype.

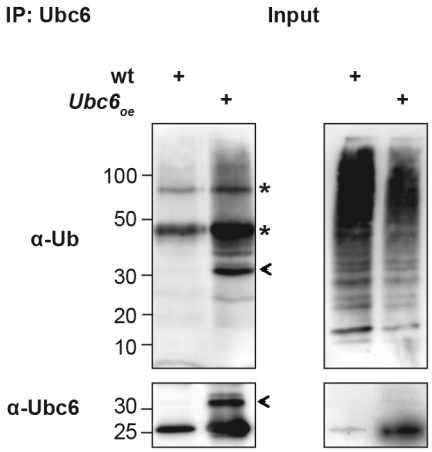

Figure 3.36 – Overproduced Ubc6 is mono-ubiquitylated. Immunoprecipitation experiments of Ubc6 under wt and overexpression conditions. Samples were analyzed by SDS-PAGE and immunoblotting and were probed for Ubc6 and Ub. Mono-ubiquitylated Ubc6 is highlighted with an arrowhead. Unspecific cross-reaction signals of antibodies are marked with an asterisk.

4 | Discussion

The Doa10 Ub ligase is a key player in ER-associated protein degradation (ERAD) and nuclear protein quality control. Its substrate spectrum covers a huge variety of different clients including cytosolic and nuclear but also integral-membrane proteins. The proteolysis of a majority of these polypeptides depends on the activity of two E2 enzymes: Ubc6 and Ubc7. To this date, it was unknown how the ligase facilitates the ubiquitylation of such a heterogeneous substrate pool and which role Ubc6 and Ubc7 play in this process. In this study it was demonstrated that Ubc6 and Ubc7 act in a sequential manner at the Doa10 ligase to ensure efficient poly-ubiquitylation of target proteins. Both enzymes exhibit highly specialized activities during the ubiquitylation cascade at the Doa10 complex. The ability of Ubc6 to attach Ub moieties not only to lysine residues within a substrate but also to hydroxylated amino acids like serine and threonine residues expands the target range of Doa10 towards clients that do not expose suitable lysine residues as Ub acceptor sites.

4.1 Ubc6 and Ubc7 act in a sequential manner on Doa10 substrates

Genetic data imply that proteolysis of Doa10 client proteins depends on the enzymatic activity of the Ub conjugating enzymes Ubc6 and Ubc7 (figure 3.1) [136, 141, 170]. In this study, it was demonstrated that both enzymes act in a successive manner on Doa10 substrates to facilitate efficient poly-ubiquitylation. In a first reaction step, Ubc6 conjugates single Ub moieties to Doa10 substrates. This is followed by an extension of these moieties with K48-linked poly-Ub chains, which are synthesized by Ubc7 (figure 4.1). These conclusions are mainly based on *in vitro* observations. Recent work analyzed the contribution

of Ubc6 and Ubc7 in the processing of Doa10 substrates *in vivo* [155]. The authors observed that the Doa10 substrate Vma12-*DegAB* is decorated with low molecular weight Ub moieties in absence of Ubc7. In cells devoid of Ubc6 or Doa10 no modification of the Doa10 client was detected. Under wt conditions, Vma12-*DegAB* was heavily poly-ubiquitylated with K48-linked Ub chains. Furthermore, Weber *et al.* were able to bypass the necessity for Ubc6-mediated Ub chain initiation by fusing Ub molecules to Doa10 target proteins. In summery, these *in vivo* data support the conclusions from this study and the postulated model for Doa10 substrate ubiquitylation. Similar consecutive ubiquitylation models were recently proposed for the APC and $SCF^{\beta TrCP2}$ ligase complexes as well as for auto-ubiquitylation of the RING ligase BRCA1 [95, 183, 193]. Nevertheless, this study verifies for the first time the requirement for such a tandem ubiquitylation mechanism during protein quality control (PQC). PQC client proteins are highly diverse in their structural properties and amino acid composition [194]. Hence, the initial attachment of a Ub molecule to an acceptor site within differing peptide environments provides a challenge for PQC ligases [195]. Consequently, a tandem ubiquitylation model, as presented in figure 4.1, may account for an adaptation of the Doa10 ubiquitylation capacity towards a diverse protein landscape of its clients.

To this date, tandem ubiquitylation models have been proposed for a small number of Ub ligases and only for Doa10-mediated quality control a biological relevance was shown *in vivo* [95, 155, 183, 193]. However, recent work suggests that such sequential engagement of E2 enzymes is a more common phenomenon, especially in higher eukaryotes. The E2 enzyme Ube2W, for example, attaches single Ub moieties to the disordered N-terminus of its client proteins in human [196, 197]. It was proposed that Ube2W together with Ube2N sequentially ubiquitylate the cytosolic antibody receptor TRIM21, which in turn activates the removal of antibody-coated virus particles during innate immunity [198]. Appointed combinations of E2 enzymes seem to be of advantage to allow flexible adaptation to certain cellular requirements and provide an additional layer of regulation to the ubiquitylation of proteins. Concordantly, much more effort must be put into identifying relevant E2-E3 ligase complexes *in vivo* and investigation of tandem ubiquitylation models on a broad range. It seems

feasible to regard the inventory of E2 enzymes within the cell as a toolbox containing a number of instruments with differing abilities to catalyze Ub linkages. The preferences of certain E2 enzymes for some ligases as well as their restriction to certain cellular compartments ensures the tight regulation and specificity of the Ub code.

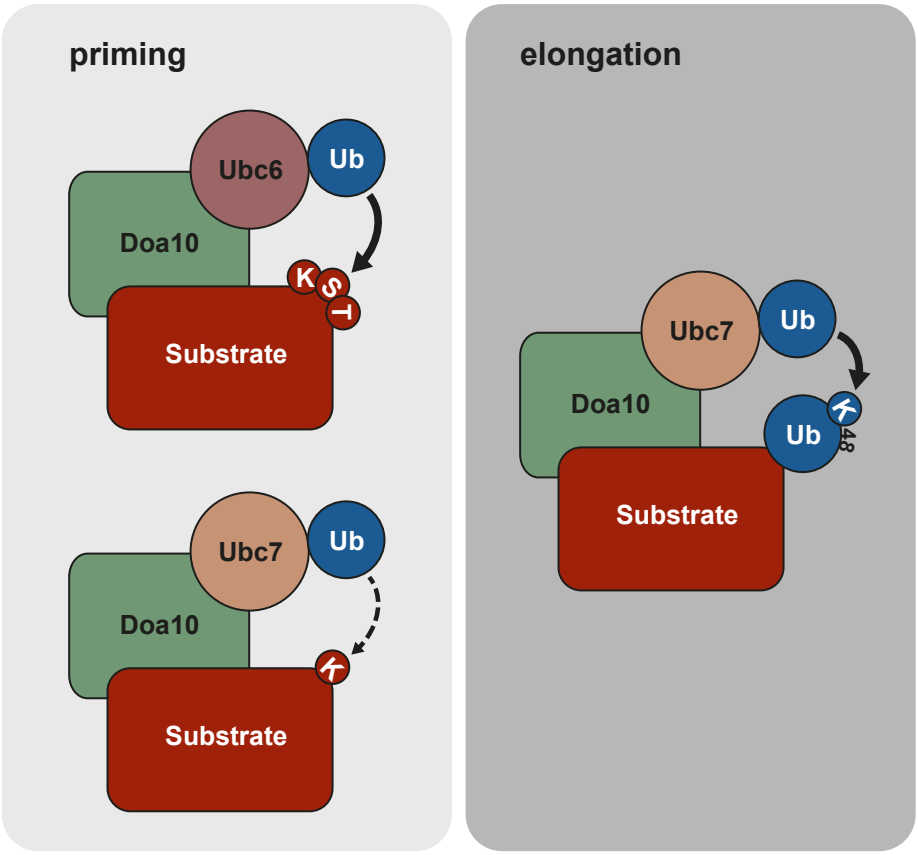

Figure 4.1 – Schematic representation of the enzymatic activities of Ubc6 and Ubc7 towards Doa10 clients. Ubc6 adds single Ub species to lysine residues (K) but also to hydroxylated amino acids as serine (S) and threonine (T) within Doa10 target proteins. This priming step allows the subsequent attachment of K48-linked poly-Ub chains by Ubc7. In some instances, Ubc7 is able to initiate ubiquitylation directly on Doa10 substrates. However, this event appears to be less efficient as compared to the priming reaction catalyzed by Ubc6. The figure was adapted from Weber *et al.* [155].

4.2 Ubc6 predominantly attaches single Ub moieties to Doa10 client proteins

Ubc6 and Ubc7 fulfill distinct functions in the ubiquitylation of Doa10 client proteins. Ubc6 initiates ubiquitylation by attaching single or presumably low molecular weight Ub species to a target protein. In this process, Ubc6 is highly flexible in choosing ubiquitylation sites (section 3.1.4). Concordantly, it was shown that Ubc6 is not able to form significant amounts of poly-Ub chains *in vitro* (section 3.1.5). Furthermore, the low molecular conjugates synthesized by Ubc6 do not exhibit a homogenous Ub-linkage type but contain a mixture of K48- and K63-linked Ub species. This matches the observation that the activity of Ubc6 alone cannot promote the proteolysis of Doa10 target proteins. Thus, Ubc6 is not able to generate a Ub signal, which is recognized by the 26S proteasome. In a recent publication, Xu *et al.* reported that Ubc6 primarily catalyzes K11-linked and, with lesser efficiency, also other Ub chains *in vitro* [28]. The authors used prolonged incubation times of about two hours for their assays. In the present work the typical reaction times were much shorter and no evidence for Ub chain synthesis by Ubc6 was found. This is further proof for the limited ability of Ubc6 to synthesize higher Ub conjugates. Concordantly, the biological relevance of a chain forming activity by Ubc6 remains to be determined *in vivo* in presence of the highly processive Ub chain elongating enzyme Ubc7. A question, which is yet not answered, concerns the preference of Ubc6 to catalyze mono-ubiquitylation. Studies characterizing structural features in E2 enzymes, which prevent Ub chain formation, are limited to date. Recent work indicates that a disordered N-terminal extension limits poly-Ub chain formation of the UBE2E Ub conjugating enzyme family [103]. A C-terminally truncated Ubc6 variant (Ubc6ΔL) did not exhibit changes in its catalytically activity suggesting that the activity of this E2 is not restricted by this extension (figure 3.4 b). For other E2 enzymes as UbcH5 and Ube2S, it was suggested that backside binding of a free Ub molecule increases processivity in Ub chain formation [100, 199]. Interestingly, a similar mechanism was also proposed to inhibit chain formation for other E2 enzymes [101]. It remains to be determined if Ubc6 interacts through such a backside binding site with Ub and how this influences the overall activity of the E2 enzyme. The surface of

Ubc6 exhibits a positive electrostatic potential, which is rather unusual for an E2 enzyme [200]. This characteristic might account for the unique catalytic propensities of Ubc6 and its family members. Another factor, which seems to determine the activity of E2 enzymes, is the binding strength of the E2 enzyme to the E3 RING domain [101]. Strong E2-E3 interactions reduce the conformational freedom of the E2-bound Ub moiety, which in turn promotes Ub chain formation. Generally, further structural and mutational studies are required to shed light on the reasons that restrict the ubiquitylation capacity of Ubc6 towards Ub chain elongation.

4.3 Ubc7 is a highly specialized E2 enzyme synthesizing K48-linked Ub chains

In contrast to Ubc6, Ubc7 efficiently catalyze K48-linked poly-Ub chains (section 3.1.5 and [142]). An acidic loop close to the catalytic center of Ubc7 (figure 4.2) presumably positions lysine 48 of the acceptor Ub molecule in favor for an attack by the donor Ub [94, 143, 201]. These structural characteristics probably limit the ability of Ub7 to attach Ub moieties directly to client proteins. Lysine residues in target proteins might be difficult to access and located in various peptide environments, which in turn complicates mounting of the first Ub by Ubc7. This assumption is validated by the observation that the Doa10 substrates Sbh2 (figure 3.26) and also a mutant variant of the ATP-binding cassette a-factor transporter Ste6* can be still degraded in absence of Ubc6 although in a less efficient manner [170, 187, 202]. A similar behavior was also shown for other chain specific E2 enzymes UBE2S (K11 specific) and UBE2N-UBE2V1 (K63 specific), which lack the capability for Ub chain initiation [96, 183, 203, 204]. In contrast, Cdc34 is able to catalyze both the initiation and the elongation with K48-linked Ub chains [94]. However, the attachment of the first Ub molecule is extremely slow and rate limiting when compared to the subsequent rapid synthesis of poly-Ub chains. Consequently, the Doa10 ligase employs two E2 enzymes to circumvent this limitation. Because Ubc7 is extremely proficient in generating Ub signals, which are recognized by the 26S proteasome, it is mandatory to constrain its activity and prevent unspecific protein degradation. This is partially archived through its interaction partner Cue1, which controls

recruitment of Ubc7 to the ER-membrane and stimulates its activity [144–146]. Additionally, the necessity for Ubc6 to initiate ubiquitylation might serve as another layer of regulation to control Ubc7 activity at the Doa10 ligase.

Ubc7 is also part of the protein quality control ligase Hrd1, which facilitates the ubiquitylation of ER luminal and ER integral-membrane clients [149, 205]. Strikingly, Ubc7 is the only E2 enzyme, which is known to be required for the decoration of Hrd1 clients with K48-linked Ub chains. Presumably, Ubc7 is able to initiate ubiquitylation in the context of this ligase. Hrd1 target proteins are partially unfolded during their retro-translocation to the cytosol, which might allow access of Ubc7 to appropriate ubiquitylation sites. Additionally, the Doa10 and Hrd1 RING domains differentially stimulated chain elongation catalyzed by Ubc7 [158]. Cohen *et al.* propose, that the Hrd1 RING domain stabilizes the closed conformation of the Ubc7~Ub conjugate substantially better than the Doa10 RING domain, which might in turn affect processivity of Ubc7 [82, 83, 111]. Nevertheless, circumstances, which enable Ubc7 to directly ubiquitylated client proteins, need to be studied in more detail.

4.4 The unique properties of the Ub conjugation enzyme Ubc6 are conserved in human

UBE2J2, the human Ubc6 orthologue, displays comparably ubiquitylation activity *in vitro* as the yeast protein (figure 3.6). Furthermore, both proteins share a high degree of sequence identity in the catalytically core domain, which most likely determines their enzymatic activity [172, 173]. Thus, it seems feasibly that UBE2J2 also acts as priming E2 enzyme in human protein quality control. This is supported by the observation that the human orthologue of Ubc7, UBE2G2, co-localizes with UBE2J2 and both proteins are implicated in ER associated protein degradation (ERAD) [206, 207]. Immunoprecipitation experiments indicated that UBE2J2 interacts with the ligase TMEM129 in the ubiquitylation of MHC class I molecules during virus infection [208, 209]. However, it is not the only E2 enzymes whose depletion diminished proteolysis of TMEM129 target proteins. UBE2K, which specifically catalyzes the synthesis of K48-linked Ub chains, is also required for the degradation of MHC class I

proteins [98, 208, 210]. Thus, both enzymes presumably act sequentially on TMEM129 client proteins but further proof for such a tandem ubiquitylation mechanism is still missing. ERAD in higher eukaryotes is more complex when compared to yeast. Consequently, only a few functional E2-E3 pairs of this process are characterized to date. Further studies are required, to validate a priming function of UBE2J2 *in vivo* and identify the involved Ub ligase complexes.

Similar to Ubc6, UBE2J2 is a short-lived protein, whose turnover depends on its own catalytically activity [211]. The linker region of Ubc6 was shown to convey degradation [152]. The corresponding area of Ubc6 is predicted to be unstructured (IUPred [212], data not shown). Most disordered regions are not conserved during evolution because they do not depend on a defined structural fold to fulfill their function [213]. Concordantly, the linker regions of human UBE2J2 and yeast Ubc6 differ in their sequence (figure 3.6). However, the overall length of this segment is similar. Auto-ubiquitylation of UBE2J2 was not detected in the course of the *in vitro* ubiquitylation assay (figure 3.6). Thus, further experiments are necessary to determine, if the human E2 enzymes is also ubiquitylated within its linker region and to identify the ligase that controls the proteolysis of the protein. It can be speculated that the constitutive turnover of Ubc6 family members might represent a regulatory aspect to control the enzymatic activity of this protein family.

4.5 Ubiquitylation of hydroxylated amino acids expands the Doa10 target range

Previous studies indicate that hydroxylated amino acids serve as Ub acceptor sites in protein degradation [70, 73, 75]. Asi2, a Doa10 substrate, was degraded even when all internal lysine residues were substituted to arginine residues [214]. Additionally, Boban *et al.* were able to show that the ubiquitylation of this lysine less Asi2 variant was susceptible to high pH levels, implying that the ubiquitylation of this mutant occurs on hydroxylated amino acids. In this study, the ability of Ubc6 to catalyze the attachment of Ub to serine or threonine residues was directly shown by mass spectrometry (figure 3.22). It was demon-

strated that ubiquitylation of hydroxylated amino acids plays an important role during auto-ubiquitylation of Ubc6 and Doa10 client ubiquitylation in absence of accessible lysine residues (section 3.2.2 and 3.2.4). There were no hints that Ubc6 is able to attach Ub moieties to cysteine residues or to the N-terminus of a protein, though this particular issue was not systematically investigate in the course of this study. Furthermore, it needs to be determined if Ubc6 preferentially attaches Ub to lysine residues rather than to hydroxylated amino acids or if the general accessibility of the available amino acids in a target protein plays a more important role during Ub chain initiation.

Previous studies postulated that E3 ligases modulate the activities of E2 enzymes to conduct the ubiquitylation of serine or threonine residues. In contrast, this study demonstrates that the catalysis of such ubiquitylation events depends primarily on the intrinsic propensities of Ubc6. Initial studies showed that the ubiquitylation of some natural ERAD substrates in human is pH labile [75]. Moreover, proteolysis of the T-cell Antigen Receptor α-Chain is facilitated by ubiquitylation of non-lysine residues [74, 215]. Still, it is not clear at the moment, how abundant ubiquitylation of hydroxylated amino acids is within cells. However, it can be assumed that it is more widespread than anticipated since most high throughput screens to identify ubiquitylated proteins and ubiquitylation sites employ protocols that disassemble oxyester and also thioester linkages. Thus, high throughput screens with milder conditions preserving these linkage types need to be conducted to survey the actual distribution of such non-canonical ubiquitylation events.

The active site region of Ubc6 exhibits significant differences from reactive centers of other E2 enzymes in yeast (red box in figure 4.2). Especially, the HPN motive close to the active site cysteine residue is implicated in being mandatory for structural arrangements within the catalytic center [80, 81]. Because these and other residues are not conserved in Ubc6, the enzyme most likely employs a different catalytic strategy for Ub transfer. The unique properties of the Ubc6 active site region, which are preserved in eukaryotes, might account for the flexibility of this class of E2 enzymes in choosing ubiquitylation sites (figure 3.6 and [172]). This assumption is supported by observations reporting that

UBE2J2 might ubiquitylate MHC class I proteins on hydroxylated amino acids during viral infection [216]. The conservation of these unique propensities of the Ubc6 E2 enzyme family most likely reflects the requirement for such an activity in PQC systems to ensure degradation of target proteins exposing unusual features with inaccessible or no lysine residues. Malfolded proteins most likely do not expose a homogenous conformation but collapse randomly. Thus, individual proteins might expose different sequence properties and ubiquitylation must be initiated at different sites. Consequently, the ability of Ubc6 to target not only lysine residues but also hydroxylated amino acids most likely ensures the efficient degradation of all conformers of a malfolded client protein.

Interestingly, the number of non-canonical ubiquitylation events in ERAD seems to increase during viral infections. The HIV virus for example initiates the ubiquitylation of BST-2, an immunity regulator, on cysteine, serine and threonine residues for degradation to weaken the immune response of the host [68]. Degradation of MHC class I proteins after infection by human cytomegalovirus and herpesvirus was shown to depend on UBE2J2 [73, 208, 216]. It is not known, whether viruses preferentially engage UBE2J2 for degradation of host proteins. However, the utilization of a promiscuous E2 enzyme to trigger degradation of normally stable host proteins appears to be of advantage for virus propagation.

4.6 Implications of Ubc6 turnover on Doa10 ligase function

Ubc6 is a short-lived protein with a half-life of about 55 min [133, 152]. Its proteolysis depends on its catalytic activity and on Ubc7 and Doa10 (figure 3.14). In the course of this study no indications for a regulatory functions of Ubc6 turnover were obtained. Unfortunately, Ubc6 variants that were catalytically active but were not subjected to constant degradation are not available. Previous observations of Kreft *et al.* indicate that Ubc6 proteolysis is not a prerequisite for the function of the Doa10 ligase *in vivo* [217]. They mutated a highly conserved glutamate residue within the 5th trans-membrane domain of the Doa10 ligase, which results in diminished or accelerated Ubc6

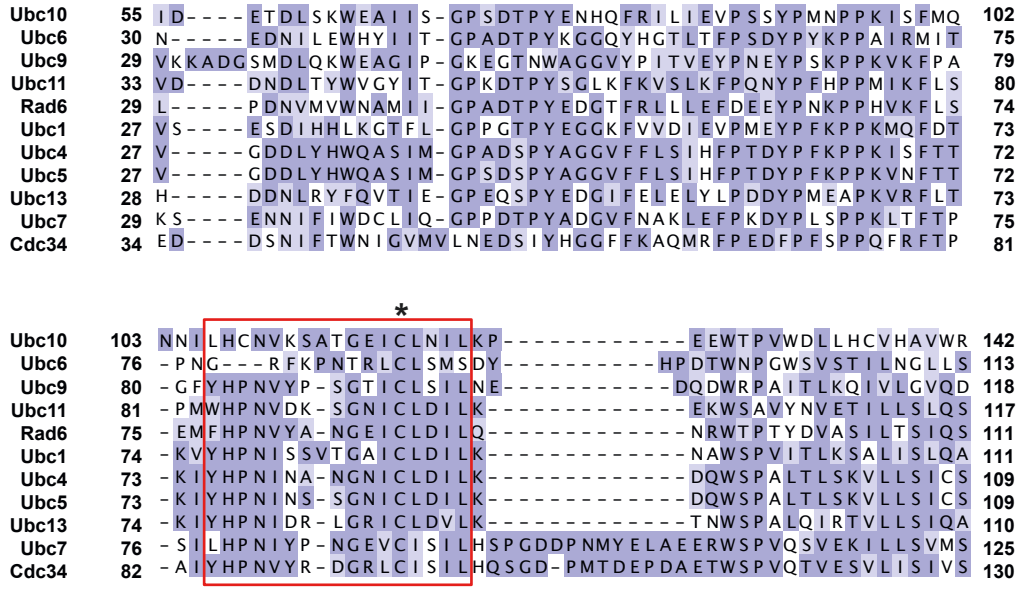

Figure 4.2 – Multiple sequence alignment of yeast Ub conjugating enzymes. Clustal Omega sequence alignment [175] of the catalytic core domains of nine E2 enzymes from yeast. The alignment was edited with Jalview and colored according to BLOSUM62 (BLOcks SUbstitution Matrix) [176]. The conserved active site cysteine is marked with an asterisk and the surrounding amino acids are highlighted with a red box.

turnover dependent on the amino acid substitution. Processing of other Doa10 client proteins was not affected by these mutations. Kreft *et al.* propose that Ubc6 can occupy at least two different binding sites at the ligase: one is responsible for Ub transfer from Ubc6 to a substrate whereas the other might be a general site for binding of integral-membrane clients. However, the authors could not provide a mechanistic explanation for their observations and further studies are required to understand their findings. Ubc6 auto-ubiquitylates itself in absence of the Doa10 ligase *in vitro* and *in vivo* (section 3.1.7). This phenomenon has been observed for several other E2 enzymes before [174]. The E2 enzyme Ube2T was shown to mono-ubiquitylate itself at a certain lysine residue within its catalytically core domain, which in turn restricts its ubiquitylation capacity towards client proteins [218]. To investigate, if a similar auto-regulatory mechanism also applies for Ubc6 function, ubiquitylated Ubc6 was purified. Due to residual amounts of unmodified Ubc6, which unspecifically

bound to the affinity resin, a definite conclusion could not be drawn from these experiments (section 3.1.7). However, it was observed that Ubc6 is able to attach several mono-Ub species to itself in *cis* during the *in vitro* ubiquitylation assay (figure 3.15). Hence, it seems improbable that the activity of Ubc6 is restricted when a Ub moiety is fused to its C-terminal region because the enzyme can attach an additional Ub molecule to a different acceptor site within its linker region. Another indication for this assumption is the lack of a specific ubiquitylation site within Ubc6 (section 3.2.1). Because Ubc6 was stronger mono-ubiquitylated in cell devoid of *DOA10* than in cells lacking Ubc7, questions were raised whether Ubc6 ubiquitylation can only take place when the E2 is not bound to the Doa10 ligase. The disordered linker region of Ubc6 might be quite flexible in absence of a binding partner, which presumably allows free access to this area for Ub transfer. In context of the Doa10 ligase the dynamics of this region could be much more constrained and certain amino acids might not be accessible for Ub conjugation. Based on this assumption unmodified Ubc6 would stay at the ligase and mainly attach Ub moieties to Doa10 target proteins. Ubc6, which is not engaged by Doa10, would ubiquitylate itself and possibly be recruited to the aforementioned integral-membrane substrate binding site of the Doa10 ligase for poly-ubiquitylation by Ubc7. The proposed model seems conceivably, through there are many open questions, which need to be addressed in order to validate such a scenario.

4.7 Regulation of Ubc6 and Ubc7 activity at the Doa10 ligase

Tandem ubiquitylation mechanisms may represent a more general phenomenon in the Ub field to allow efficient poly-ubiquitylation of target proteins. However, it is little known how ligase complexes orchestrate the activity of two sequentially acting E2 enzymes. The anaphase promoting complex (APC) was the first ligase, which was shown to employ two E2 enzymes in substrate ubiquitylation [95]. For human APC, it was demonstrated that priming and elongating E2 enzymes depend on different binding sites at the complex to enable their optimal performance during ubiquitylation [181]. The Ub chain elongating enzyme is positioned favorably towards the acceptor Ub molecule in order to increase

processivity, which in turn counteracts the activity of the chain initiating E2 enzyme. The yeast APC complex employs the E2 enzyme Ubc4 (initiating E2) and Ubc1 (elongating E2) for substrate ubiquitylation. Both enzymes are thought to compete for the same binding site at the ligase. A recent study from Girard *et al.* proposes that the UBA domain of Ubc1 increases the affinity for the APC complex, which in turn enhances its ability to compete with Ubc4 for binding [219]. In the presented study it was shown that Ubc6 and Ubc7 occupy the same docking site on the Doa10 RING domain (section 3.1.6). However, no evidence was found that high amounts of Ubc6 or Ubc7/Cue1 diminish Doa10R poly-ubiquitylation *in vitro* (data not shown). Interactions of E2 enzymes with RING domains are very transient and dynamic [13, 92]. If Ubc6 and Ubc7 display different affinities for the RING domain remains elusive and further studies are necessary to determine dissociation constants for the individual E2 enzymes with Doa10R. Additional interaction surfaces of the ligase could increase the affinity for certain E2 enzymes as for example shown for Ubc1 and the APC complex [219]. The trans-membrane anchor of Ubc6 was shown to be important for interaction with the Doa10 ligase [151, 152, 217]. If the linker region of Ubc6 specifically interacts with parts of the E3 ligase is not know to date. Ubc7 is recruited by its adapter protein Cue1 to the ER membrane [144]. Co-localization of the Ubc7/Cue1 complex to Doa10 depends on the N-terminal trans-membrane anchor of Cue1 (unpublished data). Furthermore, a C-terminally truncated Doa10 variant abolishes Ubc7 recruitment [217]. Hence, both E2 enzymes Ubc6 and Ubc7 are stably recruited to the Doa10 ligase most likely through interactions of trans-membrane segments. This was further validated by observations that Ubc6 and Ubc7 co-localize with Doa10 even when the RING domain is disrupted (figure 3.35). Additionally, both E2 enzymes bind in the absence of the other enzyme to the ligase complex [201]. Thus, it can be excluded that Ubc6 recruitment must occur prior to the recruitment of Ubc7 to Doa10. How both E2 enzymes interact with Doa10 in detail remains elusive. Nevertheless, it can be speculated that there is a mechanism, which increases the processivity of Ubc7 towards K48-linked Ub chain synthesis upon initiation of the ubiquitylation cascade. Such a stimulation of Ubc7 activity might outperform the relatively low Ub-conjugating activity of Ubc6. Studies on Cue1, for example, demonstrated that the processivity

of Ubc7 chain elongation correlates with the increasing length of the acceptor Ub chain whereas the stimulatory influence of the RING domain decreases (unpublished data, Maximilian von Delbrück, AG Sommer). In such a scenario, Ubc7-mediated chain elongation would be a self-stimulatory process when Ubc6 initiated the ubiquitylation in a prior step.

4.8 Overproduction of Ubc6 interferes with the integrity of the Doa10 ligase

UBC6 was initially identified as E2 encoding gene that when overexpressed suppresses the temperature sensitive growth defect of a *sec61-2* yeast strain [151]. Further studies revealed that the deletion as well as the increased expression of this gene abolishes the degradation of the folding-deficient Sec61-2 protein and other ERAD substrates [151, 173, 220]. Obviously, a defined amount of Ubc6 is required for the degradation of Doa10 substrates, whereas an excessive portion impairs this process (section 3.3.1). One explanation for this phenomenon is competition of the E2 enzymes Ubc6 and Ubc7 for binding to the ligase. However, this assumption was excluded because Cue1 and Ubc7 levels were not alter at the ligase upon the overproduction of Ubc6. Additionally, increased levels of Ubc7/Cue1 did not supress the *UBC6* overexpression phenotype. Elevated cellular amounts of Ubc6 lead to a tremendous increase of the Ubc6 population, which co-localized with Doa10 when compared to the wt situation. Thus, Ubc6 level seem to be not saturated under wt conditions. The negative effect of *UBC6* overexpression was subjected to its catalytically core domain since the overproduction of a truncated Ubc6 variant, lacking the UBC domain, did not interfere with Doa10 dependent substrate proteolysis. Initial experiments indicate that Doa10 substrates are still ubiquitylated upon overproduction of Ubc6. Hence, increased levels of Ubc6 at the Doa10 ligase might disrupt the Ub signal initiating degradation, which is normally generated when E2 levels are balanced. Two scenarios can be envisioned: On the one hand, Ubc6 could attach Ub moieties to random lysine residues within the growing Ub chain and thereby disrupt the homogeneity of the chain. In consequence, the client protein would not be further processed by downstream factors such as the proteasome. On the other hand, Ubc6 could attach multiple mono-Ub

moieties to the substrate, which in turn may perturb Ubc7 processivity due to the increased number of presented Ub acceptor sites. De-ubiquitylating processes always counteract ubiquitylation reactions. The ER localized deubiquitylating enzyme Ubp1 might interfere with Doa10-mediated proteolysis [221]. An increased retention time of substrates during ubiquitylation most likely raises the possibility for Ubp1 or other DUBs to remove already attached Ub moieties thereby preventing their efficient degradation [222]. Additionally, multiple mono-Ub could also impede the optimal orientation of Ubc7 for Ub donor transfer towards the Ub acceptor molecule due to steric restrictions of neighboring Ub molecules [94, 223]. A similar scenario was observed at the $SCF^{\beta TrCP2}$ ligase complex [193]. High amounts of UbcH5, the Ub chain initiating E2 enzyme, resulted in hyper-mono-ubiquitylation of the substrate, which interfered with subsequent chain elongation. However, mechanistic reasons for this observation remain elusive. Ubc6 is known to mono-ubiquitylate itself at several residues in one molecule. Thus, it seems likely that Ubc6 is able to attach several Ub moieties also to one substrate molecule *in vivo*. This would also explain, why degradation of the small Doa10 substrate Sbh2 is not affected by elevated Ubc6 levels (figure 3.32). Due to its limited size Ubc6 might not be able to attach multiple Ub moieties to Sbh2. Hence, the substrate is processed almost with similar half-life during *UBC6* overexpression as compared to wt conditions. Nevertheless, extensive investigations are necessary to understand the mechanistic reasons for the *UBC6* overexpression phenotype.

5 | Bibliography

[1] K. N. Swatek and D. Komander. Ubiquitin modifications. *Cell Res*, 26(4): 399–422, 2016.

[2] S. Vijay-Kumar, C. E. Bugg, and W. J. Cook. Structure of ubiquitin refined at 1.8 Å resolution. *J Mol Biol*, 194(3):531–544, 1987.

[3] L. Nisius and S. Grzesiek. Key stabilizing elements of protein structure identified through pressure and temperature perturbation of its hydrogen bond network. *Nature Chem*, 4(9):711–717, 2012.

[4] R. E. Lenkinski, D. M. Chen, J. D. Glickson, and G. Goldstein. Nuclear magnetic resonance studies of the denaturation of ubiquitin. *Biochim Biophys Acta*, 494(1):126–130, 1977.

[5] D. Finley, E. Ozkaynak, and A. Varshavsky. The yeast polyubiquitin gene is essential for resistance to high temperatures, starvation, and other stresses. *Cell*, 48(6):1035–1046, 1987.

[6] M. S. Briggs and H. Roder. Early hydrogen-bonding events in the folding reaction of ubiquitin. *Proc Natl Acad Sci U S A*, 89(6):2017–2021, 1992.

[7] O. F. Lange, N.-A. Lakomek, C. Fares, G. F. Schroder, K. F. A. Walter, S. Becker, J. Meiler, H. Grubmuller, C. Griesinger, and B. L. de Groot. Recognition dynamics up to microseconds revealed from an rdc-derived ubiquitin ensemble in solution. *Science*, 320(5882):1471–1475, 2008.

[8] D. Komander and M. Rape. The ubiquitin code. *Annu Rev Biochem*, 81(1): 203–229, Jul 2012.

[9] I. Dikic, S. Wakatsuki, and K. J. Walters. Ubiquitin-binding domains - from structures to functions. *Nat Rev Mol Cell Biol*, 10(10):659–671, 2009.

[10] J. Herrmann, L. O. Lerman, and A. Lerman. Ubiquitin and ubiquitin-like proteins in protein regulation. *Circ Res*, 100(9):1276–1291, May 2007.

[11] A. G. Van Der Veen and H. L. Ploegh. Ubiquitin-like proteins. *Annu Rev Biochem*, 81(1):323–357, Jul 2012.

[12] B. A. Schulman and J. W. Harper. Ubiquitin-like protein activation by e1 enzymes: the apex for downstream signalling pathways. *Nat Rev Mol Cell Biol*, 10(5):319–331, Aug 2009.

[13] Y. Ye and M. Rape. Building ubiquitin chains: E2 enzymes at work. *Nat Rev Mol Cell Biol*, 10(11):755–764, 2009.

[14] M. B. Metzger, J. N. Pruneda, R. E. Klevit, and A. M. Weissman. Ring-type e3 ligases: Master manipulators of e2 ubiquitin-conjugating enzymes and ubiquitination. *Biochim Biophys Acta*, 1843(1), 2014.

[15] M. D. Stewart, T. Ritterhoff, R. E. Klevit, and P. S. Brzovic. E2 enzymes: more than just middle men. *Cell Res*, 26(4):423–440, 2016.

[16] R. Budhidarmo, Y. Nakatani, and C. L. Day. Rings hold the key to ubiquitin transfer. *Trends Biochem Sci*, 37(2):58–65, 2012.

[17] Martin Scheffner and Sharad Kumar. Mammalian hect ubiquitin-protein ligases: Biological and pathophysiological aspects. *Biochim Biophys Acta*, 1843(1):61–74, 2014.

[18] D. E. Spratt, H. Walden, and G. S. Shaw. Rbr e3 ubiquitin ligases: new structures, new insights, new questions. *Biochem. J*, 458(3):421–437, 2014.

[19] M. Koegl, T. Hoppe, S. Schlenker, H. D. Ulrich, T. U. Mayer, and S. Jentsch. A novel ubiquitination factor, e4, is involved in multiubiquitin chain assembly. *Cell*, 96(5):635–644, 1999.

[20] D. D. Sahtoe and T. K. Sixma. Layers of dub regulation. *Trends Biochem Sci*, 40(8):456–467, 2015.

[21] O. Kerscher, R. Felberbaum, and M. Hochstrasser. Modification of proteins by ubiquitin and ubiquitin-like proteins. *Annu Rev Cell Dev Biol*, 22(1):159–180, 2006.

[22] D. Mukhopadhyay and H. Riezman. Proteasome-independent functions of ubiquitin in endocytosis and signaling. *Science*, 315(5809):201–205, Dec 2007.

[23] M. Leeb and A. Wutz. Ring1b is crucial for the regulation of developmental control genes and prc1 proteins but not x inactivation in embryonic cells. *J Cell Biol*, 178(2):219–229, 2007.

[24] M. Ohtsubo, S. Yasunaga, Y. Ohno, M. Tsumura, S. Okada, N. Ishikawa, K. Shirao, A. Kikuchi, H. Nishitani, M. Kobayashi, and Y. Takihara. Polycomb-group complex 1 acts as an e3 ubiquitin ligase for geminin to sustain hematopoietic stem cell activity. *Proc Natl Acad Sci U S A*, 105(30):10396–10401, 2008.

[25] M. Zeng, L. Ren, K. Mizuno, K. Nestoras, H. Wang, Z. Tang, L. Guo, D. Kong, Q. Hu, Q. He, L. Du, A. M. Carr, and C. Liu. Crl4wdr70 regulates h2b

monoubiquitination and facilitates exo1-dependent resection. *Nat Comms*, 7 (11364), 2016.

[26] N. Shabek, Y. Herman-Bachinsky, S. Buchsbaum, O. Lewinson, M. Haj-Yahya, M. Hejjaoui, H. A. Lashuel, T. Sommer, A. Brik, and A. Ciechanover. The size of the proteasomal substrate determines whether its degradation will be mediated by mono- or polyubiquitylation. *Molecular Cell*, 48(1):87–97, 2012.

[27] L.-Y. Tang, M. Yamashita, N. P. Coussens, Y. Tang, X. Wang, C. Li, C.-X. Deng, S. Y. Cheng, and Y. E. Zhang. Ablation of smurf2 reveals an inhibition in tgf-beta signalling through multiple mono-ubiquitination of smad3. *EMBO J*, 30(23):4777–4789, 2011.

[28] P. Xu, D. M. Duong, N. T. Seyfried, D. Cheng, Y. Xie, J. Robert, J. Rush, M. Hochstrasser, D. Finley, and J. Peng. Quantitative proteomics reveals the function of unconventional ubiquitin chains in proteasomal degradation. *Cell*, 137(1):133–145, 2009.

[29] I. Ziv, Y. Matiuhin, D. S. Kirkpatrick, Z. Erpapazoglou, S. Leon, M. Pantazopoulou, W. Kim, S. P. Gygi, R. Haguenauer-Tsapis, N. Reis, M. H. Glickman, and O. Kleifeld. A perturbed ubiquitin landscape distinguishes between ubiquitin in trafficking and in proteolysis. *Mol Cell Proteomics*, 10(5):M111.009753.

[30] E. B. Dammer, C. H. Na, P. Xu, N. T. Seyfried, D. M. Duong, D. Cheng, M. Gearing, H. Rees, J. J. Lah, A. I. Levey, J. Rush, and J. Peng. Polyubiquitin linkage profiles in three models of proteolytic stress suggest the etiology of alzheimer disease. *J Biol Chem*, 286(12):10457–10465, 2011.

[31] Schrödinger, LLC. The PyMOL molecular graphics system, version 1.8. November 2015.

[32] W.j. Cook, L.c. Jeffrey, M. Carson, Z. Chen, and C.m. Pickart. Structure of a diubiquitin conjugate and a model for interaction with ubiquitin conjugating enzyme (e2). *J Biol Chem*, 267(23):16467–16471, 1992.

[33] M. J. Eddins, R. Varadan, D. Fushman, C. M. Pickart, and C. Wolberger. Crystal structure and solution nmr studies of lys48-linked tetraubiquitin at neutral ph. *J Mol Biol*, 367(1):204–211, 2007.

[34] R. Varadan, O. Walker, C. Pickart, and D. Fushman. Structural properties of polyubiquitin chains in solution. *J Mol Biol*, 324(4):637–647, 2002.

[35] V. Chau, J. Tobias, A. Bachmair, D. Marriott, D. Ecker, D. Gonda, and A. Varshavsky. A multiubiquitin chain is confined to specific lysine in a targeted short-lived protein. *Science*, 243(4898):1576–1583, 1989.

[36] D. Finley, S. Sadis, B. P. Monia, P. Boucher, D. J. Ecker, S. T. Crooke,

and V. Chau. Inhibition of proteolysis and cell cycle progression in a multiubiquitination-deficient yeast mutant. *Mol Cell Biol*, 14(8):5501–5509, 1994.

[37] S. Virdee, Y. Ye, D. P. Nguyen, D. Komander, and J. W. Chin. Engineered diubiquitin synthesis reveals lys29-isopeptide specificity of an otu deubiquitinase. *Nat Chem Biol*, 6(10):750–757, 2010.

[38] A. Bremm, S. M. V. Freund, and D. Komander. Lys11-linked ubiquitin chains adopt compact conformations and are preferentially hydrolyzed by the deubiquitinase cezanne. *Nat Struct Mol Biol*, 17(8):939–947, Nov 2010.

[39] M. A. Michel, P. R. Elliott, K. N. Swatek, M. Simicek, J. N. Pruneda, J. L. Wagstaff, S. M.v. Freund, and D. Komander. Assembly and specific recognition of k29- and k33-linked polyubiquitin. *Mol Cell*, 58(1):95–109, 2015.

[40] Y. A. Kristariyanto, S. Y. Choi, S. A. A. Rehman, M. S. Ritorto, D. G Campbell, N. A. Morrice, R. Toth, and Y. Kulathu. Assembly and structure of lys 33 -linked polyubiquitin reveals distinct conformations. *Biochem J*, 467(2):345–352, 2015.

[41] K. E. Wickliffe, A. Williamson, H.-J. Meyer, A. Kelly, and M. Rape. K11-linked ubiquitin chains as novel regulators of cell division. *Trends Cell Biol*, 21(11): 656–663, 2011.

[42] A. Ordureau, S. A. Sarraf, D. M. Duda, J. M. Heo, M. P. Jedrychowski, V. O. Sviderskiy, J. L. Olszewski, J. T. Koerber, T. Xie, S. A. Beausoleil, J. A. Wells, S. P. Gygi, B. A. Schulman, and J. W. Harper. Quantitative proteomics reveal a feedforward mechanism for mitochondrial parkin translocation and ubiquitin chain synthesis. *Mol Cell*, 56(3):360–375, 2014.

[43] C. N. Cunningham, J. M. Baughman, L. Phu, J. S. Tea, C. Yu, M. Coons, D. S. Kirkpatrick, B. Bingol, and J. E. Corn. Usp30 and parkin homeostatically regulate atypical ubiquitin chains on mitochondria. *Nat Cell Biol*, 17(2):160–169, 2015.

[44] W. C. Yuan, Y. R. Lee, S. Y. Lin, L. Y. Chang, Y. P. Tan, C. C. Hung, J. C. Kuo, C. H. Liu, M. Y. Lin, M. Xu, Z. J. Chen, and R. H. Chen. K33-linked polyubiquitination of coronin 7 by cul3-klhl20 ubiquitin e3 ligase regulates protein trafficking. *Mol Cell*, 54(4):586–600, 2014.

[45] R. Varadan, M. Assfalg, A. Haririnia, S. Raasi, C. Pickart, and D. Fushman. Solution conformation of lys63-linked di-ubiquitin chain provides clues to functional diversity of polyubiquitin signaling. *J Biol Chem*, 279(8):7055–7063, 2003.

[46] T. Tenno, K. Fujiwara, H. Tochio, K. Iwai, E. H. Morita, H. Hayashi, S. Murata, H. Hiroaki, M. Sato, K. Tanaka, and M. Shirakawa. Structural basis for distinct roles of lys63- and lys48-linked polyubiquitin chains. *Genes Cells*, 9(10):865–875, Jul 2004.

[47] S. D. Weeks, K. C. Grasty, L. Hernandez-Cuebas, and P. J. Loll. Crystal structures of lys-63-linked tri- and di-ubiquitin reveal a highly extended chain architecture. *Proteins*, 77(4):753–759, 2009.

[48] A. B. Datta, G. L. Hura, and C. Wolberger. The structure and conformation of lys63-linked tetraubiquitin. *J Mol Biol*, 392(5):1117–1124, 2009.

[49] Y. A. Kristariyanto, S. A. Abdul-Rehman, D. G. Campbell, N. A. Morrice, C. Johnson, R. Toth, and Y. Kulathu. K29-selective ubiquitin binding domain reveals structural basis of specificity and heterotypic nature of k29 polyubiquitin. *Mol Cell*, 58(1):83–94, 2015.

[50] Z. J. Chen and L. J. Sun. Nonproteolytic functions of ubiquitin in cell signaling. *Mol Cell*, 33(3):275–286, 2009.

[51] J. Jin, X. Xie, Y. Xiao, H. Hu, Q. Zou, X. Cheng, and S. C. Sun. Epigenetic regulation of the expression of il12 and il23 and autoimmune inflammation by the deubiquitinase trabid. *Nat Immunol*, 17(3):259–268, 2016.

[52] J. You and C. M. Pickart. A hect domain e3 enzyme assembles novel polyubiquitin chains. *J Biol Chem*, 276(23):19871–19878, 2001.

[53] D. Komander, F. Reyes-Turcu, J. D. F. Licchesi, P. Odenwaelder, K. D. Wilkinson, and D. Barford. Molecular discrimination of structurally equivalent lys 63-linked and linear polyubiquitin chains. *EMBO Rep*, 10(6):662–662, 2009.

[54] B. Gerlach, S. M. Cordier, A. C. Schmukle, C. H. Emmerich, E. Rieser, T. L. Haas, A. I. Webb, J. A. Rickard, H. Anderton, W. W.-L. Wong, U. Nachbur, L. Gangoda, U. Warnken, A. W. Purcell, J. Silke, and H. Walczak. Linear ubiquitination prevents inflammation and regulates immune signalling. *Nature*, 471(7340):591–596, 2011.

[55] Y. Sasaki, S. Sano, M. Nakahara, S. Murata, K. Kometani, Y. Aiba, S. Sakamoto, Y. Watanabe, K. Tanaka, T. Kurosaki, and K. Iwai. Defective immune responses in mice lacking lubac-mediated linear ubiquitination in b cells. *EMBO J*, 32 (18):2463–2476, 2013.

[56] K. Husnjak and I. Dikic. Ubiquitin-binding proteins: Decoders of ubiquitin-mediated cellular functions. *Annu Rev Biochem*, 81(1):291–322, Jul 2012.

[57] D. S. Kirkpatrick, N. A. Hathaway, J. Hanna, S. Elsasser, J. Rush, D. Finley, R. W. King, and S. P. Gygi. Quantitative analysis of in vitro ubiquitinated

cyclin b1 reveals complex chain topology. *Nat Cell Biol*, 8(7):700–710, 2006.

[58] H.-J. Meyer and M. Rape. Enhanced protein degradation by branched ubiquitin chains. *Cell*, 157(4):910–921, 2014.

[59] G. S. McDowell and A. Philpott. Non-canonical ubiquitylation: mechanisms and consequences. *Int J Biochem Cell Biol*, 45(8):1833–1842, 2013.

[60] K. Breitschopf, E. Bengal, T. Ziv, A. Admon, and A. Ciechanover. A novel site for ubiquitination: the n-terminal residue, and not internal lysines of myod, is essential for conjugation and degradation of the protein. *EMBO J*, 17(20): 5964–5973, 1998.

[61] P. Coulombe, G. Rodier, E. Bonneil, P. Thibault, and S. Meloche. N-terminal ubiquitination of extracellular signal-regulated kinase 3 and p21 directs their degradation by the proteasome. *Mol Cell Biol*, 24(14):6140–6150, 2004.

[62] R. Ben-Saadon, I. Fajerman, T. Ziv, U. Hellman, A. L. Schwartz, and A. Ciechanover. The tumor suppressor protein p16ink4a and the human papillomavirus oncoprotein-58 e7 are naturally occurring lysine-less proteins that are degraded by the ubiquitin system: Direct evidence for ubiquitination at the n-terminal residue. *J Biol Chem*, 279(40):41414–41421, 2004.

[63] Y. Kravtsova-Ivantsiv and A. Ciechanover. Non-canonical ubiquitin-based signals for proteasomal degradation. *J Cell Sci*, 125(3):539–548, Jan 2012.

[64] C. Caron, C. Boyault, and S. Khochbin. Regulatory cross-talk between lysine acetylation and ubiquitination: role in the control of protein stability. *Bioessays*, 27(4):408–415, Apr 2005.

[65] J. M. D. Vosper, G. S. Mcdowell, C. J. Hindley, C. S. Fiore-Heriche, R. Kucerova, I. Horan, and A. Philpott. Ubiquitylation on canonical and non-canonical sites targets the transcription factor neurogenin for ubiquitin-mediated proteolysis. *J Biol Chem*, 284(23):15458–15468, 2009.

[66] J. Song, J. Wang, A. A. Jozwiak, W. Hu, P. M. Swiderski, and Y. Chen. Stability of thioester intermediates in ubiquitin-like modifications. *Protein Sci*, 18(12):2492–2499, 2009.

[67] A. F. Carvalho, C. P. Grou, M. P. Pinto, I. S. Alencastre, J. Costa-Rodrigues, M. Fransen, C. Sá-Miranda, and J. E. Azevedo. Functional characterization of two missense mutations in pex5p - c11s and n526k. *Biochim Biophys Acta*, 1773(7):1141–1148, 2007.

[68] A. A. Tokarev, J. Munguia, and J. C. Guatelli. Serine-threonine ubiquitination mediates downregulation of bst-2/tetherin and relief of restricted virion release by hiv-1 vpu. *J Virol*, 85(1):51–63, 2011.

[69] J. G. Magadán, F. J. Pérez-Victoria, R. Sougrat, Y. Ye, K. Strebel, and J. S. Bonifacino. Multilayered mechanism of cd4 downregulation by hiv-1 vpu involving distinct er retention and erad targeting steps. *PLoS Pathog*, 6(4), 2010.

[70] S. W. Tait, E. de Vries, C. Maas, A. M. Keller, C. S. D'Santos, and J. Borst. Apoptosis induction by bid requires unconventional ubiquitination and degradation of its n-terminal fragment. *J Cell Biol*, 179(7):1453–1466, 2007.

[71] K. Cadwell and L. Coscoy. Ubiquitination on nonlysine residues by a viral e3 ubiquitin ligase. *Science*, 309(5731):127–130, Jan 2005.

[72] K. Cadwell and L. Coscoy. The specificities of kaposi's sarcoma-associated herpesvirus-encoded e3 ubiquitin ligases are determined by the positions of lysine or cysteine residues within the intracytoplasmic domains of their targets. *J Virol*, 82(8):4184–4189, 2008.

[73] X. Wang, R. A. Herr, W. J. Chua, L. Lybarger, E. J. Wiertz, and T. H. Hansen. Ubiquitination of serine, threonine, or lysine residues on the cytoplasmic tail can induce erad of mhc-i by viral e3 ligase mk3. *J Cell Biol*, 177(4):613–624, 2007.

[74] S. Ishikura, A. M. Weissman, and J. S. Bonifacino. Serine residues in the cytosolic tail of the t-cell antigen receptor - chain mediate ubiquitination and endoplasmic reticulum-associated degradation of the unassembled protein. *J Biol Chem*, 285(31):23916–23924, Feb 2010.

[75] Y. Shimizu, Y. Okuda-Shimizu, and L. M. Hendershot. Ubiquitylation of an erad substrate occurs on multiple types of amino acids. *Mol Cell*, 40(6):917–926, 2010.

[76] C. Michelle, P. Vourc'h, L. Mignon, and C. R. Andres. What was the set of ubiquitin and ubiquitin-like conjugating enzymes in the eukaryote common ancestor? *J Mol Evol*, 68(6):616–628, 2009.

[77] Y. Lin, W. C. Hwang, and R. Basavappa. Structural and functional analysis of the human mitotic-specific ubiquitin-conjugating enzyme, ubch10. *J Biol Chem*, 277(24):21913–21921, Jan 2002.

[78] E. Ozkan, H. Yu, and J. Deisenhofer. Mechanistic insight into the allosteric activation of a ubiquitin-conjugating enzyme by ring-type ubiquitin ligases. *Proc Natl Acad Sci U S A*, 102(52):18890–18895, 2005.

[79] M. J. Eddins, C. M. Carlile, K. M. Gomez, C. M. Pickart, and C. Wolberger. Mms2-ubc13 covalently bound to ubiquitin reveals the structural basis of linkage-specific polyubiquitin chain formation. *Nat Struct Mol Biol*, 13(10):

915–920, 2006.

[80] P. Y. Wu, M. Hanlon, M. Eddins, C. Tsui, R. S. Rogers, J. P. Jensen, M. J. Matunis, A. M. Weisman, C. P. Wolberger, and C. M. Pickart. A conserved catalytic residue in the ubiquitin-conjugating enzyme family. *EMBO J*, 22(19): 5241–5250, 2003.

[81] C. E. Berndsen, R. Wiener, I. W. Yu, A. E. Ringel, and C. Wolberger. A conserved asparagine has a structural role in ubiquitin-conjugating enzymes. *Nat Chem Biol*, 9(3):154–156, 2013.

[82] A. Plechanovova, E. G. Jaffray, M. H. Tatham, J. H. Naismith, and R. T. Hay. Structure of a ring e3 ligase and ubiquitin-loaded e2 primed for catalysis. *Nature*, 489(7414):115–120, 2012.

[83] H. Dou, L. Buetow, G. J. Sibbet, K. Cameron, and D. T. Huang. Birc7-e2 ubiquitin conjugate structure reveals the mechanism of ubiquitin transfer by a ring dimer. *Nat Struct Mol Biol*, 19(9):876–883, 2012.

[84] D. Reverter and C. D. Lima. Insights into e3 ligase activity revealed by a sumo-rangap1-ubc9-nup358 complex. *Nature*, 435(7042):687–692, 2005.

[85] L. M. Lois and C. D. Lima. Structures of the sumo e1 provide mechanistic insights into sumo activation and e2 recruitment to e1. *EMBO J*, 24(3):439–451, 2005.

[86] D. T. Huang, H. W. Hunt, M. Zhuang, M. D. Ohi, J. M. Holton, and B. A. Schulman. Basis for a ubiquitin-like protein thioester switch toggling e1-e2 affinity. *Nature*, 445(7126):394–398, 2007.

[87] I. Lee and H. Schindelin. Structural insights into e1-catalyzed ubiquitin activation and transfer to conjugating enzymes. *Cell*, 134(2):268–278, 2008.

[88] N. Zheng, P. Wang, P. D. Jeffrey, and N. P. Pavletich. Structure of a cbl-ubch7 complex: Ring domain function in ubiquitin-protein ligases. *Cell*, 18(102): 533–539, 2000.

[89] C. Dominguez, A. M. Bonvin, G. S. Winkler, F. M. Van Schaik, H. T. Timmers, and R. Boelens. Structural model of the ubch5b/cnot4 complex revealed by combining nmr, mutagenesis, and docking approaches. *Structure*, 12(4):633–644, 2004.

[90] M. Zhang, M. Windheim, S. M. Roe, M. Peggie, P. Cohen, C. Prodromou, and L. H. Pearl. Chaperoned ubiquitylation - crystal structures of the chip u box e3 ubiquitin ligase and a chip-ubc13-uev1a complex. *Mol Cell*, 20(4):525–538, 2005.

[91] Q. Yin, SC. Lin, B. Lamothe, M. Lu, YC. Lo, G. Hura, L. Zheng, R. L. Rich,

A. D. Campos, D. G. Myszka, M. J. Leonardo, B. G. Darnay, and H. Wu. E2 interaction and dimerization in the crystal structure of traf6. *Nat Struct Mol Biol*, 16(6):658–666, 2009.

[92] Z. M. Eletr, D. T. Huang, D. M. Duda, B. A. Schulman, and B. Kuhlman. E2 conjugating enzymes must disengage from their e1 enzymes before e3-dependent ubiquitin and ubiquitin-like transfer. *Nat Struct Mol Biol*, 12(10):933–934, 2005.

[93] J. Jin, X. Li, S. P. Gygi, and J. W. Harper. Dual e1 activation systems for ubiquitin differentially regulate e2 enzyme charging. *Nature*, 447(7148): 1135–1138, 2007.

[94] M. D. Petroski and R. J. Deshaies. Mechanism of lysine 48-linked ubiquitin-chain synthesis by the cullin-ring ubiquitin-ligase complex scf-cdc34. *Cell*, 123 (6):1107–1120, 2005.

[95] M. C. Rodrigo-Brenni and D. O. Morgan. Sequential e2s drive polyubiquitin chain assembly on apc targets. *Cell*, 130(1):127–139, 2007.

[96] M. Windheim, M. Peggie, and P. Cohen. Two different classes of e2 ubiquitin-conjugating enzymes are required for the mono-ubiquitination of proteins and elongation by polyubiquitin chains with a specific topology. *Biochem J*, 409(3): 723–729, 2008.

[97] R. M. Hofmann and C. M. Pickart. Noncanonical mms2-encoded ubiquitin-conjugating enzyme functions in assembly of novel polyubiquitin chains for dna repair. *Cell*, 96(5):645–653, 1999.

[98] Z. Chen and C. M. Pickart. A 25-kilodalton ubiquitin carrier protein (e2) catalyzes multi-ubiquitin chain synthesis via lysine 48 of ubiquitin. *J Biol Chem*, 265(35):21835–21842, 1990.

[99] M. J. Lewis, L. F. Saltibus, D. D. Hau, W. Xiao, and L. Spyracopoulos. Structural basis for non-covalent interaction between ubiquitin and the ubiquitin conjugating enzyme variant human mms2. *J Biomol NMR*, 34(2):89–100, 2006.

[100] P. S. Brzovic, A. Lissounov, D. E. Christensen, D. W. Hoyt, and R. E. Klevit. A ubch5/ubiquitin noncovalent complex is required for processive brca1-directed ubiquitination. *Mol Cell*, 21(6):873–880, 2006.

[101] L. Nguyen, K. S. Plafker, A. Starnes, M. Cook, R. E. Klevit, and S. M. Plafker. The ubiquitin-conjugating enzyme, ubcm2, is restricted to monoubiquitylation by a two-fold mechanism that involves backside residues of e2 and lys48 of ubiquitin. *Biochemistry*, 53(24):4004–4014, 2014.

[102] P. A. Banka, A. P. Behera, S. Sarkar, and A. B. Datta. Ring e3-catalyzed e2 self-ubiquitination attenuates the activity of ube2e ubiquitin-conjugating

enzymes. *J Mol Biol*, 427(13):2290–2304, 2015.

[103] F. R. Schumacher, G. Wilson, and C. L. Day. The n-terminal extension of ube2e ubiquitin-conjugating enzymes limits chain assembly. *J Mol Biol*, 425 (22):4099–4111, 2013.

[104] C. E. Berndsen and C. Wolberger. New insights into ubiquitin e3 ligase mechanism. *Nat Struct Mol Biol*, 21(4):301–307, 2014.

[105] K. L. Lorick, J. P. Jensen, S. Fang, A. M. Ong, S. Hatakeyama, and A. M. Weissman. Ring fingers mediate ubiquitin-conjugating enzyme (e2)-dependent ubiquitination. *Proc Natl Acad Sci U S A*, 96(20):11364–11369, 1999.

[106] P. S. Brzovic, J. E. Meza, M. C. King, and R. E. Klevit. Brca1 ring domain cancer-predisposing mutations: Structural consequences and effects on protein-protein interactions. *J Biol Chem*, 28:41399–41406, 2001.

[107] C. W. Liew, H. Sun, T. Hunter, and C. L. Day. Ring domain dimerization is essential for rnf4 function. *Biochem J*, 431(1):23–29, 2010.

[108] M. D. Ohi, C. W. Vander Kooi, J. A. Rosenberg, W. J. Chazin, and K. L. Gould. Structural insights into the u-box, a domain associated with multi-ubiquitination. *Nat Struct Biol*, 10(4):250–255, 2003.

[109] M. L. Bentley, J. E. Corn, K. C. Dong, Q. Phung, T. K. Cheung, and A. G. Cochran. Recognition of ubch5c and the nucleosome by the bmi1/ring1b ubiquitin ligase complex. *EMBO J*, 30(16):3285–3297, 2011.

[110] S. J. Campbell, R. A. Edwards, C. C. Leung, D. Neculai, C. D. Hodge, S. Dhe-Paganon, and J. N. Glover. Molecular insights into the function of ring finger (rnf)-containing proteins hrnf8 and hrnf168 in ubc13/mms2-dependent ubiquitylation. *J Biol Chem*, 287(28):23900–23910, 2012.

[111] J. N. Pruneda, P. J. Littlefield, S. E. Soss, K. A. Nordquist, W. J. Chazin, P. S. Brzovic, and R. E. Klevit. Structure of an e3:e2 ub complex reveals an allosteric mechanism shared among ring/u-box ligases. *Mol Cell*, 47(6):933–942, 2012.

[112] A. Saha, S. Lewis, G. Kleiger, B. Kuhlman, and R. J. Deshaies. Essential role for ubiquitin-ubiquitin-conjugating enzyme interaction in ubiquitin discharge from cdc34 to substrate. *Mol Cell*, 42(1):75–83, 2011.

[113] R. Das, J. Mariano, Y. C. Tsai, R. C. Kalathur, Z. Kostova, J. Li, S. G. Tarasov, R. L. McFeeters, A. S. Altieri, X. Ji, R. A. Byrd, and A. M. Weissman. Allosteric activation of e2-ring finger-mediated ubiquitylation by a structurally defined specific e2-binding region of gp78. *Mol Cell*, 34(6):674–685, 2009.

[114] V. Notenboom, R. G. Hibbert, S. E. van Rossum-Fikkert, J. V. Olsen, M. Mann,

and T. K. Sixma. Functional characterization of rad18 domains for rad6, ubiquitin, dna binding and pcna modification. *Nucleic Acids Res*, 35(17): 5819–5830, 2007.

[115] R. I. Morimoto and A. M. Cuervo. Protein homeostasis and aging: taking care of proteins from the cradle to the grave. *J Gerontol A Biol Sci Med Sci*, 64(2): 167–170, 2009.

[116] C. Hetz and B. Mollereau. Disturbance of endoplasmic reticulum proteostasis in neurodegenerative diseases. *Nat Rev Neurosci*, 15(4):233–249, 2014.

[117] L. Yang, D. Zhao, J. Ren, and J. Yang. Endoplasmic reticulum stress and protein quality control in diabetic cardiomyopathy. *Biochim Biophys Acta*, 1852 (2):209–218, 2014.

[118] S. Shao and R. S. Hegde. Target selection during protein quality control. *Trends Biochem Sci*, 41(2):124–137, 2016.

[119] Bracher A. Hayer-Hartl M. Hartl, F. U. Molecular chaperones in protein folding and proteostasis. *Nature*, 475(7356), 2011.

[120] J. Tyedmers, A. Mogk, and B. Bukau. Cellular strategies for controlling protein aggregation. *Nat Rev Mol Cell Biol*, 11(11):777–788, 2010.

[121] C. Hirsch, R. Gauss, and T. Sommer. Coping with stress: cellular relaxation techniques. *Trends Cell Biol*, 16(12):657–663, 2006.

[122] T. R. Jahn and S. E. Radford. The yin and yang of protein folding. *FEBS J*, 272(23):5962–5970, 2005.

[123] J. F. Diaz-Villanueva, R. Diaz-Molina, and V. Garcia-Gonzalez. Protein folding and mechanisms of proteostasis. *Int J Mol Sci*, 16(8):17193–17230, 2015.

[124] A. Buchberger, B. Bukau, and T. Sommer. Protein quality control in the cytosol and the endoplasmic reticulum: Brothers in arms. *Mol Cell*, 40(2):238–252, 2010.

[125] J. L. Brodsky. Just a trim, please: Refining er degradation through deubiquitination. *Cell*, 154(3):479–481, 2013.

[126] A. Stolz, W. Hilt, A. Buchberger, and D. H. Wolf. Cdc48: a power machine in protein degradation. *Trends Biochem Sci*, 36(10):515–523, 2011.

[127] B. Medicherla, Z. Kostova, A. Schaefer, and D. H. Wolf. A genomic screen identifies dsk2p and rad23p as essential components of er-associated degradation. *EMBO Rep*, 5(7):692–697, 2004.

[128] H. Richly, M. Rape, S. Braun, S. Rumpf, C. Hoege, and S. Jentsch. A series of ubiquitin binding factors connects cdc48/p97 to substrate multiubiquitylation and proteasomal targeting. *Cell*, 120(1):73–84, 2005.

[129] D. Finley. Recognition and processing of ubiquitin-protein conjugates by the proteasome. *Annu Rev Biochem*, 78(1):477–513, 2009.

[130] F. Förster, P. Unverdorben, P. Sledz, and W. Baumeister. Unveiling the long-held secrets of the 26s proteasome. *Structure*, 21(9):1551–1562, 2013.

[131] J. S. Thrower, L. Hoffman, M. Rechtsteiner, and C. M. Pickart. Recognition of the polyubiquitin proteolytic signal. *EMBO J*, 19(1):94–102, 2000.

[132] Y. Lu, B. H. Lee, R. W. King, D. Finley, and M. W. Kirschner. Substrate degradation by the proteasome: A single-molecule kinetic analysis. *Science*, 348(6231):1250834–1250834, 2015.

[133] R. Swanson, M. Locher, and M. Hochstrasser. A conserved ubiquitin ligase of the nuclear envelope/endoplasmic reticulum that functions in both er-associated and matalpha2 repressor degradation. *Genes Dev*, 15(20):2660–2674, 2001.

[134] M. Deng and M. Hochstrasser. Spatially regulated ubiquitin ligation by an er/nuclear membrane ligase. *Nature*, 443(7113):827–831, 2006.

[135] S. G. Kreft, L. Wang, and M. Hochstrasser. Membrane topology of the yeast endoplasmic reticulum-localized ubiquitin ligase doa10 and comparison with its human ortholog teb4 (march-vi). *J Biol Chem*, 281(8):4646–4653, 2006.

[136] T. Ravid, S. G. Kreft, and M. Hochstrasser. Membrane and soluble substrates of the doa10 ubiquitin ligase are degraded by distinct pathways. *EMBO J*, 25 (3):533–543, 2006.

[137] M. J. Maurer, E. D. Spear, A. T. Yu, E. J. Lee, S. Shahzad, and S. Michaelis. Degradation signals for ubiquitin-proteasome dependent cytosolic protein quality control (cytoqc) in yeast. *G3 (Bethesda)*, 2016.

[138] D. Zattas, J. M. Berk, S. G. Kreft, and M. Hochstrasser. A conserved c-terminal element in the yeast doa10 and human march6 ubiquitin ligases required for selective substrate degradation. *J Biol Chem*, 291(23):12105–12118, 2016.

[139] S. Han, Y. Liu, and A. Chang. Cytoplasmic hsp70 promotes ubiquitination for endoplasmic reticulum-associated degradation of a misfolded mutant of the yeast plasma membrane atpase, pma1. *J Biol Chem*, 282(36):26140–26149, 2007.

[140] K. Nakatsukasa, G. Huyer, S. Michaelis, and J. L. Brodsky. Dissecting the er-associated degradation of a misfolded polytopic membrane protein. *Cell*, 132 (1):101–112, 2008.

[141] P. Chen, P. Johnson, T. Sommer, S. Jentsch, and M. Hochstrasser. Multiple ubiquitin-conjugating enzymes participate in the in vivo degradation of the yeast mat alpha 2 repressor. *Cell*, 74(2):357–369, 1993.

[142] K. Bagola, M. von Delbruck, G. Dittmar, M. Scheffner, I. Ziv, M. H. Glickman, A. Ciechanover, and T. Sommer. Ubiquitin binding by a cue domain regulates ubiquitin chain formation by erad e3 ligases. *Mol Cell*, 50(4):528–539, 2013.

[143] W. J. Cook, P. D. Martin, B. F. Edwards, R. K. Yamazaki, and V. Chau. Crystal structure of a class i ubiquitin conjugating enzyme (ubc7) from saccharomyces cerevisiae at 2.9 angstroms resolution. *Biochemistry*, 36(7):1621–1627, 1997.

[144] T. Biederer, C. Volkwein, and T. Sommer. Role of cue1p in ubiquitination and degradation at the er surface. *Science*, 278(5344):1806–1809, 1997.

[145] O. A. Bazirgan and R. Y. Hampton. Cue1p is an activator of ubc7p e2 activity in vitro and in vivo. *J Biol Chem*, 283(19):12797–12810, 2008.

[146] Z. Kostova, J. Mariano, S. Scholz, C. Koenig, and A. M. Weissman. A ubc7p-binding domain in cue1p activates er-associated protein degradation. *J Cell Sci*, 122(Pt 9):1374–1381, 2009.

[147] M. Von Delbrück, A. Kniss, V. V. Rogov, L. Pluska, K. Bagola, F. Löhr, P. Güntert, T. Sommer, and V. Dötsch. The cue domain of cue1 aligns growing ubiquitin chains with ubc7 for rapid elongation. *Molecular Cell*, 62(6):918–928, 2016.

[148] T. Ravid and M. Hochstrasser. Autoregulation of an e2 enzyme by ubiquitin-chain assembly on its catalytic residue. *Nat Cell Biol*, 9(4):422–427, 2007.

[149] O. A. Bazirgan, R. M. Garza, and R. Y. Hampton. Determinants of ring-e2 fidelity for hrd1p, a membrane-anchored ubiquitin ligase. *J Biol Chem*, 281 (51):38989–9001, 2006.

[150] O. Foresti, V. Rodriguez-Vaello, C. Funaya, and P. Carvalho. Quality control of inner nuclear membrane proteins by the asi complex. *Science*, 346(6210): 751–755, 2014.

[151] T. Sommer and S. Jentsch. A protein translocation defect linked to ubiquitin conjugation at the endoplasmic reticulum. *Nature*, 365(6442).

[152] J. Walter, J. Urban, C. Volkwein, and T. Sommer. Sec61p-independent degradation of the tail-anchored er membrane protein ubc6p. *EMBO J*, 20(12): 3124–3131, 2001.

[153] A. Khmelinskii, E. Blaszczak, M. Pantazopoulou, B. Fischer, D. J. Omnus, G. Le Dez, A. Brossard, A. Gunnarsson, Joseph D. Barry, M. Meurer, and et al. Protein quality control at the inner nuclear membrane. *Nature*, 516(7531): 410–413, 2014.

[154] M. M. Hiller, A. Finger, M. Schweiger, and D. H. Wolf. Er degradation of a misfolded luminal protein by the cytosolic ubiquitin-proteasome pathway.

Science, 273(5282):1725–1728, 1996.

[155] A. Weber, I. Cohen, O. Popp, G. Dittmar, Y. Reiss, T. Sommer, T. Ravid, and E. Jarosch. Sequential poly-ubiquitylation by specialized conjugating enzymes expands the versatility of a quality control ubiquitin ligase. *Mol Cell*, 63: 827–839, 2016.

[156] O. Neuber, E. Jarosch, C. Volkwein, J. Walter, and T. Sommer. Ubx2 links the cdc48 complex to er-associated protein degradation. *Nat Cell Biol*, 7(10): 993–998, 2005.

[157] K. Finke, K. Plath, S. Panzner, S. Prehn, T. A. Rapoport, E. Hartmann, and T. Sommer. A second trimeric complex containing homologs of the sec61p complex functions in protein transport across the er membrane of s. cerevisiae. *EMBO J*, 15(7):1482–1494, 1996.

[158] I. Cohen, R. Wiener, Y. Reiss, and T. Ravid. Distinct activation of an e2 ubiquitin-conjugating enzyme by its cognate e3 ligases. *Proc Natl Acad Sci U S A*, 112(7):625–632, 2015.

[159] C. E. Berndsen and C. Wolberger. A spectrophotometric assay for conjugation of ubiquitin and ubiquitin-like proteins. *Anal Biochem*, 418(1):102–110, 2011.

[160] U. Lenk and T. Sommer. Ubiquitin-mediated proteolysis of a short-lived regulatory protein depends on its cellular localization. *J Biol Chem*, 275(50): 39403–39410, 2000.

[161] U. K. Laemmli. Cleavage of structural proteins during the assembly of the head of bacteriophage t4. *Nature*, 227(5259):680–685, 1970.

[162] O. H. Lowry, N. J. Rosebrough, A. L. Farr, and R. J. Randall. Protein measurement with the folin phenol reagent. *J Biol Chem*, 193(1):265–275, 1951.

[163] L. Whitmore and B. A. Wallace. Dichroweb, an online server for protein secondary structure analyses from circular dichroism spectroscopic data. *Nucleic Acids Res*, 32(Web server issue):668–673, 2004.

[164] A. Shevchenko, H. Tomas, J. Havlis, J. V. Olsen, and M. Mann. In-gel digestion for mass spectrometric characterization of proteins and proteomes. *Nat Protoc*, 1(6):2856–2860, 2006.

[165] J. Rappsilber, M. Mann, and Y. Ishihama. Protocol for micro-purification, enrichment, pre-fractionation and storage of peptides for proteomics using stagetips. *Nat Protoc*, 2(8):1896–1906, 2007.

[166] J. Cox and M. Mann. Maxquant enables high peptide identification rates, individualized p.p.b.-range mass accuracies and proteome-wide protein quantification. *Nat Biotechnol*, 26(12):1367–1372, 2008.

[167] H. Mirzaei, R. S. Rogers, B. Grimes, J. Eng, A. Aderem, and R. Aebersold. Characterizing the connectivity of poly-ubiquitin chains by selected reaction monitoring mass spectrometry. *Mol Biosyst*, 6(10):2004–2014, 2010.

[168] L. M. de Godoy, J. V. Olsen, J. Cox, M. L. Nielsen, N. C. Hubner, F. Frohlich, T. C. Walther, and M. Mann. Comprehensive mass-spectrometry-based proteome quantification of haploid versus diploid yeast. *Nature*, 455(7217):1251–1254, 2008.

[169] R Development Core Team. *R: A Language and Environment for Statistical Computing*. R Foundation for Statistical Computing, Vienna, Austria, 2008. URL `http://www.R-project.org`. ISBN 3-900051-07-0.

[170] G. Huyer, W. F. Piluek, Z. Fansler, S. G. Kreft, M. Hochstrasser, J. L. Brodsky, and S. Michaelis. Distinct machinery is required in saccharomyces cerevisiae for the endoplasmic reticulum-associated degradation of a multispanning membrane protein and a soluble luminal protein. *J Biol Chem*, 279(37):38369–38378, 2004.

[171] H. T. Kim, K. P. Kim, F. Lledias, A. F. Kisselev, K. M. Scaglione, D. Skowyra, S. P. Gygi, and A. L. Goldberg. Certain pairs of ubiquitin-conjugating enzymes (e2s) and ubiquitin-protein ligases (e3s) synthesize nondegradable forked ubiquitin chains containing all possible isopeptide linkages. *J Biol Chem*, 282(24): 17375–17386, 2007.

[172] D. Lester, C. Farquharson, G. Russell, and B. Houston. Identification of a family of noncanonical ubiquitin-conjugating enzymes structurally related to yeast ubc6. *Biochem Biophys Res Commun*, 269(2):474–480, 2000.

[173] U. Lenk, H. Yu, J. Walter, M. S. Gelman, E. Hartmann, R. R. Kopito, and T. Sommer. A role for mammalian ubc6 homologues in er-associated protein degradation. *J Cell Sci*, 115(Pt 14):3007–3014, 2002.

[174] Y. David, T. Ziv, A. Admon, and A. Navon. The e2 ubiquitin-conjugating enzymes direct polyubiquitination to preferred lysines. *J Biol Chem*, 285(12): 8595–8604, 2010.

[175] F. Sievers, A. Wilm, D. Dineen, T. J. Gibson, K. Karplus, W. Li, R. Lopez, H. McWilliam, M. Remmert, J. Soding, J. D. Thompson, and D. G. Higgins. Fast, scalable generation of high-quality protein multiple sequence alignments using clustal omega. *Mol Syst Biol*, 7(539), 2011.

[176] A. M. Waterhouse, J. B. Procter, D. M. Martin, M. Clamp, and G. J. Barton. Jalview version 2–a multiple sequence alignment editor and analysis workbench. *Bioinformatics*, 25(9):1189–1191, 2009.

[177] X. Wang, R. A. Herr, and T. H. Hansen. Ubiquitination of substrates by

esterification. *Traffic*, 13(1):19–24, 2012.

[178] H. Ahn, J. Lim, and W. Son. Solution structure of ring domain of e3 ubiquitin ligase doa10. *PDB*, 2014.

[179] L. Buetow, M. Gabrielsen, N. G. Anthony, H. Dou, A. Patel, H. Aitkenhead, G. J. Sibbet, B. O. Smith, and D. T. Huang. Activation of a primed ring e3-e2-ubiquitin complex by non-covalent ubiquitin. *Mol Cell*, 58(2):297–310, 2015.

[180] R. S. Ranaweera and X. Yang. Auto-ubiquitination of mdm2 enhances its substrate ubiquitin ligase activity. *J Biol Chem*, 288(26):18939–18946, 2013.

[181] N. G. Brown, E. R. Watson, F. Weissmann, M. A. Jarvis, R. VanderLinden, C. R. Grace, J. J. Frye, R. Qiao, P. Dube, G. Petzold, S. E. Cho, O. Alsharif, J. Bao, I. F. Davidson, J. J. Zheng, A. Nourse, I. Kurinov, J. M. Peters, H. Stark, and B. A. Schulman. Mechanism of polyubiquitination by human anaphase-promoting complex: Ring repurposing for ubiquitin chain assembly. *Mol Cell*, 56(2):246–260, 2014.

[182] P. C. Roehm and J. M. Berg. Sequential metal binding by the ring finger domain of brca1. *Biochemistry*, 36(33):10240–10245, 1997.

[183] D. E. Christensen, P. S. Brzovic, and R. E. Klevit. E2-brca1 ring interactions dictate synthesis of mono- or specific polyubiquitin chain linkages. *Nat Struct Mol Biol*, 14(10):941–948, 2007.

[184] K. E. Stoll, P. S. Brzovic, T. N. Davis, and R. E. Klevit. The essential ubc4/ubc5 function in yeast is hect e3-dependent, and ring e3-dependent pathways require only monoubiquitin transfer by ubc4. *J Biol Chem*, 286(17):15165–15170, 2011.

[185] M. Biasini, S. Bienert, A. Waterhouse, K. Arnold, G. Studer, T. Schmidt, F. Kiefer, T. Gallo Cassarino, M. Bertoni, L. Bordoli, and T. Schwede. Swiss-model: modelling protein tertiary and quaternary structure using evolutionary information. *Nucleic Acids Res*, 42:252–258, 2014.

[186] D. M. Wenzel, K. E. Stoll, and R. E. Klevit. E2s: structurally economical and functionally replete. *Biochem J*, 433(1):31–42, 2011.

[187] G. Habeck, F. A. Ebner, H. Shimada-Kreft, and S. G. Kreft. The yeast erad-c ubiquitin ligase doa10 recognizes an intramembrane degron. *J Cell Biol*, 209 (2):261–273, 2015.

[188] R. J. Deshaies and R. Schekman. A yeast mutant defective at an early stage in import of secretory protein precursors into the endoplasmic reticulum. *J Cell Biol*, 105(2):633–645, 1987.

[189] T. Biederer, C. Volkwein, and T. Sommer. Degradation of subunits of the

sec61p complex, an integral component of the er membrane, by the ubiquitin-proteasome pathway. *EMBO J.*, 15(9):2069–2076, 1996.

[190] A. B. Futcher and B. S. Cox. Copy number and the stability of 2-micron circle-based artificial plasmids of saccharomyces cerevisiae. *J Bacteriol*, 157(1): 283–290, 1984.

[191] A. Finger, M. Knop, and D. H. Wolf. Analysis of two mutated vacuolar proteins reveals a degradation pathway in the endoplasmic reticulum or a related compartment of yeast. *Eur J Biochem*, 218(2):565–574, 1993.

[192] O. S. Alfassy, I. Cohen, Y. Reiss, B. Tirosh, and T. Ravid. Placing a disrupted degradation motif at the c terminus of proteasome substrates attenuates degradation without impairing ubiquitylation. *J Biol Chem*, 288(18):12645–12653, 2013.

[193] K. Wu, J. Kovacev, and Z. Q. Pan. Priming and extending: a ubch5/cdc34 e2 handoff mechanism for polyubiquitination on a scf substrate. *Mol Cell*, 37(6): 784–796, 2010.

[194] T. Ravid and M. Hochstrasser. Diversity of degradation signals in the ubiquitin-proteasome system. *Nat Rev Mol Cell Biol*, 9(9):679–689, 2008.

[195] F. Mattiroli and T. K. Sixma. Lysine-targeting specificity in ubiquitin and ubiquitin-like modification pathways. *Nat Struct Mol Biol*, 21(4):308–316, 2014.

[196] K. M. Scaglione, V. Basrur, N. S. Ashraf, J. R. Konen, K. S. J. Elenitoba-Johnson, S. V. Todi, and H. L. Paulson. The ubiquitin-conjugating enzyme (e2) ube2w ubiquitinates the n terminus of substrates. *J Biol Chem*, 288(26): 18784–18788, 2013.

[197] V. Vittal, L. Shi, D. M. Wenzel, K. M. Scaglione, E. D. Duncan, V. Basrur, K. S. J. Elenitoba-Johnson, D. Baker, H. L. Paulson, P. S. Brzovic, and R. E. Klevit. Intrinsic disorder drives n-terminal ubiquitination by ube2w. *Nat Chem Biol*, 11(1):83–89, Jan 2014.

[198] A. J. Fletcher, D. L. Mallery, R. E. Watkinson, C. F. Dickson, and L. C. James. Sequential ubiquitination and deubiquitination enzymes synchronize the dual sensor and effector functions of trim21. *Proc Natl Acad Sci U S A*, 112(32): 10014–10019, 2015.

[199] K. E. Wickliffe, S. Lorenz, D. E. Wemmer, J. Kuriyan, and M. Rape. The mechanism of linkage-specific ubiquitin chain elongation by a single-subunit e2. *Cell*, 144(5):769–781, 2011.

[200] P. J. Winn, T. L. Religa, J. N. Battey, A. Banerjee, and R. C. Wade. Determinants of functionality in the ubiquitin conjugating enzyme family. *Structure*,

12(9):1563–1574, 2004.

[201] Katrin Bagola. *Aktivität Ubiquitin-konjugierender Enzyme an den RING-LIgasen des ERAD-Systems*. Phd thesis, 2012.

[202] M. B. Metzger, M. J. Maurer, B. M. Dancy, and S. Michaelis. Degradation of a cytosolic protein requires endoplasmic reticulum-associated degradation machinery. *J Biol Chem*, 283(47):32302–32316, 2008.

[203] A. Williamson, K. E. Wickliffe, B. G. Mellone, L. Song, G. H. Karpen, and M. Rape. Identification of a physiological e2 module for the human anaphase-promoting complex. *Proc Natl Acad Sci U S A*, 106(43):18213–18218, 2009.

[204] M. D. Petroski, X. Zhou, G. Dong, S. Daniel-Issakani, D. G. Payan, and J. Huang. Substrate modification with lysine 63-linked ubiquitin chains through the ubc13-uev1a ubiquitin-conjugating enzyme. *J Biol Chem*, 282(41):29936–29945, 2007.

[205] C. Hirsch, R. Gauss, S. C. Horn, O. Neuber, and T. Sommer. The ubiquitylation machinery of the endoplasmic reticulum. *Nature*, 458(7237):453–460, 2009.

[206] S. Tiwari and A. M. Weissman. Endoplasmic reticulum (er)-associated degradation of t cell receptor subunits. involvement of er-associated ubiquitin-conjugating enzymes (e2s). *J Biol Chem*, 276(19):16193–16200, 2001.

[207] Z. Kostova, Y. C. Tsai, and A. M. Weissman. Ubiquitin ligases, critical mediators of endoplasmic reticulum-associated degradation. *Semin Cell Dev Biol*, 18(6): 770–779, 2007.

[208] M. L. van de Weijer, M. C. Bassik, R. D. Luteijn, C. M. Voorburg, M. A. Lohuis, E. Kremmer, R. C. Hoeben, E. M. LeProust, S. Chen, H. Hoelen, M. E. Ressing, W. Patena, J. S. Weissman, M. T. McManus, E. J. Wiertz, and R. J. Lebbink. A high-coverage shrna screen identifies tmem129 as an e3 ligase involved in er-associated protein degradation. *Nat Commun*, 5(3832), 2014.

[209] D. J. van den Boomen, R. T. Timms, G. L. Grice, H. R. Stagg, K. Skodt, G. Dougan, J. A. Nathan, and P. J. Lehner. Tmem129 is a derlin-1 associated erad e3 ligase essential for virus-induced degradation of mhc-i. *Proc Natl Acad Sci U S A*, 111(31):11425–11430, 2014.

[210] R. Rajsbaum, G. A. Versteeg, S. Schmid, A. M. Maestre, A. Belicha-Villanueva, C. Martinez-Romero, J. R. Patel, J. Morrison, G. Pisanelli, L. Miorin, M. Laurent-Rolle, H. M. Moulton, D. A. Stein, A. Fernandez-Sesma, B. R. tenOever, and A. Garcia-Sastre. Unanchored k48-linked polyubiquitin synthesized by the e3-ubiquitin ligase trim6 stimulates the interferon-ikkepsilon kinase-mediated antiviral response. *Immunity*, 40(6):880–895, 2014.

[211] S. Y. Lam, C. Murphy, L. A. Foley, S. A. Ross, T. C. Wang, and J. V. Fleming. The human ubiquitin conjugating enzyme ube2j2 (ubc6) is a substrate for proteasomal degradation. *Biochem Biophys Res Commun*, 451(3):361–366, 2014.

[212] Z. Dosztanyi, V. Csizmok, P. Tompa, and I. Simon. Iupred: web server for the prediction of intrinsically unstructured regions of proteins based on estimated energy content. *Bioinformatics*, 21(16):3433–3434, 2005.

[213] M. M. Babu, R. W. Kriwacki, and R. V. Pappu. Versatility from protein disorder. *Science*, 337(6101):1460–1461, 2012.

[214] M. Boban, P. O. Ljungdahl, and R. Foisner. Atypical ubiquitylation in yeast targets lysine-less asi2 for proteasomal degradation. *J Biol Chem*, 290(4): 2489–2495, 2015.

[215] H. Yu and R. R. Kopito. The role of multiubiquitination in dislocation and degradation of the alpha subunit of the t cell antigen receptor. *J Biol Chem*, 274(52):36852–36858, 1999.

[216] X. Wang, R. A. Herr, M. Rabelink, R. C. Hoeben, E. J. Wiertz, and T. H. Hansen. Ube2j2 ubiquitinates hydroxylated amino acids on er-associated degradation substrates. *J Cell Biol*, 187(5):655–668, 2009.

[217] S. G. Kreft and M. Hochstrasser. An unusual transmembrane helix in the endoplasmic reticulum ubiquitin ligase doa10 modulates degradation of its cognate e2 enzyme. *J Biol Chem*, 286(23):20163–20174, May 2011.

[218] Y. J. Machida, Y. Machida, Y. Chen, A. M. Gurtan, G. M. Kupfer, A. D. D'andrea, and A. Dutta. Ube2t is the e2 in the fanconi anemia pathway and undergoes negative autoregulation. *Mol Cell*, 23(4):589–596, 2006.

[219] J. R. Girard, J. L. Tenthorey, and D. O. Morgan. An e2 accessory domain increases affinity for the anaphase-promoting complex and ensures e2 competition. *J Biol Chem*, 290(40):24614–24625, 2015.

[220] J. D. Laney, E. F. Mobley, and M. Hochstrasser. The short-lived mat 2 transcriptional repressor is protected from degradation in vivo by interactions with its corepressors tup1 and ssn6. *Mol Cell Biol*, 26(1):371–380, 2005.

[221] T. Ast, N. Aviram, S. G. Chuartzman, and M. Schuldiner. A cytosolic degradation pathway, prerad, monitors pre-inserted secretory pathway proteins. *J Cell Sci*, 127(14):3017–3023, 2014.

[222] Z.-R. Zhang, J. S. Bonifacino, and R. S. Hegde. Deubiquitinases sharpen substrate discrimination during membrane protein degradation from the er. *Cell*, 154(3):609–622, 2013.

[223] R. Suryadinata, J. K. Holien, G. Yang, M. W. Parker, E. Papaleo, and B. Sarcevic. Molecular and structural insight into lysine selection on substrate and ubiquitin lysine 48 by the ubiquitin-conjugating enzyme cdc34. *Cell Cycle*, 12 (11):1732–1744, 2013.

A | List of abbreviations

AAA - ATPases Associated with diverse cellular Activities
APC - anaphase promoting complex
ATP - adenosine triphosphate
a.u. - arbitrary unit
BSA - bovine serum albumin
bp - base pair
Brij58 - polyethylene glycol hexadecyl ether
CST - Cell Signaling Technology Inc.
CD - circular dichroism
CHX - cycloheximide
CID - collision-induced dissociation
Cue - coupling of ubiquitin conjugation to ER degradation
DNA - deoxyribonucleic acid
Doa - degradation-of-Matα
DTT - dithiothreitol
DUB - Deubiquitinase
E1 - ubiquitin activating enzyme
E2 - ubiquitin conjugating enzyme
E3 - ubiquitin ligase
EDTA - ethylenediaminetetraacetic acid
ER - endoplasmic reticolum
ERAD - ER associated protein degradation
FDR - false discovery rate
FTMS - Fourier Transform Mass Spectrometry
fw - forward
GFP - green fluorescent protein

GST - glutathione S-transferase
HA - haemagglutinin
HECT - Homologous to the E6-AP carboxyl terminus
HMG - 3-hydroxy-3-methyl-glutaryl
Hrd - HMG-CoA reductase degradation
HRP - horseradish peroxidase
Hsp - heat shock protein
IgG - immunoglobulin G
IP - immunoprecipitation
IPTG - isopropyl β-D-1-thiogalactopyranoside
kb - kilo bases (1 kb=1000 bp)
kDa - kilodalton
Mda - megadalton
LB - lysogeny broth
LC - liquid chromatography
Mat - mating type
MHC - major histocompatibility complex
MS - mass spectrometry
ND - not determined
NEM - N-Ethylmaleimide
NMR - Nuclear magnetic resonance
OD_{600} - optical density at a wavelength of 600 nm
PAGE - polyacrylamide gel electrophoresis
PBS - phosphate-buffered saline
PCR - polymerase chain reaction
PDB - Protein Data Bank
PEG - polyethylene glycol
PMSF - phenylmethanesulfonyl fluoride
PQC - protein quality control
PVDF - polyvinylidene fluoride
RBR - RING between RING
RING - really interesting new gene
RNA - ribonucleic acid
rev - reverse

rpm - revolutions per minute
Rpn - Proteasome Regulatory Particle, Non-ATPase-like
SD - synthetic drop-out
SDS - sodium dodecyl sulfate
Sec61 - secretory61
TB - terrific broth
TBT - Tris buffer with tween
TM - trans-membrane domain
Tris - Tris(hydroxymethyl)aminomethane
Ub - ubiquitin
Ubc - ubiquitin conjugating domain
UBD - ubiquitin binding domain
UBL - ubiquitin-like protein
UPS - ubiquitin proteasome system
UV - ultraviolet
v/v - ratio volume per volume
w/o - without
wt - wild type
w/v - ration weight per volume
YPD - yeast extract peptone dextrose

B | Selbstständigkeitserklärung

Hiermit versichere ich, dass ich die vorliegende Arbeit eigenständig und nur mit den angegebenen Hilfen und Hilfsmitteln angefertigt habe. Ich habe die dem Verfahren zugrunde liegende Promotionsordnung der Mathematisch-Naturwissenschaftlichen Fakultät I der Humboldt-Universität zu Berlin vom 06. Juli 2009 zur Kenntnis genommen. Ich habe mich anderwärts nicht um einen Doktorgrad beworben und besitze keinen entsprechenden Titel.

Berlin, der 29. September 2016

Annika Katharina Weber

C | Publikationen und Vorträge

Publikationen

a) A. Weber, I. Cohen, O. Popp, G. Dittmar, Y. Reiss, T. Sommer, T. Ravid, E. Jarosch. Sequential poly-ubiquitylation by specialized conjugating enzymes expands the versatility of a quality control ubiquitin ligase. *Mol Cell*, 63:827-839, 2016

b) T. Sommer, A. Weber, E. Jarosch. News and Views: Rsp5/Nedd4 clears cells of heat-damaged proteins. *Nat Cell Biol*, 16(12):1130-1132, 2014

c) R. S. Schweizer, R. A. Aponte, S. Zimmermann, A. Weber, J. Reinstein. Fine Tuning of a Biological Machine: DnaK Gains Improved Chaperone Activity by Altered Allosteric Communication and Substrate Binding. *Chembiochem*, 12(10):1559-1573, 2011

Vorträge und Posterpräsentationen

a) 2016, FASEB Konferenz, Ubiquitin and cellular regulation, Big Sky Montana, USA, Posterpräsentation

b) 2016, Cancer Club, MDC Berlin, Deutschland, Vortrag

c) 2015, The Ubiquitin Family Meeting, Cold Spring Harbor, USA, Posterpräsentation

d) 2014, EMBO Konferenz, Ubiquitin and ubiquitin-like proteins: At the crossroads from chromatin to protein, Buenos Aires, Argentinien, Posterpräsentation

e) 2013, EMBO Konferenz, Ubiquitin and ubiquitin-like proteins: From structure to function, Riva del Garda, Italien, Posterpräsentation